CHAPTER

THIRTEEN

DESIGN OF HETEROGENEOUS CATALYTIC REACTORS

Our objective in this chapter is to predict the performance of large heterogeneous reactors using the kinetics and transport rates developed in Chaps. 9 to 11. It is not necessary to consider further the individual transport processes within and external to the catalyst pellet. Methods of combining these steps with the kinetics of the chemical reactions to obtain a global rate were summarized in Chap. 12. However, Example 13-2 illustrates again how these individual processes can be combined to predict the conversion in an entire fixed-bed reactor. The major goal now is to use the global rate information to evaluate the composition of the effluent from a reactor for a specified set of design conditions.† The design conditions that must be fixed are the temperature, pressure, and composition of the feed stream, the dimensions of the reactor and catalyst pellets, and enough information about the surroundings to evaluate the heat flux through the reactor walls.

As noted in Chap. 1, a common catalytic reactor is the fixed-bed type, in which the reaction mixture flows continuously through a tube filled with a stationary bed of catalyst pellets (Fig. 1-4*a*). Because of its importance, and because considerable information is available on its performance, most attention will be given to this reactor type. Fluidized-bed, trickle-bed, and slurry reactors are also

† An a priori design procedure, in contrast to a succession of larger experimental reactors, has been ably summarized by R. H. Wilhelm [*J. Pure Appl. Chem.*, 5, 403 (1962)] for fixed beds. This review includes relations between the intrinsic and global rates and, as such, summarizes the effects of external and internal transport processes described in Chaps. 10 to 12. Also, an extensive review of more recent developments in reactor theory and design is available: "Chemical Reactor Theory," Leon Lapidus and Neal R. Amundson (eds.), Prentice-Hall, Englewood Cliffs, N.J., 1977. See particularly Chap. 6 on design of fixed-bed reactors and Chaps. 10 and 11 on fluidized-bed reactors.

considered later in the chapter. Some of the design methods given are applicable also to fluid-solid noncatalytic reactions. The global rate and integrated conversion-time relationships for noncatalytic gas-solid reactions will be considered in Chap. 14.

Only reactors operating at pseudo-steady state are discussed; that is, the design methods presented are applicable when conditions such as catalyst activity do not change significantly in time intervals of the order of the residence time in the reactor. Brief comments about transient conditions are included in Sec. 13-7, but these refer to changes from one stable state to another.

FIXED-BED REACTORS

Quantitative design methods of increasing complexity are considered in Secs. 13-3 to 13-6. First, however, let us summarize construction and operating characteristics of fixed-bed reactors.

13-1 Construction and Operation

Fixed-bed reactors consist of one or more tubes packed with catalyst particles and operated in a vertical position. The catalyst particles may be a variety of sizes and shapes: granular, pelleted, cylinders, spheres, etc. In some instances, particularly with metallic catalysts such as platinum, instead of using single particles, wires of the metal are made into screens. Multiple layers of these screens constitute the catalyst bed. Such screen or gauze catalysts are used in commercial processes for the oxidation of ammonia and the oxidation of acetaldehyde to acetic acid.

Because of the necessity of removing or adding heat, it may not be possible to use a single large-diameter tube packed with catalyst. In this event the reactor may be built up of a number of tubes encased in a single body, as illustrated in Fig 13-1. The energy exchange with the surroundings is obtained by circulating, or perhaps boiling, a fluid in the space between the tubes. If the heat of reaction is large, each catalyst tube must be small (tubes as small as 1.0-in. diameter have been used) in order to prevent excessive temperatures within the reaction mixture (for an exothermic reaction). The problem of deciding how large the tube diameter should be, and thus how many tubes are necessary, to achieve a given production forms an important problem in the design of such reactors.

A disadvantage of this method of cooling is that the rate of heat transfer to the fluid surrounding the tubes is about the same all along the tube length, but the major share of the reaction usually takes place near the entrance. For example, in an exothermic reaction the rate will be relatively large at the entrance to the reactor tube owing to the high concentrations of reactants existing there. It will become even higher as the reaction mixture moves a short distance into the tube, because the heat liberated by the high rate of reaction is greater than that which can be transferred to the cooling fluid. Hence the temperature of the reaction mixture will rise, causing an increase in the rate of reaction. This continues as the mixture moves up the tube, until the disappearance of reactants has a larger effect on the rate than the increase in temperature. Farther along the tube the rate will

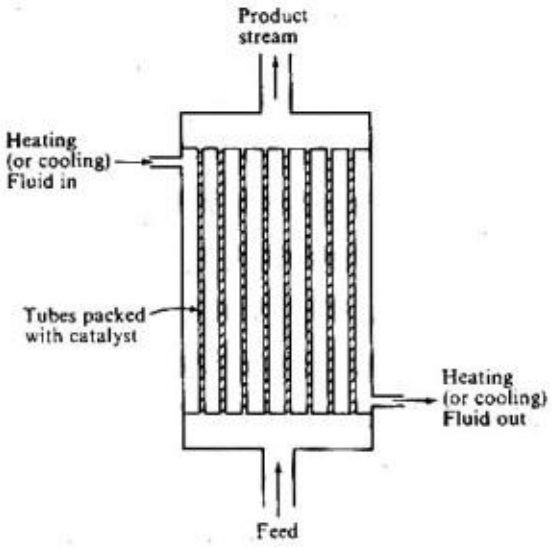

Figure 13-1 Multitube, fixed-bed reactor.

decrease. The smaller amount of heat can now be removed through the wall with the result that the temperature decreases. This situation leads to a maximum in the curve of temperature vs. reactor-tube length. An example is shown in Fig. 13-2 for a TVA ammonia-synthesis reactor. Such a maximum temperature (hot spot) is characteristic of an exothermic reaction in a tubular reactor (Chap. 5).

As mentioned in Chaps. 1 and 5, other means of cooling may be employed besides circulating a fluid around the catalyst tube. Dividing the reactor into parts with intercoolers between each part (see Fig. 13-3) is a common procedure.

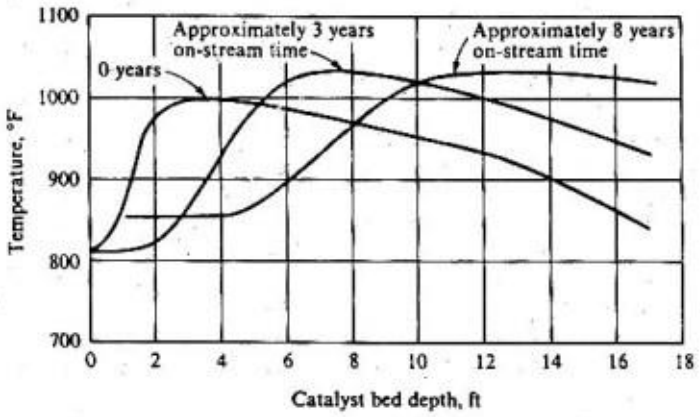

Figure 13-2 Variation in temperature profile with on-stream time in fixed-bed ammonia-synthesis reactor [*by permission from A. V. Slack, H. Y. Allgood, and H. E. Maune, Chem. Eng. Progr., 49, 393 (1953)*].

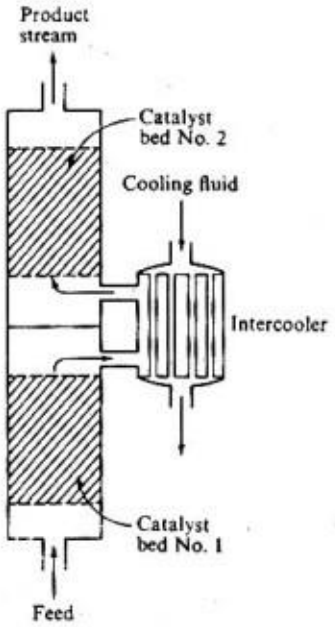

Figure 13-3 Divided reactor with inter-cooler between catalyst beds.

Another scheme which has been satisfactory for reactions of moderate heat of reaction, such as the dehydrogenation of butene, is to add a large quantity of an inert component (steam) to the reaction mixture.

The particular scheme employed for cooling (or heating) the fixed-bed reactor depends on a number of factors: cost of construction, cost of operation, maintenance, and special features of the reaction, such as the deactivation of the catalyst and the magnitude of ΔH. For example, the heat of reaction of naphthalene oxidation is so high that small externally cooled tubes provide about the only way to prevent excessive temperatures in fixed-bed equipment. In sulfur dioxide oxidation the much smaller heat of reaction permits the use of less expensive large-diameter adiabatic catalyst bins in series, with external intercoolers for removing the heat evolved. In dehydrogenation of butene the heat of reaction is not extremely high, so that small-diameter catalyst tubes are not required. Here the use of external heat exchangers is possible (the reaction is endothermic, and energy must be supplied to maintain the temperature), and a satisfactory system can be designed by alternating adiabatic reaction sections with heat exchangers. However, in this case there are several auxiliary advantages in adding a hot inert material (steam) to supply the energy. The blanketing effect of the steam molecules reduces the polymerization of the butadiene product. Also, the steam lowers the partial pressure of the hydrocarbons, and in so doing improves the equilibrium conversion.

All of the operating devices for energy exchange have the objective of preventing excessive temperatures or maintaining a required temperature level; i.e., they are attempts to achieve isothermal operation of the reactor. There are many

advantages to operating at near-isothermal conditions. For example, in the naphthalene oxidation process it is necessary to control the temperature to prevent the oxidation from going all the way to carbon dioxide and water. This is a common situation in partial-oxidation reactions. A second example is the air oxidation of ethylene where ethylene oxide is the desired product. Another reason for avoiding excessive temperatures is to prevent loss of catalyst activity. Changes in structure of the solid catalyst particles as the temperature is increased may reduce their activity and shorten their useful life. For example, the iron oxide catalyst for the ammonia-synthesis reaction shows a more rapid decrease in activity with time if the synthesis unit is operated above the normal temperature range of 400 to 550°C.

The reason for limiting the temperature in sulfur dioxide oxidation is based on two factors: excessive temperatures decrease the catalyst activity, as just mentioned, and the equilibrium yield is adversely affected at high temperatures. This last point is the important one in explaining the need to maintain the temperature level in the dehydrogenation of butene. Still other factors, such as physical properties of the equipment, may require limiting the temperature level. For example, in reactors operated at very high temperatures, particularly under pressure, it may be necessary to cool the reactor-tube wall to preserve the life of the tube itself.

The problem of regenerating the catalyst to restore activity may be a serious one in the fixed-bed reactor. In a great many instances the catalyst is too valuable to discard. If the catalyst activity decreases rapidly with time, frequent regeneration may be necessary. Even when the cost is so low that regeneration is not required, shutting down the process and starting up again after new catalyst has been added is an expensive procedure. If this is necessary at frequent intervals, the entire process may become uneconomical. The exact economic limit on shutdown time depends on the particular process, but in general, if the activity cannot be maintained over a period of several months, the cost of shutdowns is likely to be prohibitive. Regeneration *in situ* is one way out of this difficulty. However, *in situ* regeneration requires two or more reactors if continuous operation is to be maintained, and hence increases the initial cost of the installation. The most successful fixed-bed reactor systems are those where the catalyst activity is sustained for long periods without regeneration. The fixed-bed reactor requires a minimum of auxiliary equipment and is particularly suitable for small commercial units.

In order to prolong the time between regenerations and shutdowns, the reactor tube may be made longer than required for the reaction. For example, suppose a 3-ft length of catalyst bed is necessary to approach the equilibrium conversion with fresh catalyst of high activity. The reactor may be built with tubes 10 ft long. Initially, the desired conversion will be obtained in the first 3 ft. As the catalyst activity decreases, the section of the bed in which the reaction is mainly accomplished will move through the bed, until finally all 10 ft are deactivated. This technique has been employed successfully in ammonia synthesis reactors.

13-2 Outline of the Design Problem

The global rate of reaction tells how much reaction is occurring at any location in the reactor, in terms of *bulk* concentrations and temperature. To evaluate temperatures and concentrations, energy- and mass-conservation equations are form-

ulated according to Eqs. (3-1) and (5-1) for a fluid flowing through a bed of catalyst pellets. The solution of these equations gives the temperature and concentrations at any location, including the reactor exit. In fixed-bed reactor design it is assumed that all properties are constant in a volume element associated with a single catalyst pellet. This means that the global rate is the same within this volume element. Two methods have been used to solve the conservation equations. The most common approach is to assume that the volume element is small with respect to the reactor as a whole. Then the temperature and concentrations are regarded as continuous functions of reactor position, and the conservation expressions become differential equations. This is the method that will be used in the examples in this chapter. The second method† considers the volume element (associated with one catalyst pellet) to be an individual cell, or finite stage, within which mixing is complete so that the cell has uniform properties. The reactor is visualized as an interconnected assembly of these cells. Mass and energy transfer between cells is assumed to occur only by fluid flowing from one cell to adjacent cells. In this procedure the mass- and energy-conservation expressions become an assembly of algebraic (difference) equations.

When temperature gradients exist in the reactor, analytical solution of either the differential or difference equations is not possible. The design process requires numerical solution by a stepwise procedure. Machine computation is necessary. The procedure is illustrated in Secs. 13-4 to 13-6.

The complexity of the design problem depends primarily on the type (radial or axial) and magnitude of the temperature variation in the reactor. The reactants normally enter the catalyst bed at uniform temperature and composition, but as they pass through the bed and reaction occurs, the accompanying heat of reaction and heat exchange with the surroundings can cause both longitudinal and radial variations in temperature. The severity of these variations depends upon the heat of reaction and heat exchange with the surroundings. In the simplest case the entire reactor operates isothermally and there is no variation of axial velocity in the radial direction. The global rate is a function only of concentration. Further, the concentrations will change only in the axial direction. A *one-dimensional* model can be used in developing the mass-conservation equations as described in Sec. 13-3. An analytical solution for the conversion in the exit stream is sometimes possible (see Example 13-2).

It is infrequent in practice to achieve isothermal operation. Either the heat of reaction must be very low (as in isomerization reactions) or the reactant concentration must be very small (as in removal of pollutants from water or air by oxidation). However, in large-scale reactors, adiabatic operation is often closely approached. Again, a one-dimensional model may be employed, but both energy- and mass-conservation equations are needed to describe the conversion in the axial direction. The design procedure is discussed in Sec. 13-4 and illustrated in Example 13-3.

The most complex design problem arises when heat transfer through the reactor wall must be taken into account. This type of operation occurs when it is

† The mixing-cell or finite-stage model is described by H. A. Deans and L. Lapidus [*AIChE J.* 6, 656, 663 (1960)] and by M. L. McGuire and L. Lapidus [*AIChE J.* 11, 85 (1965)].

necessary to supply or remove heat through the wall, and the rate of energy transfer is not sufficient to approach isothermal operation. It is a frequent occurrence in commercial, fixed-bed reactors because of their size and because fluid velocities must be low enough to allow for the required residence time. The presence of the catalyst pellets prevents sufficient turbulence and mixing to obtain uniform concentration and temperature profiles. The concentration, temperature, and the global rate, will vary in both the radial and the axial direction. A *two-dimensional* model is needed for a correct formulation of the conservation equations. A relatively simple two-dimensional model is discussed and illustrated in Sec. 13-6. An approximate, simpler solution can be achieved if all the radial temperature variation is assumed to be concentrated in a thin layer of fluid at the reactor wall. Then with the plug-flow assumption the temperature would be uniform across the reactor radius except for a sharp change at the wall. Also, there would be no radial gradient in concentration. A one-dimensional model can be used for this approximate solution, as illustrated in Sec. 13-5. The computer time required to compute temperature and concentration profiles when radial gradients are accounted for depends upon the type of two-dimensional model employed. This subject is discussed briefly in Sec. 13-6. The approach followed in this introductory text is to illustrate the concepts with relatively simple models and provide references to more advanced methods.†

No mention has been made of the pressure drop in fixed-bed reactors. In most cases Δp is small with respect to the total pressure so that ignoring this effect is justified. However, for gaseous reactions at low pressures the change in pressure may affect the global rate significantly. Also, the Δp is needed for designing pumping equipment. For packed beds the pressure drop may be estimated from the Ergun equation.‡

ISOTHERMAL AND ADIABATIC FIXED-BED REACTORS

13-3 Isothermal Operation

In Chap. 4 the plug-flow model was used as a basis for designing homogeneous tubular-flow reactors. The equation employed to calculate the conversion in the effluent stream was Eq. (3-18). We shall find that the same equations and the same calculational procedure may be used for fixed-bed catalytic reactors, provided that plug-flow behavior is a valid assumption. All that is necessary is to replace the homogeneous rate of reaction in those equations with the global rate for the catalytic reaction, and replace the reactor volume with mass of catalyst. In

† Reviews of fixed-bed reactor design are available: V. Hlavacek and J. Votruba in "Chemical Reactor Theory," Leon Lapidus and Neal R. Amundson (eds.), chap. 6, Prentice-Hall, Englewood Cliffs, N.J. (1977); G. F. Froment, *Ind. Eng. Chem.* **59**(2), 18 (1967); J. Beek, *Adv. Chem. Eng.* 3, 303 (1962).

‡ S. Ergun, *Chem. Eng. Prog.* **48**, 89 (1952); D. Mehta and M. C. Hawley, *Ind. Eng. Chem., Proc. Des. Dev.* **8**, 280 (1969).

the isothermal case deviations from plug-flow behavior arise from variations of axial velocity in the radial direction and from axial dispersion. The radial variation in velocity leads to a residence-time distribution, as does axial dispersion. The effects on the conversion of these deviations from plug-flow performance were discussed in Chap. 6. In isothermal fixed-bed reactors these effects are usually small for isothermal conditions, so that plug-flow equations are satisfactory. However, deviations are potentially large in nonisothermal reactors, and radial variations in particular must be taken into account. We consider first the two-dimensional form of the mass-conversion equation and then present the plug-flow, one-dimensional version normally applicable for isothermal conditions.

A section of a fixed-bed catalytic reactor is shown in Fig. 13-4. Consider a small volume element of radius r, width Δr, and height Δz, through which reaction mixture flows isothermally. Suppose that radial and axial mass transfer can be expressed by Fick's law, with $(D_e)_r$ and $(D_e)_L$ as *effective* diffusivities,† based on the total (void and nonvoid) area perpendicular to the direction of diffusion. The volume of the element, which is $2\pi r\,\Delta r\,\Delta z$, contains both solid catalyst pellets and surrounding fluid. The concentration in the fluid phase is constant within the element, and the global rate is known in terms of this bulk-fluid concentration. The axial velocity of the reacting fluid can vary in the radial direction. It will be described as a local superficial velocity $u(r)$ based on the total (void plus nonvoid) cross-sectional area.

We now apply Eq. (3-1) to obtain a mass-conservation expression for reactant in the volume element. For steady state, the result in differential form is

$$\frac{\partial}{\partial r}\left(r(D_e)_r\frac{\partial C}{\partial r}\right) + r\frac{\partial}{\partial z}\left(-uC + (D_e)_L\frac{\partial C}{\partial z}\right) - \mathbf{r}_p\rho_B r = 0 \qquad (13\text{-}1)$$

where r_p = *global* rate of disappearance of reactant per unit mass of catalyst
ρ_B = density of catalyst in the bed
u = superficial velocity in the axial direction

† These diffusivities include both molecular and turbulent contributions. In fixed beds some convection exists even at low velocities.

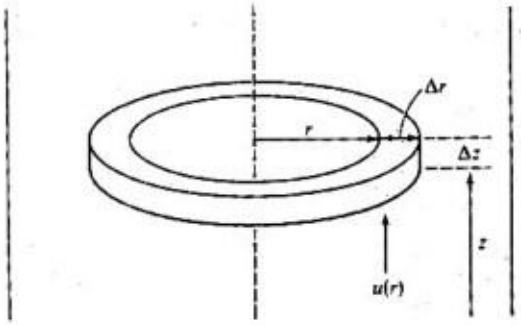

Figure 13-4 Annular element in a fixed-bed catalytic reactor.

If the diffusivities are not sensitive to r or to z and the velocity is not a function of z,† Eq. (13-1) may be written

$$(D_e)_r\left(\frac{1}{r}\frac{\partial C}{\partial r}+\frac{\partial^2 C}{\partial r^2}\right)-u\frac{\partial C}{\partial z}+(D_e)_L\frac{\partial^2 C}{\partial z^2}-\mathbf{r}_p\rho_B=0 \tag{13-2}$$

If the velocity varies with z (due to changes in temperature or number of moles in a gaseous reaction), Eq. (13-1) should be used. If the concentration entering the reactor is C_0, and if there is no axial dispersion in the feed line, the boundary conditions for Eq. (13-2) are

$$\frac{dC}{dz}=0 \qquad \text{at } z=L \tag{13-3}$$

$$uC_0=-(D_e)_L\left(\frac{\partial C}{\partial z}\right)_{>0}+u(C)_{>0} \qquad \text{at } z=0 \text{ for all } r \tag{13-4}$$

$$\frac{\partial C}{\partial r}=0 \qquad \text{at } r=r_0 \text{ for all } z \tag{13-5}$$

$$\frac{\partial C}{\partial r}=0 \qquad \text{at } r=0 \text{ for all } z \tag{13-6}$$

It is instructive to write Eq. (13-2) in dimensionless form by introducing the conversion x and dimensionless coordinates r^* and z^* based on the diameter of the catalyst pellet:

$$x=\frac{C_0-C}{C_0} \tag{13-7}‡$$

$$r^*=\frac{r}{d_p} \tag{13-8}$$

$$z^*=\frac{z}{d_p} \tag{13-9}$$

In terms of these variables Eq. (13-2) becomes

$$-\frac{1}{\mathrm{Pe}_r}\left[\frac{1}{r^*}\frac{\partial x}{\partial r^*}+\frac{\partial^2 x}{(\partial r^*)^2}\right]+\frac{\partial x}{\partial z^*}-\frac{1}{\mathrm{Pe}_L}\frac{\partial^2 x}{(\partial z^*)^2}-\frac{\mathbf{r}_p\rho_B d_p}{C_0 u}=0 \tag{13-10}$$

where

$$\mathrm{Pe}_r=\frac{ud_p}{(D_e)_r} \tag{13-11}$$

$$\mathrm{Pe}_L=\frac{ud_p}{(D_e)_L} \tag{13-12}$$

† This requirement is met for constant fluid density; that is, isothermal conditions for a liquid-phase reaction mixture, and isothermal conditions and no change in total molal flow rate for a gas-phase reaction mixture.

‡ For this equation to be valid for a gaseous reaction, there must be no change in total molal flow rate as well as isothermal operating conditions.

Equation (13-10) shows that the conversion depends on the dimensionless reaction-rate group $r_p \rho_B d_p C_0 u$ and the radial and axial Peclet numbers, defined by Eqs. (13-11) and (13-12).

When the velocity u varies with *radial location*, a stepwise numerical solution of Eq. (13-10) or Eq. (13-2) would be needed. Axial velocities do vary with radial position in fixed beds. The typical profile† is flat in the center of the tube, increases slowly until a maximum velocity is reached about one pellet diameter from the wall, and then decreases sharply to zero at the wall. The radial gradients are a function of the ratio of tube to pellet diameter. Excluding the zero value at the wall, the deviation between the actual velocity at any radius and the average value for the whole tube is small when $d/d_p > 30$.

Radial Peclet numbers have been measured,‡ and some of the results are shown in Fig. 13-5. Above a modified Reynolds number $d_p G/\mu$ of about 40, Pe, is independent of flow rate and has a magnitude of about 10. As implied in Sec. 13-2 the two terms involving radial gradients in Eq. (13-10) are generally small for isothermal operation. The only way§ that concentration gradients can develop is through the variation of velocity with r. Also, the relatively large value of Pe_r further reduces the magnitude of these two terms. If we neglect them, Eq. (13-10) reduces to

$$\frac{\partial x}{\partial z^*} - \frac{1}{\mathrm{Pe}_L}\frac{\partial^2 x}{(\partial z^*)^2} - \frac{r_p \rho_B d_p}{C_0 u} = 0 \tag{13-13}$$

† C. E. Schwartz and J. M. Smith, *Ind. Eng. Chem.*, 45, 1209 (1953).

‡ R. W. Fahien and J. M. Smith, *AIChE J.*, 1, 28 (1955); C. L. de Ligny, *Chem. Eng. Sci.*, 25, 1175 (1970).

§ Note that this is not so if radial temperature gradients exist. Then the rate can vary significantly with r, and large concentration gradients develop. In such a case use is made of the data in Fig. 13-5 as described in Example 13-7.

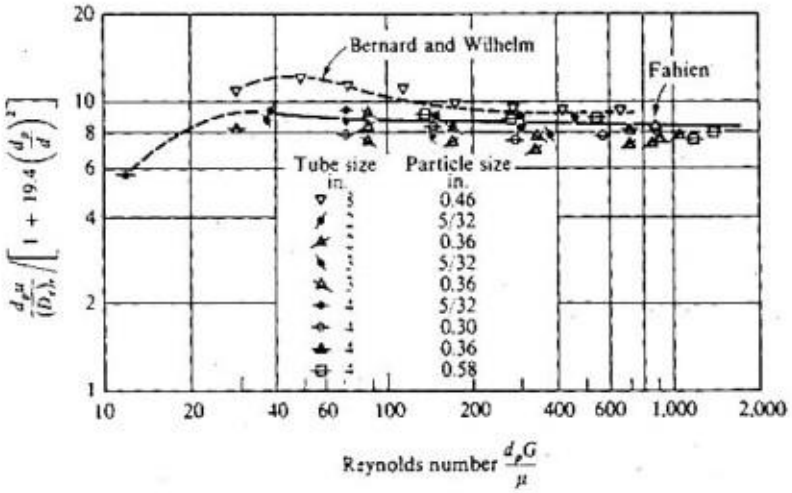

Figure 13-5 Correlation of average Peclet number, $d_p u/(D_e)_r$, with Reynolds number and d_p/d.

or, in dimensional form,

$$-u\frac{\partial C}{\partial z} + (D_e)_L\frac{\partial^2 C}{\partial z^2} - \mathbf{r}_p\rho_B = 0 \tag{13-14}$$

This expression retains the effect of axial dispersion. It is identical to Eq. (6-43), except that the rate for a homogeneous reaction has been replaced with the global rate $\mathbf{r}_p\rho_B$, per unit volume, for a heterogeneous catalytic reaction. In Sec. 6-9 Eq. (6-43) was solved analytically for first-order kinetics to give Eq. (6-47). That result can be adapted for fixed-bed catalytic reactors. The first-order *global* rate would be

$$\mathbf{r}_p = k_o C \qquad \text{g mol/(s)(g catalyst)} \tag{13-15}$$

where k_o is an overall rate constant that includes the effects of fluid-to-particle and intraparticle mass-transfer effects. The solution of Eq. (13-14) is the same as Eq. (6-47), but instead of Eq. (6-48) we have

$$\beta = \left(1 + 4k_0\rho_B\frac{(D_e)_L}{u^2}\right)^{1/2} \tag{13-16}$$

If the catalytic rate equation were not first order, numerical solution of Eq. (13-14) with Eqs. (13-3) and (13-4) would be necessary.

To utilize Eq. (6-47), or solutions of Eq. (13-14) for other kinetics, requires the axial diffusivity $(D_e)_L$ as well as the global rate. $(D_e)_L$ has been measured for both gases and liquids flowing through fixed beds. The experimental data of McHenry and Wilhelm† (for gases) and theoretical predictions‡ both indicate that $\mathrm{Pe}_L = 2$ for Reynolds numbers above about 10. For liquids§ Pe_L is less, particularly at low Reynolds numbers. A more detailed correlation including bed porosity and Schmidt number is available¶.

The significance of the axial dispersion term in Eq. (13-14) depends on the length L of the reactor, the effective diffusivity, and the velocity. Its importance decreases as the velocity and length increase. For low velocities ($\mathrm{Re} < 1$) in short reactors, longitudinal dispersion can be significant.†† In most other cases axial dispersion is negligible. Then Eq. (13-14) takes the form

$$-u\frac{dC}{dz} = \mathbf{r}_p\rho_B \tag{13-17}$$

† K. W. McHenry, Jr., and R. H. Wilhelm, *AIChE J.*, 3, 83 (1957).

‡ R. Aris and N. D. Amundson, *AIChE J.*, 3, 280 (1957).

§ J. J. Carberry and R. H. Bretton, *AIChE J.*, 4, 367 (1958); E. J. Cairns and J. M. Prausnitz, *Chem. Eng. Sci.*, 12, 20 (1960).

¶ D. J. Gunn, *Chem. Eng.*, No. 219, 153 (1968).

†† Criteria for neglecting axial dispersion in isothermal and adiabatic reactors are given by Carberry and Wendel [*AIChE J.*, 9, 129 (1963)], Hlavacek and Marek [*Chem. Eng. Sci.* 21, 501 (1966)] and Levenspiel and Bischoff [*Adv. Chem. Eng.*, 4, 95 (1963)].

Multiplying the numerator and the denominator by the cross-sectional area of the reactor gives

$$-Q\frac{dC}{dV} = \mathbf{r}_p\rho_B$$

or

$$\frac{V}{Q} = -\frac{1}{\rho_B}\int_{C_0}^{C}\frac{dC}{\mathbf{r}_p} = \frac{C_0}{\rho_B}\int_{C_0}^{C}\frac{dx}{\mathbf{r}_p} \tag{13-18}$$

Since $V\rho_B$ is the mass of catalyst in the reactor and $C_0Q = F$, an alternate form, which is also applicable for variable fluid density, is Eq. (12-2):

$$\frac{W}{F} = \int\frac{dx}{\mathbf{r}_p} \tag{12-2}$$

Equation (12-2) is of the same form as Equation (3-18). The application of these equations to reactor design is the same as discussed in Chap. 4, for example, in Example 4-7.

Example 13-1 Derive Eq. (13-2) by starting with the point, mass-conservation equation (continuity equation) for species j in a reacting system:

$$\frac{\partial C_j}{\partial t} = -\nabla\cdot D_e(\nabla C_j) + \nabla\cdot(C_j\mathbf{v}) = \sum_i \mathbf{r}_{ij} \tag{A}$$†

where $\mathbf{r}_i$ is the rate of *production* of species j, by reaction i, per unit volume of reactor. Note the assumptions involved.

SOLUTION For steady state $\partial C_j/\partial t = 0$. In the cylindrical coordinates of a tubular reactor the radial component of the velocity will be zero and we can assume angular symmetry. Then the divergence of the convective flux of j is

$$\nabla\cdot(C_j\mathbf{v}) = \frac{\partial}{\partial z}(C_j v_z) \tag{B}$$

where v_z is now the velocity in the axial direction. In cylindrical coordinates the divergence of the gradient of the diffusion flux is

$$\nabla\cdot D_e(\nabla C_j) = \frac{\partial}{\partial z}\left[(D_e)_L\left(\frac{\partial C_j}{\partial z}\right)\right] + \frac{1}{r}\frac{\partial}{\partial r}\left[r(D_e)_r\frac{\partial C}{\partial r}\right] \tag{C}$$

For one reaction, and in terms of the global rate of disappearance per unit mass, $\mathbf{r}_p$,

$$\sum_i \mathbf{r}_{ij} = -\rho_B\mathbf{r}_p \tag{D}$$

† See books on transport phenomena for derivation of the species continuity equation; for example, R. B. Bird, W. E. Stewart, and E. N. Lightfoot, "Transport Phenomena," p. 556, John Wiley & Sons, New York (1960).

Substituting Eqs. (B) to (D) in Eq. (A) gives

$$-\frac{\partial}{\partial z}\left[(D_e)_L\left(\frac{\partial C_j}{\partial z}\right)\right]-\frac{1}{r}\frac{\partial}{\partial r}\left[r(D_e)_r\frac{\partial C}{\partial r}\right]+\frac{\partial}{\partial z}(C_j v_z)=-\rho_B \mathbf{r}_p \qquad \text{(E)}$$

Finally, if the axial and radial diffusivities are not sensitive to r or to z, and if the velocity is not a function of z, Eq. (E) becomes

$$-(D_e)_r\left(\frac{1}{r}\frac{\partial C_j}{\partial r}+\frac{\partial^2 C_j}{\partial r^2}\right)+v_z\frac{\partial C_j}{\partial z}-(D_e)_L\frac{\partial^2 C_j}{\partial z^2}+\rho_B \mathbf{r}_p=0 \qquad \text{(F)}$$

This equation is identical with Eq. (13-2) where we have used u, rather than v_z, to be the velocity in the axial direction.

We have mentioned that in this chapter it is supposed that the global rate of reaction is known from the methods of Chaps. 9 to 11. That is, the intrinsic rate has been combined with external and intraparticle transport rates to obtain the global rate as a function of bulk concentrations and temperature. However, it is perhaps helpful to illustrate how all the individual transport effects are combined to predict reactor performance. For isothermal conditions and first-order kinetics, it is possible to obtain a simple analytical solution which clearly displays the influence of axial dispersion, fluid-to-particle mass transport, intraparticle diffusion, and intrinsic reaction. This is done in Example 13-2.

Example 13-2 An irreversible first-order reaction occurs on the interior pore surface of catalyst particles in a fixed-bed tubular reactor. Assume isothermal operation and the dispersion model for the reaction mixture flowing through the bed. The reactant concentration in the feed is C_0. Derive an equation for the conversion in the reactor effluent. How is the equation simplified if:

(*a*) intraparticle diffusion resistance is unimportant?
(*b*) fluid-to-particle (or external) mass transfer resistance is unimportant?
(*c*) the global rate is controlled by the intrinsic reaction at an interior site?
(*d*) axial dispersion is unimportant (plug-flow conditions)?
(*e*) both conditions (*c*) and (*d*) apply?

SOLUTION

A. Intrinsic reaction and intraparticle diffusion. The rate of the intrinsic reaction per unit mass of catalyst is

$$\mathbf{r}=k_1 C' \qquad \text{(A)}$$

where the prime on C designates the *intraparticle* concentration. The mass-conservation equation within the particle (assumed to be spherical) is given by Eq. (11-46). Its solution gives the concentration profile [Eq. (11-49)]. This, in turn, can be used to express the rate of reaction for the whole particle, $\mathbf{r}_p$, in terms of the concentration C_s' (which is equal to C_s) at the outer surface of the particle. The result for $\mathbf{r}_p$ is Eq. (11-53), which may be written

$$\mathbf{r}_p=\eta k_1 C_s=\frac{1}{\Phi_s}\left|\frac{1}{\tanh 3\Phi_s}-\frac{1}{3\Phi_s}\right|k_1 C_s \qquad \text{(11-53)}$$

This expression combines the effects of intrinsic reaction and intraparticle diffusion to give the rate for one particle (per unit mass of catalyst) in terms of the Thiele modulus Φ_s.

B. External mass transfer. The next step is to express $\mathbf{r}_p$ in terms of the bulk concentration; that is, convert Eq. (11-53) to a form involving C_b instead of C_s, thus giving an expression for the global rate. This is done by equating the mass-transfer rate from bulk gas to catalyst surface to the rate of reaction, as discussed in Chap. 10 (and illustrated in Example 11-8). Equating Eqs. (10-1) and (11-53),

$$k_m a_m (C_b - C_s) = \eta k_1 C_s \tag{B}$$

where a_m, the outer surface area per unit mass, is $6/d_p\rho_p$ for a spherical particle of diameter d_p and density ρ_p.

Eliminating C_s from Eqs. (11-53) and (B) in order to express $\mathbf{r}_p$ in terms of C_b gives

$$\mathbf{r}_p = \left[\frac{1}{d_p\rho_p/6k_m + 1/\eta k_1}\right] C_b \tag{C}$$

C. Reactor Model. For the dispersion model the mass-conservation expression is Eq. (13-14) with $\mathbf{r}_p$ given by Eq. (C). As noted, the solution of Eq. (13-14) with its boundary conditions is Eq. (6-47) with β given by Eq. (13-16). Thus the conversion x, in the effluent is

$$\left(\frac{C}{C_0}\right)_b = 1 - x$$

$$= \frac{4\beta}{(1+\beta)^2 \exp\left[-\frac{1}{2}\frac{uL}{(D_e)_L}(1-\beta)\right] - (1-\beta)^2 \exp\left[-\frac{1}{2}\frac{uL}{(D_e)_L}(1+\beta)\right]} \tag{D}$$

where

$$\beta = \left(1 + 4k_v\rho_B\frac{(D_e)_L}{u^2}\right)^{1/2} \tag{E}$$

Comparison of Eqs. (13-15) and (C) shows that the overall rate constant is

$$k_v = \frac{1}{d_p\rho_p/6k_m + 1/\eta k_1} \tag{F}$$

Equation (F) can be written in dimensionless terms by multiplying by $d_p\rho_B/u$ to give

$$\frac{k_v\, d_p\rho_B}{u} = \left[\frac{1}{S} + \frac{1}{\eta\Lambda}\right]^{-1} \tag{G}$$

where $S = \dfrac{6\rho_B k_m}{\rho_p u}$; external mass-transfer parameter (H)

$\Lambda = \dfrac{k_1\rho_B d_p}{u}$; intrinsic reaction parameter (I)

Then β may be expressed in terms of these parameters and the Peclet number Pe_L:

$$\beta = \left[1 + 4\left(\frac{1}{S} + \frac{1}{\eta\Lambda}\right)^{-1}\left(\frac{u}{d_p}\right)\frac{(D_e)_L}{u^2}\right]^{1/2} = \left[1 + 4\left(\frac{1}{S} + \frac{1}{\eta\Lambda}\right)^{-1}\frac{1}{Pe_L}\right]^{1/2} \quad (J)$$

Finally, Eq. (D) can be written in terms of Pe_L:

$$1 - x = \frac{4\beta}{(1+\beta)^2 \exp\left[-\frac{1}{2}(L/d_p)\,Pe_L(1-\beta)\right] - (1-\beta)^2 \exp\left[-\frac{1}{2}(L/d_p)\,Pe_L(1+\beta)\right]} \quad (K)$$

Equation (K) is the required solution which expresses the conversion in terms of the axial dispersion parameter Pe_L and, through β, in terms of S, Λ, and the intraparticle diffusion parameter (the effectiveness factor η). Note that the product $L/d_p(Pe_L) = Lu/(D_e)_L$ is a Peclet number based upon L length. This indicates that the importance of axial dispersion depends upon the reactor length.

(*a*) If intraparticle diffusion is unimportant, η in Eq. (J) becomes unity.

(*b*) If external diffusion is unimportant, k_m becomes relatively large; then S is much larger than $\eta\Lambda$ and Eq. (J) for β becomes

$$\beta = (1 + 4\eta\Lambda/Pe_L)^{1/2} \quad (L)$$

(*c*) If intrinsic kinetics controls the global rate, $k_o = k_1$: this is the same as neglecting both external and internal mass transfer resistances. Then Eq. (J) becomes

$$\beta = (1 + 4\Lambda/Pe_L)^{1/2} \quad (M)$$

(*d*) If axial dispersion is unimportant, Pe_L is very large and $\beta \to 1.0$. Then Eq. (K) becomes indeterminate. However, Eq. (13-17) is applicable and may be integrated directly with $\mathbf{r}_p$ given by Eq. (13-15):

$$-u\frac{dC_b}{dz} = k_0 C_b \rho_B$$

or, in integrated form,

$$\left(\frac{C}{C_0}\right)_b = \exp\left(-k_0\rho_B L/u\right) \quad (N)$$

Substituting Eq. (F) for k_o,

$$\left(\frac{C}{C_0}\right)_b = 1 - x = \exp\left(-\frac{\rho_B L/u}{d_p\rho_p/6k_m + 1/\eta k_1}\right)$$

or, in terms of the dimensionless parameters

$$1 - x = \exp\left[-\frac{L/d_p}{(1/S) + (1/\eta\Lambda)}\right] \quad (P)$$

This result was also obtained in Example 12-1 where experimental conversion data were interpreted in terms of a plug-flow model which included external and intraparticle mass transfer. Equations (I) for the global rate and (K) for the effluent concentration in Example 12-1 are of the same form as Eqs. (C) and (P) of this example.

(*e*) If axial dispersion is unimportant and also intrinsic kinetics controls the global rate, Eq. (P) is applicable with $S \to \infty$ and $\eta \to 1$. Hence,

$$1 - x = \exp\left[-(\Lambda L/d_p)\right] = \exp\left[-\left(\frac{k_1 \rho_B L}{u}\right)\right] \qquad \text{(Q)}$$

In this equation the only rate constant is that for intrinsic kinetics. Equation (Q) is analogous to Eq. (4-18) developed for ideal-flow (plug flow) in a tubular reactor for a first-order homogeneous reaction.

13-4 Adiabatic Operation

Large-diameter or well-insulated reactors approach adiabatic operation more closely than isothermal operation. Therefore, an adiabatic, one-dimensional model may be a good representation of actual behavior. With this model, as for isothermal operation, radial gradients in concentrations and temperature are generally small because they are caused solely by radial variation in the axial velocity.

If axial dispersion of heat is included, the two-dimensional energy conservation equation is

$$(k_e)_r\left(\frac{1}{r}\frac{\partial T}{\partial r} + \frac{\partial^2 T}{\partial r^2}\right) - (u\rho)c_p\frac{\partial T}{\partial z} + (k_e)_L\frac{\partial^2 T}{\partial z^2} - \mathbf{r}_p\rho_B(\Delta H) = 0 \qquad (13\text{-}19)$$

This expression is analogous to Eq. (13-2) for mass transfer and involves the same kinds of assumptions. It is obtained from Eq. (5-1) by including terms for axial and radial transfer of heat. The quantities $(k_e)_r$ and $(k_e)_L$ are *effective* thermal conductivities in the radial and axial directions and are analogous to $(D_e)_r$ and $(D_e)_L$.

For the *adiabatic* model the radial dispersion term disappears so that Eq. (13-19) becomes

$$-u\rho c_p\frac{\partial T}{\partial z} + (k_e)_L\frac{\partial^2 T}{\partial z^2} - \mathbf{r}_p\rho_B(\Delta H) = 0 \qquad (13\text{-}20)$$

This is analogous to the mass-conservation expression [Eq. (13-14)].

The axial dispersion term† in the energy-conservation equation may be more important‡ than axial dispersion of mass. However, for the relatively high velocities and long bed depths encountered in commercial reactors it is normal that axial dispersion of both heat and mass can be neglected. If this is not so, the

† The axial effective thermal conductivity $(k_e)_L$ may be estimated from the correlation of J. Votruba, V. Hlavacek, and M. Marek, *Chem. Eng. Sci.* **27**, 1845 (1972).

‡ L. C. Young and B. A. Finlayson, *Ind. Eng. Chem. Fundam.* **12**, 412 (1973); Hlavacek, V., et al., *Chem. Eng. Sci.* **28**, 1897 (1973).

solution of Eqs. (13-14) and (13-20) becomes a boundary-value problem with boundary conditions applicable at the entrance and exit of the catalyst bed. The situation is analogous to the dispersion model considered for homogeneous tubular reactions in Sec. 6-9. However, now the energy-conservation equation is also involved and complex numerical solution techniques† are necessary. Even with high-speed computers considerable time is required.

If we neglect axial dispersion of heat and mass, Eq. (13-20) reduces to

$$u\rho C_p \frac{dT}{dz} = \mathbf{r}_p \rho_B (-\Delta H) \tag{13-21}$$

and the mass-conservation expression is Eq. (12-2). As done in Chap. 5 for adiabatic, homogeneous reactors [see Eqs. (5-15) and (5-16)], we can combine Eqs. (13-21) and (12-2) so as to integrate the energy equation. Thus, substituting $\mathbf{r}_p$ from the differential form [Eq. (12-2)] into Eq. (13-21) gives

$$u\rho c_p \frac{dT}{dz} = \rho_B (-\Delta H) F \frac{dx}{dW}$$

$$dT = \frac{\rho_B (-\Delta H) F}{u\rho c_p} \left(\frac{dz}{dW}\right) dx$$

Since $dW = (\rho_B A_c\, dz)$ and $u\rho A_c = F_t$,

$$dT = (-\Delta H) \frac{F}{F_t c_p} dx \tag{13-22}$$

The flow rates F and F_t are the mass-feed rates of reactant and of total mixture. For constant, ΔH, integration yields

$$T - T_f = (-\Delta H) \frac{F}{F_t c_p} (x - x_f) \tag{13-23}$$

where x_f and T_f are the conversion and temperature of the feed.

With the temperature given by Eq. (13-23), the global rate can be evaluated at any conversion. Then only Eq. (12-2) need be integrated to determine the conversion for any catalyst bed depth or mass W. The calculations, which are similar to those for homogeneous reactors (Example 5-2), are illustrated in Example 13-3.

Example 13-3 Wenner and Dybdal‡ studied the catalytic dehydrogenation of ethyl benzene and found that with a certain catalyst the rate could be represented by the reaction

$$C_6H_5C_2H_5 \rightleftharpoons C_6H_5CH{=}CH_2 + H_2$$

† Orthogonal collocation [J. V. Villadsen and W. E. Stewart, *Chem. Eng. Sci.* 22, 1483 (1967)] has proven to be an efficient procedure for solution of such equations [L. C. Young and B. A. Finlayson, loc. cit.].

‡ R. R. Wenner and F. C. Dybdal, *Chem. Eng. Progr.*, 44, 275 (1948).

The global rate was given as

$$r_p = k\left(p_E - \frac{1}{K} p_s p_H\right)$$

where p_E = partial pressure of ethyl benzene
p_s = partial pressure of styrene
p_H = partial pressure of hydrogen

The specific reaction rate and equilibrium constants are

$$\log k = -\frac{4770}{T} + 4.10$$

where k is the pound moles of styrene produced per hr(atm)(lb catalyst) and T is in degrees Kelvin; in SI units, $k_{SI} = 2.74 \times 10^{-6}\ k$, kg mol/(s)(kPa)(kg catalyst).

t, °C	K
400	1.7×10^{-3}
500	2.5×10^{-2}
600	2.3×10^{-1}
700	1.4

Estimate the amount of catalyst necessary to produce 15 tons (13,620 kg) of styrene a day, using vertical tubes 4 ft (1.22 m) in diameter, packed with catalyst pellets. Wenner and Dybdal considered this problem by taking into account the side reactions producing benzene and toluene. However, to simplify the calculations in this introductory example, suppose that the sole reaction is the dehydrogenation to styrene, and that there is no heat exchange between the reactor and the surroundings. Assume that under normal operation the exit conversion will be 45%. However, also prepare graphs of conversion and temperature vs. catalyst bed depth, up to equilibrium conditions. The feed rate per reactor tube is 13.5 lb mol h (1.70×10^{-3} kg mol/s) for ethyl benzene and 270 lb mol/h (34.0×10^{-3} kg mol/s) for steam. In addition,

Temperature of mixed feed entering reactor	= 625°C (898 K)
Bulk density of catalyst as packed	= 90 lb/ft^3 (1440 kg/m^3)
Average pressure in reactor tubes	= 1.2 atm (121 kPa)
Heat of reaction ΔH	= 60,000 Btu/lb mol (1.39×10^5 kJ/(kg mol)
Surroundings temperature	= 70°F (294 K)

SOLUTION The reaction is endothermic, so that heat must be supplied to maintain the temperature. In this problem energy is supplied by adding steam at 625°C to the feed. An alternate approach of transferring heat from the surroundings is utilized for the same system in Example 13-4.

The operation is adiabatic so that Eq. (13-23) is applicable with $x_f = 0$. For ethylbenzene $F = 13.5$ lb mol/h. As there is a large excess of steam, it will be satisfactory to take $c_p = 0.52$. Then the heat capacity of the reaction mixture will be

$$F_t c_p = (270 \times 18 + 13.5 \times 106)(0.52)$$
$$= 3270 \text{ Btu/°F(h) or } (1.72 \text{ kJ/(K)(s)} \qquad \text{(A)}$$

Substituting numerical values in Eq. (13-23), we obtain

$$T - T_f = \frac{-60{,}000\ (13.5)}{3270} x$$
$$T - 1616 = -248x \qquad \text{(B)}$$

where T is in degrees Rankine, and 1616°R is the entering temperature of the feed.

Equation (12-2), written in differential form, with the weight of catalyst expressed as $dW = \rho_B A_c\, dz$, where A_c is the cross-sectional area, is

$$F\, dx = r_p \rho_B A_c\, dz$$
$$dz = \frac{F}{r_p \rho_B A_c} dx = \frac{13.5\, dx}{90(0.7854)(16) r_p} = \frac{0.0119}{r_p} dx \qquad \text{(C)}$$

The partial pressures can be expressed in terms of the conversion as follows: At any conversion x the moles of each component are

Steam = 20
Ethyl benzene = $1 - x$
Styrene = x
Hydrogen = x
Total moles = $21 + x$

Then

$$p_E = \frac{1 - x}{21 + x}(1.2)$$

$$p_S = p_H = \frac{x}{21 + x}(1.2)$$

Then the rate equation becomes

$$r_p = \frac{1.2}{21 + x} k \left[(1 - x) - \frac{1.2}{K} \frac{x^2}{21 + x}\right]$$

or, with the expression for k determined by Wenner and Dybdal,†

$$r_p = \frac{1.2}{21 + x}(12{,}600)e^{-19{,}800/T}\left[(1 - x) - \frac{1.2}{K}\frac{x^2}{21 + x}\right] \qquad \text{(D)}$$

Substituting this value of r_p in Eq. (C) gives an expression for the catalyst-bed depth in terms of the conversion and temperature,

$$\frac{dz}{dx} = \frac{21 + x}{1{,}270{,}000}e^{19{,}800/T}\left[(1 - x) - \frac{1.2}{K}\frac{x^2}{21 + x}\right]^{-1} \qquad \text{(E)}$$

With Eq. (B) to express T in terms of x, and the K vs. T data given in the problem statement, the entire right-hand side of Eq. (E) is in terms of x. Then we may write Eq. (E) as

$$\frac{dz}{dx} = f(x) \qquad \text{(F)}$$

This expression may be solved numerically for z as a function of x, starting at the feed ($z = 0$, $T = 1616°$R, or 898 K, for $x = 0$). Equation (F) is of the same form as Eq. (B) of Example 5-1 with one dependent variable, z. Hence, it may be solved by the Runge-Kutta procedure described in that example. The results of the computations obtained with an increment size $\Delta x = 0.01$ are given in Table 13-1.

The rate of reaction becomes zero at a conversion of about $x = 0.69$ and a temperature of 1445°R (803 K), as determined from Eqs. (B) and (D). From Fig. 13-6 it is found that a bed depth of 3.8 ft (1.16 m) is required for a

† In the exponential term T has been converted to degrees Rankine.

Table 13-1 Data for conversion of ethyl benzene to styrene in an adiabatic reactor

Conversion	Temperature, °R	Temperature, °C	Catalyst-bed depth, ft
0	1616	625	0
0.10	1591	611	0.40
0.20	1566	597	0.96
0.30	1542	584	1.75
0.40	1517	570	2.93
0.50	1492	556	4.95
0.55	1480	549	6.3
0.60	1467	542	10.0
0.62	1462	539	13.0
0.69	1445	530	∞

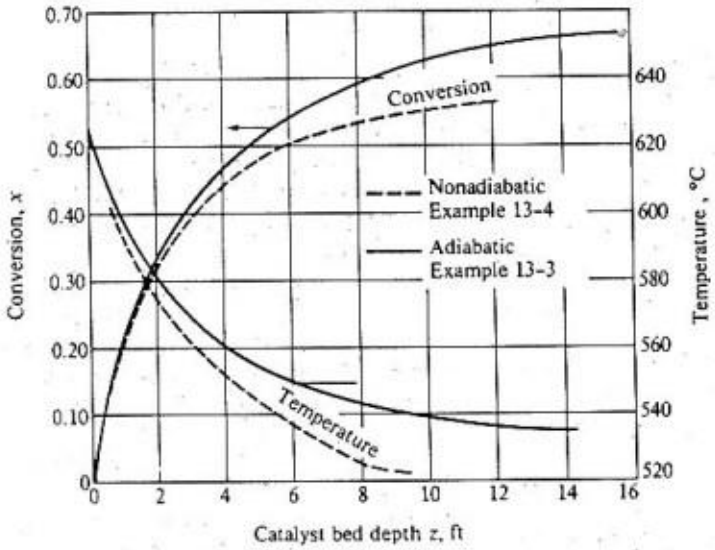

Figure 13-6 Conversion vs. catalyst-bed depth for the production of styrene from ethyl benzene.

conversion of 45%. The production of styrene from each reactor tube would be

$$\text{Production, tube} = 13.5(0.45)(104)(24)$$

$$= 15{,}200 \text{ lb/day} \qquad (7.6 \text{ tons/day}, 6900 \text{ kg/day})$$

Hence two 4-ft-diameter reactor tubes packed with catalyst to a depth of at least 3.8 ft would be required to produce 15 tons/day of crude styrene. The mass of catalyst required is

$$3.8(\pi d_t^2/4)90(15/7.6) = 8500 \text{ lb } (3860 \text{ kg})$$

NONISOTHERMAL, NONADIABATIC FIXED-BED REACTORS

In homogeneous-reactor design (Chap. 5) only heat exchange with the surroundings was considered. Radial mixing was supposed to be sufficiently good that all the resistance to energy transfer could be concentrated at the reactor wall. The temperature was assumed to be flat up to the wall, where a discontinuous change to the wall temperature occurred. The temperature of the reaction mixture changed only in the axial direction. This one-dimensional model is normally satisfactory for homogeneous reactors, because radial mixing is sufficient to give a reasonably flat profile. However, in fixed beds this is not as good an assumption, because the catalyst pellets hinder radial mixing. Hence, a two-dimensional model which accounts for radial temperature gradients within the catalyst bed may be necessary. The one- and two-dimensional models are considered separately in Secs. 13-5 and 13-6.

13-5 The One-Dimensional Model

The form of the radial temperature profile in a nonadiabatic fixed-bed reactor has been observed experimentally to have a parabolic shape. Data for the oxidation of sulfur dioxide with a platinum catalyst on $\frac{1}{8} \times \frac{1}{8}$-in. cylindrical pellets in a 2-in.-ID reactor are illustrated in Fig. 13-7. Results are shown for several catalyst-bed depths. The reactor wall was maintained at 197°C by a jacket of boiling glycol. This is an extreme case. The low wall temperature resulted in severe radial temperature gradients, more so than would exist in many commercial reactors. The longitudinal profiles are shown in Fig. 13-8 for the same experiment. These curves show the typical hot spots, or maxima, characteristic of exothermic reactions in a nonadiabatic reactor. The greatest increase above the feed temperature is at the center, $r/r_0 = 0$. This rise decreases as the wall is approached and actually disappears at a radial position of 0.9. The temperature is so low here, even in the entering stream, that very little reaction occurs. Hence the curve in Fig. 13-8 at $r/r_0 = 0.9$ is essentially a cooling curve, approaching 197°C as the bed depth increases.

A completely satisfactory design method for nonadiabatic reactors entails predicting the radial and longitudinal variations in temperature, such as those shown in Figs. 13-7 and 13-8, predicting the analogous concentration profiles, and the bulk mean conversion. To make such predictions we must know the effective

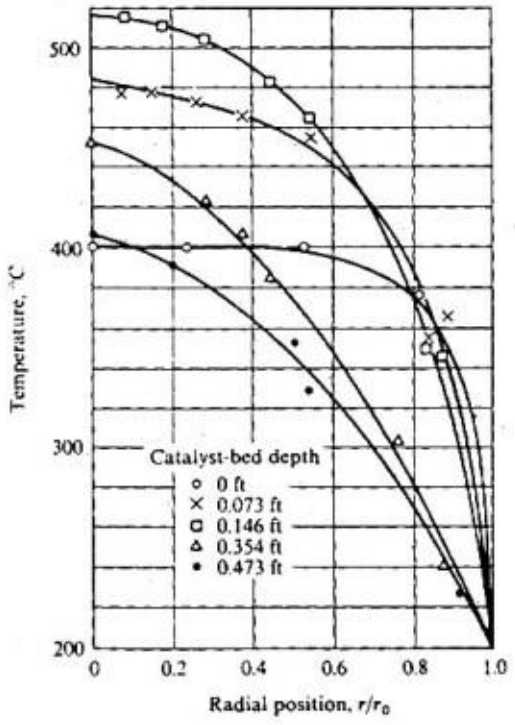

Figure 13-7 Radial temperature profiles in a fixed-bed reactor for the oxidation of SO_2 with air.

thermal conductivity and diffusivity for heat and mass transfer in the radial and axial directions since these qualities appear in the conservation expressions [Eqs. (13-2) and (13-19)]. However, it is worthwhile first to consider the one-dimensional model that eliminates the need for effective conductivities and diffusivities and gives an approximate prediction for the average temperature across the bed.

The parabolic shape of the radial temperature curves in Fig. 13-7 suggests that most of the resistance to heat transfer is near the wall of the reactor and only a small amount is in the central core. To carry this idea farther, if we assume that all the heat-transfer resistance is in a very thin layer next to the wall, the temperature profile will be as shown by the dashed lines in Fig. 13-9. The solid line is the 0.146-ft bed-depth curve of Fig. 13-7. The horizontal, dashed line represents the bulk-mean temperature obtained by integration of the data for the solid line. If the actual situation is replaced by this approximate model, the only information necessary to establish the energy exchange with the surroundings is the heat-transfer coefficient at the wall, h_w. To complete the definition of the one-dimensional model, axial dispersion of mass and energy is also neglected. With these conditions, the design procedure would be the same as for nonadiabatic, homogeneous tubular reactors, as illustrated in Example 5-2. To calculate

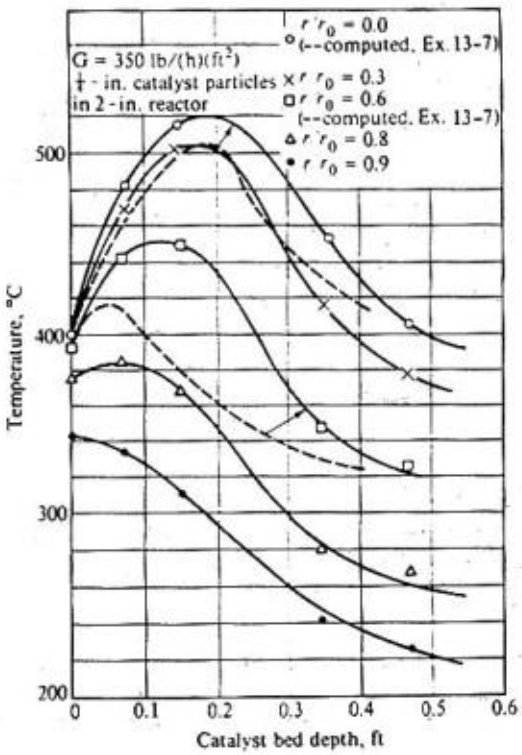

Figure 13-8 Longitudinal temperature profiles in SO_2 reactor.

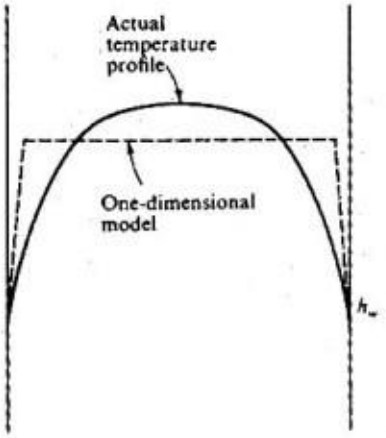

Figure 13-9 Comparison of model (one-dimensional) temperature profile with an actual profile.

the bulk conversion and temperature along the reactor length we need only plug-flow forms of the conservation equations: Eq. (12-2) for mass conservation and Eq. (5-15)† or (5-16) for energy conservation. However, before we apply the one-dimensional model it is necessary to review the available data for h_w.

Wall heat-transfer coefficients If T_b is the bulk mean temperature of the reaction fluid and T_w is the wall temperature, h_w is defined by

$$dQ = h_w(T_b - T_w)\, dA_s \tag{13-24}$$

where Q is the heat-transfer rate to the wall and A_s is the wall area. The presence of the solid particles increases the heat-transfer coefficient in a packed bed several times over that in an empty tube at the same gas flow rate. In the earliest experimental investigations of the subject,‡ the results were reported as ratios of the coefficient in the packed bed to that in the empty pipe. It was found that this ratio varied with the ratio of the pellet diameter to the tube diameter, reaching a maximum value at about $d_p/d = 0.15$. Colburn's results for the ratio of heat-transfer coefficients in packed and empty tubes, h_w h, are:

d_p/d	0.05	0.10	0.15	0.20	0.25	0.30
h_w/h	5.5	7.0	7.8	7.5	7.0	6.6

Presumably the large increase in heat-transfer coefficient for a packed tube over that for an empty tube is due to the mixing, or turbulence, caused by the presence of the solid particles. This turbulence tends to prevent the buildup of a slow-moving layer of fluid next to the wall and also increases the radial transfer of heat

† Note that Eq. (13-21), which was derived as the plug-flow form of Eq. (13-19), is the adiabatic form of Eq. (5-15).

‡ A. P. Colburn, *Ind. Eng. Chem.*, **28**, 910 (1931); *Trans. AIChE*, **26**, 166 (1931); E. Singer and R. H. Wilhelm, *Chem. Eng. Progr.*, **46**, 343 (1950).

within the fluid in the tube. Up to a point, decreasing the particle size increases the importance of these factors, and the heat transfer coefficient continues to increase. However, the maximum at a certain d_p/d ratio suggests that another factor is involved. This is concerned with the size of the radial eddies in the fluid in the bed. As the particle size continues to decrease, the size of the eddies decreases, and the distance over which each mixing process occurs is decreased. Also, there is a larger number of more-or-less stagnant films between the fluid and the solid particles which the heat must cross in reaching the wall. The maximum in the heat-transfer coefficient would represent the point at which this second factor counterbalances favorable effects of the mixing process obtained with the smaller particles.

More recent correlations of wall coefficients are available.† The recommendation of Beek‡ for gases in fixed beds is

$$h_w d_p/k_f = 2.58(\mathrm{Re})^{1/3}(\mathrm{Pr})^{1/3} + 0.094(\mathrm{Re})^{0.8}(\mathrm{Pr})^{0.4} \qquad \text{cylin. particles} \quad (13\text{-}25)$$

$$h_w d_p/k_f = 0.203(\mathrm{Re})^{1/3}(\mathrm{Pr})^{1/3} + 0.220(\mathrm{Re})^{0.8}(\mathrm{Pr})^{0.4} \qquad \text{for spherical particles} \quad (13\text{-}26)$$

where $\mathrm{Re} = d_p u\rho/\mu$ and $\mathrm{Pr} = c_p \mu/k_f$. The molecular thermal conductivity of the fluid is k_f. These correlations apply only to the coefficient at the inside wall of the tube. If the wall temperature is not known, the resistance on the outside of the tube wall must be included in calculating the heat-exchange rate with the surroundings.

Application of one-dimensional model This model requires much less computational time than the two-dimensional procedure. Hence, it is particularly useful for a preliminary design. It provides a rapid procedure for estimating reactor size and the effect of such variables as tube diameter. As the tube diameter decreases, the ratio of the heat-transfer area to the reactor volume will increase. Therefore, the temperature rise of the reaction mixture as it passes through the bed will be less, and the radial temperature variation within the bed will also be less. Hence, where it is necessary not to exceed a certain temperature in the catalyst bed, small-diameter tubes are indicated. The approximate size necessary for a given temperature can be determined by means of this simplified procedure. Problem 13-7 illustrates calculations for a phthalic anhydride reactor. The oxidation of naphthalene has a high heat of reaction, so that the size of the catalyst tubes is a critical point in the design.

Examples 13-4 to 13-6 illustrate the simplified design method for different cases. The first is for the endothermic styrene reaction, where the temperature decreases continually with catalyst-bed depth. Example 13-5 is for an exothermic reaction carried out under conditions where radial temperature gradients are not large. Example 13-6 is also for an exothermic case, but here the gradients are severe, and the simplified solution is not satisfactory.

† G. F. Froment, *Adv. Chem. Ser.*, **109**, Amer. Chem. Society, Washington, D.C. (1972); R. E. Chow, R. A. Caban, and M. M. Irizarry, *Can. Chem. Eng.*, 51, 67 (1973); S. Yagi and D. Kunii, *AIChE J.*, 6, 97 (1960).

‡ J. Beek, *Adv. Chem. Eng.*, 3, 303 (1962). Based on original correlations of T. J. Hanratty, *Chem. Eng. Sci.*, 3, 209 (1954) and of D. Thoenes, Jr., and H. Kramers, *Chem. Eng. Sci.*, 8, 271 (1958).

Example 13-4 Under actual conditions the reactor described in Example 13-3 would not be truly adiabatic. Suppose that with reasonable insulation the heat loss would correspond to a heat-transfer coefficient of $U = 1.6$ Btu (h) (ft^2 inside tube area) (°F). This value is based on the difference in temperature between the reaction mixture and the surroundings at 70°F. Determine revised curves of temperature and conversion vs. catalysed-bed depth for this nonadiabatic operation.

SOLUTION The mass conservation equation (C) and the rate expression (D) of Example 13-3 are applicable, as is their combination, Eq. (E). The expression for conservation of energy for nonadiabatic operation will be Eq. (5-16); that is

$$U(T_s - T)\,dA_h = \Delta H_R F\,dx + F_t c_p\,dT$$

Substituting numerical values,

$$1.6(530 - T)(4\pi\,dz) = (60{,}000)13.5\,dx + 3270\,dT$$

or

$$dT = -248\,dx - 0.00615(T - 530)\,dz \qquad \text{(A)}$$

Equation (E) of Example (13-3) and Eq. (A) determine the conversion and temperature as a function of catalyst bed depth. Equation (E) is of the form $dx/dz = f(x, T)$ and Eq. (A) of the form $dT/dz = f(x, T)$. Hence, the fourth order Runge-Kutta method with two dependent variables (T and x) can be used for the numerical solution. The procedure and the working equations are the same as those for Example 4-7. However, in order to gain an appreciation for the magnitudes of the numbers, let us illustrate for one increment the calculations by the Euler method (also first described in Example 4-7).

In applying the Euler method it is convenient to choose an increment of conversion. It is necessary to assume a temperature at the end of the increment in order to evaluate a reaction rate for use in Eq. (E) of Example 13-3. The assumption can be checked in Eq. (A). If $\Delta x = 0.1$, and T is assumed to be 1591°R, we have from Eq. (E):

at $z = 0$, $x = 0$ and $T = 1616$°R

$$\frac{dz}{dx} = \frac{21}{1{,}270{,}000}\left(e^{19{,}800\,\frac{1616}{}}\right)[(1 - 0) - 0]^{-1} = 3.30$$

at $x = 0.1$, $T = 1591$°R

$$\frac{dz}{dx} = \frac{21 + 0.1}{1{,}270{,}000}\left(e^{19{,}800\,\frac{1591}{}}\right)\left[(1 - 0.1) - \frac{1.2}{0.28}\frac{0.1^2}{21 + 0.1}\right]^{-1}$$

$$= 4.65$$

Then, by the Euler method,

$$\Delta z = \left(\frac{dz}{dx}\right)_{ave}\Delta x = \frac{3.30 + 4.65}{2}(0.1) = 0.40 \text{ ft.}$$

Table 13-2 Conversion of ethylbenzene to styrene in a nonadiabatic reactor

Catalyst-bed depth, ft	Conversion x	Mean bulk temperature °R	Mean bulk temperature °C
0	0	1616	625
0.40†	0.10†	1589†	610†
0.50	0.12	1583	606
0.98†	0.20†	1560†	594†
1.0	0.20	1558	593
2.0	0.31	1525	574
3.0	0.39	1501	561
4.0	0.44	1483	551
5.0	0.47	1468	543
6.0	0.50	1457	536
7.0	0.51	1447	531
8.0	0.531	1438	526
9.0	0.534	1434	524
9.0†	0.55†	1426†	519†

† Calculated by the Euler method with an increment size $\Delta x = 0.1$.

Now, checking the assumed temperature in Eq. (A), we find

$$\Delta T = -248(0.1) = 0.00615\left(\frac{1{,}616 + 1{,}591}{2} - 530\right)(0.40)$$

$$= -24.8 - 2.6 = -27.4°\text{F}$$

$$T_1 = 1{,}616 - 27 = 1589°\text{R}$$

Since this temperature is close to the assumed value, the calculations need not be repeated.

The same kind of calculations can be made for subsequent increments to give T and x for successively larger bed depths. The results marked with a dagger in Table 13-2 were obtained by the Euler method. The other values in the table and in Fig. 13-6 are the more accurate results calculated by the fourth-order Runge-Kutta procedure, using an increment size $\Delta z = 0.5$ ft.

The bed depth for a given conversion is greater than for the adiabatic case, because the temperature is less. For example, for a conversion of 50%, 6.0 ft of catalyst is required, in comparison with 4.95 ft in Example 13-3.

Example 13-5 A bench-scale study of the hydrogenation of nitrobenzene was published by Wilson† in connection with reactor design studies. Nitrobenzene and hydrogen were fed at a rate of 65.9 g mol/h to a 3.0-cm-ID reactor

† K. B. Wilson, *Trans. Inst. Chem. Engrs. (London)*, **24**, 77 (1946).

containing the granular catalyst. A thermocouple sheath, 0.9 cm in diameter, extended down the center of the tube. The void fraction was 0.424 and the pressure atmospheric. The feed entered the reactor at 427.5 K, and the tube was immersed in an oil bath maintained at the same temperature. The heat-transfer coefficient from the mean reaction temperature to the oil bath was determined experimentally to be 8.67 cal/(h)(cm^2)(°C). A large excess of hydrogen was used, so that the specific heat of the reaction mixture may be taken equal to that for hydrogen and the change in total moles as a result of reaction may be neglected. The heat of reaction is approximately constant and equal to $-152{,}100$ cal/g mol.

The entering concentration of nitrobenzene was 5.0×10^{-7} g mol/cm^3. The *global* rate of reaction was represented by the expression†

$$r_p = 5.79 \times 10^4 C^{0.578} e^{-2.958/T}$$

where r_p = g mol nitrobenzene reacting/cm^3(h), expressed in terms of void volume in reactor
C = concentration of nitrobenzene, g mol/cm^3
T = temperature, K

The experimental results for temperature vs. reactor length are shown in Fig. 13-10. From the data given, calculate temperatures up to a reactor length of 25 cm and compare them with the observed results.

† Includes effects of external and intraparticle resistances.

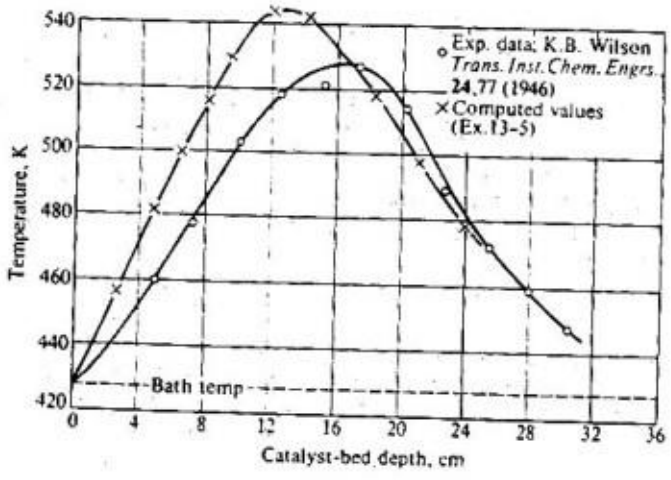

Figure 13-10 Longitudinal temperature profile in a reactor for hydrogenation of nitrobenzene.

SOLUTION The concentration depends on temperature as well as conversion. If Q is the volumetric flow rate at a point in the reactor where the concentration is C, and Q_0 is the value at the entrance, the conversion of nitrobenzene is

$$x = \frac{C_0 Q_0 - CQ}{C_0 Q_0} = 1 - \frac{C}{C_0}\frac{Q}{Q_0}$$

Since there is no change in pressure or number of moles, Q changes only because of temperature changes. Hence, assuming perfect-gas behavior, we have

$$x = 1 - \frac{C}{C_0}\frac{T}{T_0}$$

or

$$C = (1 - x)\frac{C_0 T_0}{T} = (5 \times 10^{-7})\frac{427.5}{T}(1 - x) \tag{A}$$

Substituting this expression into the rate equation gives the global rate in terms of the temperature and conversion,

$$\mathbf{r}_p = 439\left(\frac{1 - x}{T}\right)^{0.578} e^{-2.958/T} \tag{B}$$

The mass-conservation expression, Eq. 12-2, should be written in terms of the void volume because of the form in which the rate data are reported. Thus

$$F\,dx = \mathbf{r}_p(0.424)\,dV$$

The feed rate of nitrobenzene is

$$F = 65.9(22{,}400)\left(\frac{427.5}{273}\right)(5.0 \times 10^{-7}) = 1.15 \text{ g mol/h}$$

Hence,

$$1.15\,dx = \mathbf{r}_p(0.424)\frac{\pi}{4}(9 - 0.81)\,dz$$

or

$$\frac{dx}{dz} = \frac{\mathbf{r}_p}{0.423} = 1040\left(\frac{1 - x}{T}\right)^{0.578} e^{-2458/T} \tag{C}$$

The energy-conservation expression is Eq. 5-15. In numerical terms,

$$-(-152{,}100)F\,dx - 8.67\pi(3)(T - 427.5)\,dz = 65.9(6.9\,dT)$$

where 6.9 cal/(g mol)(K) is the molal heat capacity of hydrogen at 427.5 K. This equation may be simplified to

$$\frac{dT}{dz} = 385\left(\frac{dx}{dz}\right) - 0.180(T - 427.5) \tag{D}$$

If Eq. (C) is employed to eliminate dx/dz, Eq. (D) becomes

$$\frac{dT}{dz} = 4.0 \times 10^5 \left(\frac{1-x}{T}\right)^{-0.578} e^{-2958/T} - 0.180(T - 427.5) \qquad \text{(E)}$$

Equations (C) and (E) are of the form $dx/dz = f(x, T)$ and $dT/dz = f(x, T)$. Hence, they can be solved by the fourth-order Runge-Kutta method to give T and x as a function of z. The method of solution and equations are the same as those given for the similar, two-dependent variable problem of Example 4-7. The calculated results, using an increment $\Delta z = 0.5$ cm, are shown in Table 13-3 and Fig. 13-10.

As the bed depth increases the heat-loss term in Eq. (E) increases because T increases. At low conversions the heat-of-reaction term also increases. However, the decrease in reactant concentration (proportional to $1 - x$) ultimately slows the increase in the first term. The trend continues until the heat transferred to the oil bath is as large as that evolved as a result of reaction. The temperature reaches a maximum at this point, the so-called "hot spot." Figure 13-10 shows that the computed hot spot is reached at about 13 cm from the entrance to the reactor. This location is 4 cm before the experimental hot spot. Also, the experimental temperature is 20°C less than the computed value at the maximum. Three points should be mentioned in making this comparison. First, the measured temperature corresponds to the center of the tube, while the computed results are for a bulk mean temperature. Second, the thermocouples were contained in a metal sheath entering down the center of the reactor. The sheath would reduce the observed temperatures, because of longitudinal conduction, and make them more nearly comparable with the bulk mean computed values. Third, using a specific heat of hydrogen for the

Table 13-3 Temperatures and conversions in a nitrobenzene hydrogenation reactor

Catalyst bed depth cm	Conversion x	Bulk temperature °C
0	0	427.5
0.5	0.016	433
1.0	0.033	439
2.0	0.072	451
3.0	0.116	463
5.0	0.220	486
7.0	0.344	508
9.0	0.481	528
11.0	0.620	543
12.0	0.685	546
13.0	0.744	548
14.0	0.796	546
15.0	0.840	542
17.0	0.906	529
19.0	0.948	511
21.0	0.972	494

whole reaction mixture results in a value that is too low, causing the calculated temperatures to be high.

The agreement shown in Fig. 13-10 is good, in view of these three points and since the one-dimensional model neglects radial temperature gradients. The fact that a heat-transfer coefficient was determined experimentally in the same apparatus probably improved the agreement.

The simplified approach to the design of nonadiabatic reactors led to good results in Example 13-5 partly, at least, because radial temperature variations were not large. This is because the wall temperature was the same as the temperature of the entering reactants. At the hot spot the maximum temperature difference between the center and the wall was about 120°C. In Example 13-6 much larger radial temperature gradients exist, and the simplified method is not as suitable.

Example 13-6 Using the one-dimensional method, compute curves for temperature and conversion vs. catalyst-bed depth for comparison with the *experimental* data shown in Figs. 13-8 and 13-12 for the oxidation of sulfur dioxide. The reactor consisted of a cylindrical tube, 2.06 in. ID. The superficial gas mass velocity was 350 lb (h)(ft^2), and its inlet composition was 6.5 mol % SO_2 and 93.5 mol % dry air. The catalyst was prepared from $\frac{1}{8}$-in. cylindrical pellets of alumina and contained a surface coating of platinum (0.2 wt % of the pellet). The measured global rates in this case were not fitted to a kinetic equation, but are shown as a function of temperature and conversion in Table 13-4 and Fig. 13-11. Since a fixed inlet gas composition was used, independent variations of the partial pressures of oxygen, sulfur dioxide, and sulfur trioxide were not possible. Instead these pressures are all related to one variable, the extent of conversion. Hence the rate data shown in Table 13-4 as a function of conversion are sufficient for the calculations. The total pressure was essen-

Table 13-4 Experimental global rates [g mol/(h)(g catalyst)] of oxidation of SO_2 with a 0.2 % Pt-on-Al_2O_3 catalyst

	% conversion† of SO_2						
t, °C	0	10	20	30	40	50	60
350	0.011	0.0080	0.0049	0.0031			
360	0.0175	0.0121	0.00788	0.00471	0.00276	0.00181	
380	0.0325	0.0214	0.01433	0.00942	0.00607	0.00410	
400	0.0570	0.0355	0.0239	0.01631	0.0110	0.00749	0.00488
420	0.0830	0.0518	0.0344	0.02368	0.0163	0.0110	0.00745
440	0.1080	0.0752	0.0514	0.03516	0.0236	0.0159	0.0102
460	0.146	0.1000	0.0674	0.04667	0.0319	0.0215	0.0138
480	.....	0.1278	0.0898	0.0642	0.0440	0.0279	0.0189
500	.....	0.167	0.122	0.0895	0.0632	0.0394	0.0263

† Conversion refers to a constant feed composition of 6.5 mole% SO_2 and 93.5 mole% air.

Source: R. W. Olson, R. W. Schuler, and J. M. Smith, *Chem. Eng. Progr.*, **46**, 614 (1950).

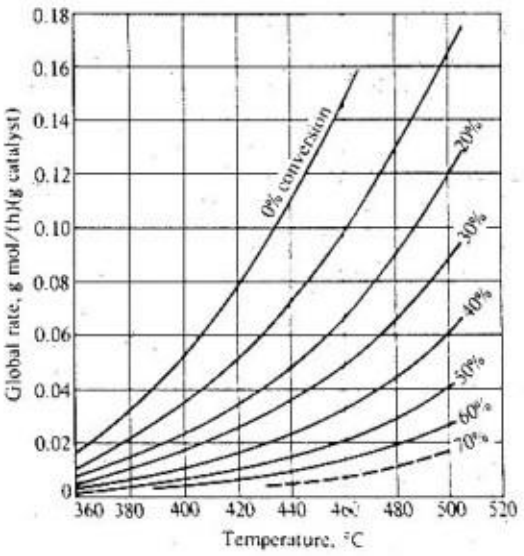

Figure 13-11 Rate of oxidation of SO_2 on $\frac{1}{4}$-in. catalyst particles containing 0.2% platinum [mass velocity 350 lb/(h)(ft^2)].

tially constant at 790 mmHg. The heat of reaction is nearly constant over a considerable temperature range and was equal to $-22{,}700$ cal/g mol of sulfur dioxide reacted. The gas mixture was predominantly air, so that its specific heat may be taken equal to that of air. The bulk density of the catalyst as packed in the reactor was 64 lb ft^3.

From Fig. 13-7 it is apparent that the entering temperature across the diameter is not constant, but varies from a maximum value of about 400°C at the center down to 197°C at the wall. Since the one-dimensional method of solution to be used in this example is based on a uniform temperature radially, we use a mean value of 364°C. In the two-dimensional model, considered in Example 13-7, the actual entering-temperature profile can be taken into account.

For the heat-transfer coefficient from gas to tube wall take $h_w = 6.3$ Btu/(h)(ft)^2(°F). The tube wall temperature is 197°C.

SOLUTION The energy conservation equation for an element of reactor height dz is, according to Eq. (5-16)

$$-(-22{,}700)F(1.8)\,dx + 6.3\pi\frac{2.06}{12}(197 - T)1.8\,dz = F_t c_p\,dT(1.8) \quad \text{(A)}$$

In this expression the conversion factor of 1.8°F/°C has been introduced so that the temperature may be expressed in degrees centigrade

$$F = 350\pi\left(\frac{1.03}{12}\right)^2\frac{1}{31.2}(0.065) = 0.017 \text{ lb mol/h}$$

The number 31.2 is the molecular weight of the feed containing 6.5 mol% SO_2. The heat capacity of the reaction mixture, assumed to be that of air at an average temperature of 350°C, is 0.26 Btu/(lb)(°F). Hence

$$F_t c_p = 350\pi\left(\frac{1.03}{12}\right)^2(0.26) = 2.11 \text{ Btu/°F}$$

Substituting these values in Eq. (A), we find

$$0.017(22{,}700)\,dx - 3.40(T - 197)\,dz = 2.11\,dT$$

or

$$\frac{dT}{dz} = 182\frac{dx}{dz} - 1.61(T - 197) \tag{B}$$

The mass-conservation expression [Eq. (12-2)] may be written

$$\pi\left(\frac{1.03}{12}\right)^2 \mathbf{r}_p \rho_B\,dz = F\,dx = 0.017\,dx$$

The bulk density of the catalyst as packed is given as 64 lb/ft^3. Hence Eq. (B) simplifies to the form

$$\frac{dx}{dz} = \frac{\mathbf{r}_p}{0.0112} \tag{C}$$

In contrast to the previous examples, the rate of reaction is not expressed in equation form, but as a tabulation of experimental rates as a function of x and T. A simple first- or second-order expression would not correlate the data for this reaction. Instead, a Langmuir type of equation, based on adsorption of oxygen on the catalyst, was necessary. This equation was developed and tested in Example 9-2. The tabulation of rates is more convenient to use in this problem than the rate equation. The units of $\mathbf{r}_P$ in Eq. (C) should be lb mol reacted/(h)(lb catalyst), but numbers in these units are numerically equivalent to g mol/(h)(g catalyst), so that the data in Table 13-4 can be used directly.

The method of solution is the same as in Example 13-5.

Table 13-5 Conversion and temperature in an SO_2 reactor calculated by the one-dimensional model

Conversion	t, °C	Catalyst-bed depth, ft
0	364	0
0.05	365	0.029
0.10	365	0.065
0.15	362	0.112
0.18	357	0.149
0.21	351	0.020
0.24	(300)	(0.5)

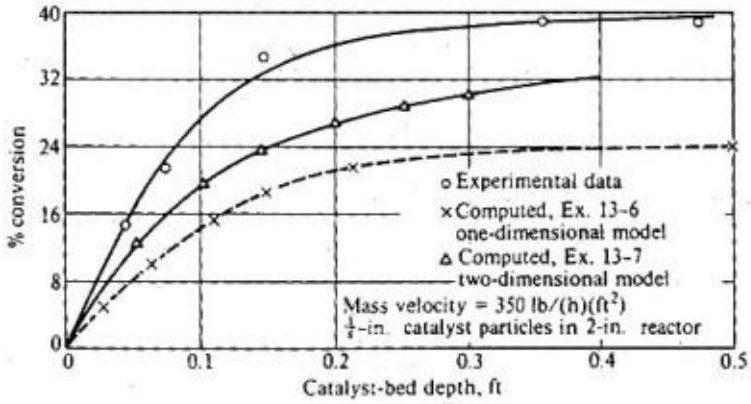

Figure 13-12 Comparison of calculated and experimental conversion values in an SO_2 reactor.

Equation (C) with $\mathbf{r}_p$ data from Table 13-4 is an expression of the form $dx/dz = f(x, T)$. Likewise, Eq. (B) is of the form $dT/dz = f(x, T)$. Hence, the numerical solution can again be carried out by the Runge-Kutta method. There are two dependent variables so that the method and equations for the calculations are the same as those used for Example 4-7. The calculations are started at the feed, $z = 0$, $x = 0$, $t = 364°C$. Increments, Δz, of catalyst bed depth are chosen and x and T at the end of each increment obtained from Eqs. (C) and (B).

The results obtained with $\Delta z = 0.001$ ft are summarized in Table 13-5 and shown in Fig. 13-12. It is apparent that the mean computed temperature never rises appreciably above the entering value of 364°C. Indeed, when a bed depth of about 0.2 ft is reached, the temperature is so low that the rate is no longer high enough to give a significant increase in conversion.

In the experimental reactor used by Schuler et al.† the low wall temperature results in severe radial temperature gradients. Hence the mean bulk temperature may be low, but the temperatures near the center of the bed may be high enough to cause a significant amount of reaction. This is a major factor in the large difference between the experimental conversion curve and the results computed in this example, both shown in Fig. 13-12. A critical quantity in the simplified design method applied to this problem is the wall heat-transfer coefficient. Small changes in h_w can cause large differences in the conversion. In the next section this example is repeated, this time with radial temperature and concentration gradients taken into account.

The one-dimensional model is particularly useful for investigating complex reactor systems. For example, Lucas and Gelbin‡ have used the approach to design multistage reactors for ammonia synthesis. Design calculations which

† R. W. Schuler, V. P. Stallings, and J. M. Smith, *Chem. Eng. Progr., Symp. Ser.* 4, **48**, 19 (1952).
‡ K. Lucas and D. Gelbin, *Brit. Chem. Eng.*, 7, 336 (1962).

included radial gradients would be time consuming, even with large digital computers. With the one-dimensional method, approximate results and the effects of changes in operating conditions can be evaluated for a series of reactors with a modest amount of computer time.

13-6 The Two-Dimensional Model

In this section the design procedure is made more accurate by taking into account radial variations in temperature and concentrations. A thorough treatment would consider the radial distribution of velocity, would account for radial concentration and temperature gradients by using Peclet numbers which themselves varied with radial position, and would allow for axial dispersion of mass and energy. Such sets of elliptical partial differential equations are difficult to solve numerically since they constitute boundary-value problems. Further, transport data adequate to allow for radial variation in velocity and the Peclet numbers are not available. Also, the boundary conditions at the entrance to the bed are complex when the temperature varies radially. Young and Finlayson† have presented the solution to this problem for the case of uniform velocity and Peclet numbers in the radial direction. For these conditions the conservation expressions are Eqs. (13-2) and (13-19). Their results indicated that, for nonisothermal nonadiabatic conditions, axial dispersion could be important even for long catalyst beds. The numerical methods required for solution of Eqs. (13-2) and (13-19) are rather involved and will not be discussed here, except to note that the orthogonal-collocation technique‡ has proven to be an efficient solution method.

To illustrate the two-dimensional model we will neglect axial dispersion of mass and energy. This means omitting the terms involving $\partial^2/\partial z^2$ in Eqs. (13-2) and (13-19). If Eq. (13-2) is expressed in terms of conversion, the two conservation expressions become (G = mass velocity)

$$\frac{\partial x}{\partial z} - \frac{d_p}{\mathrm{Pe}_r}\left(\frac{1}{r}\frac{\partial x}{\partial r} + \frac{\partial^2 x}{\partial r^2}\right) - \frac{\mathbf{r}_p \rho_B}{(G/\bar{M})y_0} = 0 \tag{13-27}$$

and

$$-Gc_p\frac{\partial T}{\partial z} + (k_e)_r\left(\frac{1}{r}\frac{\partial T}{\partial r} + \frac{\partial T}{\partial r^2}\right) - \mathbf{r}_p \rho_B \,\Delta H = 0 \tag{13-28}$$

where $(G/\bar{M})y_0 = u_0 C_0$ = molal feed rate of reactant per unit area of reactor
$\bar{M}$ = average molecular weight of the feed stream
y_0 = reactant mole fraction in the feed

The objective is to solve Eqs. (13-27) and (13-28) for the temperature and *conversion at any point in the bed. The solution of these parabolic equations is an initial value problem where the only boundary conditions (in the axial direction)* needed are at the entrance of the bed. Thus, we must know the feed temperature

† L. C. Young and B. A. Finlayson, *Ind. Eng. Chem.*, **12**, 412 (1973).

‡ B. A. Finlayson, *Chem. Eng. Sci.*, **26**, 1081 (1971); J. V. Villadsen and W. E. Stewart, *Chem. Eng. Sci.*, **22**, 1483 (1967).

and conversion profiles across the diameter of the reactor. Further boundary conditions applicable at any axial location are that the conversion is flat ($\partial x/\partial r = 0$) at both the centerline and at the wall of the tube. The temperature gradient at the centerline is zero, but the condition at the wall is determined by the heat-transfer characteristics. In the illustration that follows, the wall temperature is maintained constant by a boiling liquid (ethylene glycol) in a jacket surrounding the reactor. In other cases the wall temperature may vary with z. For example, if the fluid in the jacket or surroundings is at T_s and the heat-transfer coefficient between the inside wall surface and the surroundings is U, the proper boundary condition is

$$U(T_w - T_s) = -k_e\left(\frac{\partial T}{\partial r}\right)_w \tag{13-29}$$

where $(\partial T/\partial r)_w$ is the temperature gradient in the reactor at the wall.

The transport information needed, in addition to that for the one-dimensional model, are the radial values for D_e (or Pe) and k_e. Radial diffusivities have been presented in Sec. 13-3 (Fig. 13-5). Next, available information on effective thermal conductivities is summarized.

Effective thermal conductivities In a bed of solid particles through which fluid flows, heat can be transferred in the radial direction by several mechanisms: through the particles by conduction, through the fluid by conduction and convection, and by radiation. In writing Eqs. (13-19) and (13-28), all this heat transfer has been assumed to occur by conduction according to an *effective* thermal conductivity $(k_e)_r$. This is equivalent to supposing that the bed is replaced by a solid of thermal conductivity $(k_e)_r$. In view of the several mechanisms that are involved, $(k_e)_r$ is a property of the bed. Its value depends on a large number of variables, such as fluid flow rate, particle diameter, porosity, molecular thermal conductivity of the fluid and of the solid phases, and temperature level. Therefore, the most logical method of correlating data is to divide $(k_e)_r$ into separate contributions, each of which corresponds to a mechanism of heat transfer. Many correlations† have been developed on this basis and may be used to estimate $(k_e)_r$. For gaseous reaction mixtures the numerical range for $(k_e)_r$ is about 0.1 to 0.3 Btu/(h)(ft)(°R) [or 0.17 to 0.52 J/(m)(s)(K)] at temperatures of less than 500°F. At higher temperatures, radiation from particle to particle can lead to higher values.

Application of two-dimensional model A number of numerical methods are available‡ for solving Eqs. (13-27) and (13-28) with the appropriate boundary conditions. For simplicity, we will describe an unsophisticated, explicit method

† E. Singer and R. H. Wilhelm, *Chem. Eng. Prog.*, **46**, 343 (1950); W. B. Argo and J. M. Smith, *Chem. Eng. Prog.*, **49**, 443 (1953); John Beek, Design of Packed Catalytic Reactors, in "Advances in Chemical Engineering," vol. 3, p. 229, Academic Press, Inc., New York, 1962; S. Yagi and N. Wakao, *AIChE J.*, **5**, 71 (1960); A. P. deWasch and G. F. Froment, *Chem. Eng. Sci.*, **27**, 567 (1972).

‡ See Leon Lapidus, "Digital Computation for Chemical Engineers," McGraw-Hill Book Company, New York, 1960, and V. Hlavacek and J. Votruba, chap. 6, pp. 355-359, "Chemical Reactor Theory," ed. by Leon Lapidus and N. R. Amundson, Prentice-Hall, Englewood Cliffs, N.J., 1977.

based on writing the differential equations in difference form. The solution is carried out by starting at the reactor entrance and proceeding stepwise, first radially and then axially, to the desired catalyst bed depth.

Let n and L represent the number of increments in the radial and axial directions, respectively, and Δr and Δz their magnitude, so that

$$r = n\,\Delta r \tag{13-30}$$

$$z = L\,\Delta z \tag{13-31}$$

The temperature at any point in the bed can be represented by $T_{n,L}$, that is, the temperature at $r = n\,\Delta r$ and $z = L\,\Delta z$. Note that r is measured from the center of the bed and z from the feed entrance.

The first forward difference in temperature in the r direction can be written

$$\Delta_r T = T_{n+1,L} - T_{n,L} \tag{13-32}$$

Similarly, the first forward difference in the z direction may be written

$$\Delta_z T = T_{n,L+1} - T_{n,L} \tag{13-33}$$

The second central difference in the r direction is

$$\Delta_r^2 T = (T_{n+1,L} - T_{n,L}) - (T_{n,L} - T_{n-1,L}) \tag{13-34}$$

With these definitions, the difference form of Eq. (13-28) is

$$T_{n,L+1} = T_{n,L} + \frac{\Delta z}{(\Delta r)^2}\frac{(k_e)_r}{Gc_p} \times \left[\frac{1}{n}(T_{n+1,L} - T_{n,L}) + T_{n+1,L} - 2T_{n,L} + T_{n-1,L}\right] - \frac{\Delta H \bar{r}_p \rho_B\,\Delta z}{Gc_p} \tag{13-35}$$

Similarly, Eq. (13-27) may be written in difference form as

$$x_{n,L+1} = x_{n,L} + \frac{\Delta z}{(\Delta r)^2}\frac{d_p}{\mathrm{Pe}_r} \times \left[\frac{1}{n}(x_{n+1,L} - x_{n,L}) + x_{n+1,L} - 2x_{n,L} + x_{n-1,L}\right] + \frac{\bar{\mathbf{r}}_p \rho_B \bar{M}\,\Delta z}{Gy_0} \tag{13-36}$$

Provided the magnitude of the reaction terms involving $\mathbf{r}_p$ can be estimated, Eqs. (13-35) and (13-36) can be solved step by step to obtain the conversion. The first step is to compute values of T and x across the diameter, at $z = 1\,\Delta z$, or $L = 1$, from known values at $L = 0$. Then continue to the next longitudinal increment, $L = 2$, etc. The indeterminate form of the equations at $n = 0$ can be avoided by using the special expressions

$$T_{0,L+1} = T_{0,L} + \frac{2\,\Delta z}{(\Delta r)^2}\frac{(k_e)_r}{c_p G}(2T_{1,L} - 2T_{0,L}) - \frac{\Delta H \bar{r}_p \rho_B\,\Delta z}{Gc_p} \tag{13-37}$$

$$x_{0,L+1} = x_{0,L} + \frac{2\,\Delta z}{(\Delta r)^2}\frac{d_p}{\mathrm{Pe}_r}(2x_{1,L} - 2x_{0,L}) + \frac{\bar{\mathbf{r}}_p \rho_B \bar{M}\,\Delta z}{Gy_0} \tag{13-38}$$

derived from L'Hôpital's rule.

The effect of the reaction terms in Eqs. (13-35) and (13-36) is, for an exothermic reaction, to increase both the temperature and the conversion. Since the rate depends on the temperature and composition, and the average value for the increment L to $L+1$ is not known until Eqs. (13-35) and (13-36) are solved, a trial-and-error procedure is indicated. The calculations are illustrated in Example 13-7, where the SO_2 reactor problem of Example 13-6 is recomputed with radial variations taken into account. In this example experimental data for the global rate are available. These data were obtained for the same size of catalyst pellets and for the same gas velocity as for the integral reactor. Hence external and internal transport effects on the global rate were the same for the laboratory conditions in which $\mathbf{r}_p$ was measured as for the integral reactor to be designed. In this way the calculations discussed in Chap. 12 for evaluating a global rate to fit the transport situation in the large-scale reactor were avoided. In most cases global rates have to be evaluated from intrinsic rates, effectiveness factors, and external transport coefficients.

Example 13-7 Recompute the conversion-vs.-bed-depth curve for the SO_2 reactor of Example 13-6 by the two-dimensional method, with the assumption that $(k_e)_r$, $(D_e)_r$, and G are constant. The temperature profile at the entrance to the reactor is given in the following table and also plotted in Fig. 13-13:

Feed temperature, °C	400.1	399.5	400.1	400.4	376.5	376.1	197.0
Radial position	0.023	0.233	0.474	0.534	0.797	0.819	1.000

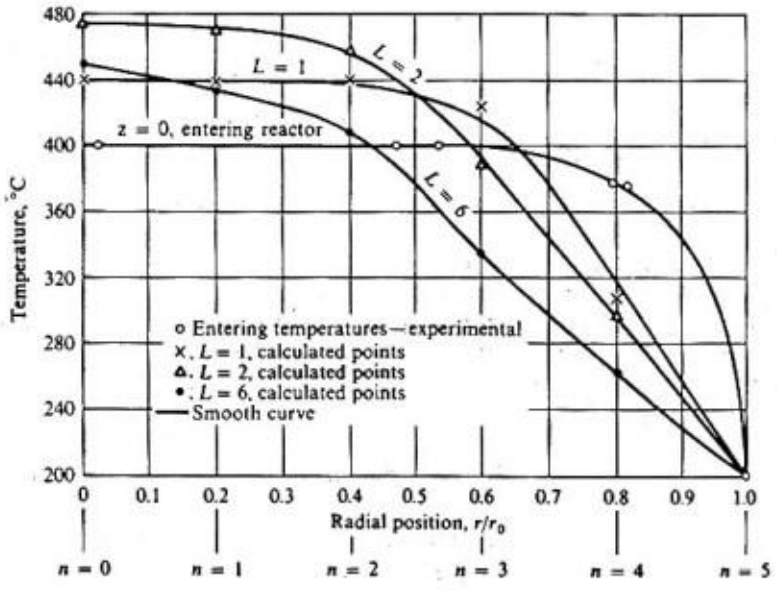

Figure 13-13 Calculated temperatures in an SO_2 reactor.

The reactants composition across the diameter may be assumed to be uniform.

SOLUTION The effective thermal conductivity calculated from the Argo† correlation is 0.216 Btu (h)(ft)(°F). The Peclet number from Fig. 13-5 is 9.6 for the conditions of this example. The quantities needed in Eqs. (13-35) and (13-36) are

$$\frac{k_e}{c_p G} = \frac{0.216}{0.26(350)} = 0.00238 \text{ ft}$$

$$\frac{d_p}{\text{Pe}_r} = \frac{1/8}{12(9.6)} = 0.00109 \text{ ft}$$

Temperature and conversion equations It is convenient to divide the radius of the bed into five increments, so that

$$\Delta r = 0.2 r_0 = 0.2\left(\frac{1.03}{12}\right) = 0.0172 \text{ ft}$$

If Δz is chosen to be 0.05 ft,

$$\frac{\Delta z}{(\Delta r)^2} = \frac{0.05}{0.0172^2} = 170 \text{ ft}^{-1}$$

Then the coefficients in Eqs. (13-35) and (13-36) are

$$\frac{k_e}{c_p G}\frac{\Delta z}{(\Delta r)^2} = 0.00238(170) = 0.404 \qquad \text{dimensionless}$$

$$\frac{d_p}{\text{Pe}_r}\frac{\Delta z}{(\Delta r)^2} = 0.00109(170) = 0.185 \qquad \text{dimensionless}$$

$$\frac{\Delta H t_p \rho_B \Delta z}{G c_p} = \frac{-22{,}700(64)(0.05)\bar{r}_p}{350(0.26)} = -798\bar{r}_p \qquad °\text{C}$$

$$\frac{t_p \rho_B \bar{M} \Delta z}{G y_0} = \frac{64(31.2)(0.05)\bar{r}_p}{350(0.065)} = 4.38\bar{r}_p \qquad \text{dimensionless}$$

Substituting these values in Eqs. (13-35) and (13-36) gives working expressions for calculating the temperature and conversion at a bed depth $L + 1$, from data at the previous bed depth L. Thus

$$T_{n,L+1} = T_{n,L} + 0.404 \times \left[\frac{1}{n}(T_{n+1,L} - T_{n,L}) + T_{n+1,L} - 2T_{n,L} + T_{n-1,L}\right] + 798\bar{r}_p \quad \text{(A)}$$

† W. B. Argo and J. M. Smith, *Chem. Eng. Progr.* **49**, 443 (1953).

$$x_{n,L+1} = x_{n,L} + 0.185 \times \left[\frac{1}{n}(x_{n+1,L} - x_{n,L}) + x_{n+1,L} - 2x_{n,L} + x_{n-1,L}\right] + 4.38\bar{\mathbf{r}}_P \quad \text{(B)}$$

Calculations for the first bed-depth increment ($L = 1$) The entering-temperature distribution is known (see Fig. 13-13), and the entering conversion will be zero at all radial positions. Starting at $n = 1$, the temperatures $T_{0,0}$, $T_{1,0}$, and $T_{2,0}$, as read from Fig. 13-13, are all 400°C. Substituting these values into Eq. (A) gives $T_{1,1}$ in terms of the average rate $\bar{\mathbf{r}}_P$ over the increment of bed depth from 0 to $L = 1$ ($z = 0.05$ ft):

$$T_{1,1} = T_{1,0} + 0.404\left[\frac{1}{1}(T_{2,0} - T_{1,0}) + T_{2,0} - 2T_{1,0} + T_{0,0}\right] + 798\bar{\mathbf{r}}_P$$
$$= 400 + 0.404(0) + 798\bar{\mathbf{r}}_P = 400 + 798\bar{\mathbf{r}}_P \quad \text{(C)}$$

Since $x_{0,0}$, $x_{1,0}$, and $x_{2,0}$ are all 0, Eq. (B) gives, for the conversion at $n = 1$ and $L = 1$,

$$x_{1,1} = 0 + 0.185(0) + 4.38\bar{\mathbf{r}}_P = 4.38\bar{\mathbf{r}}_P \quad \text{(D)}$$

Equations (C) and (D) and the rate data, Table 13-4 or Fig. 13-11, constitute three relationships of the unknown quantities $T_{1,1}$, $x_{1,1}$, and $\bar{\mathbf{r}}_P$. One method of solution is the following four-step process:

1. Assume a value of $\bar{\mathbf{r}}_P$, after obtaining $\mathbf{r}_{1,0}$ from Fig. 13-11.
2. Compute $T_{1,1}$ and $x_{1,1}$ from Eqs. (C) and (D).
3. Evaluate the rate $\mathbf{r}_{1,1}$ at the end of the increment from Fig. 13-11.
4. Average $\mathbf{r}_{1,1}$ and $\mathbf{r}_{1,0}$, and compare the result with the assumed $\bar{\mathbf{r}}_P$. If agreement is not obtained, repeat the sequence with a revised value of $\bar{\mathbf{r}}_P$.

Let us carry out these steps. At 400°C and zero conversion we have

$$\mathbf{r}_{1,0} = 0.055$$

We assume $\bar{\mathbf{r}}_P = 0.051$. Then from Eq. (C) and Eq. (D),

$$T_{1,1} = 400 + 798(0.051) = 441°\text{C}$$
$$x_{1,1} = 4.38(0.051) = 0.223$$

From Fig. 13-11 at 441°C and 22.3% conversion, $\mathbf{r}_{1,1} = 0.046$. Hence

$$\bar{\mathbf{r}}_P = \frac{0.055 + 0.046}{2} = 0.0505$$

This result is close to the assumed value of 0.051, so the calculated temperature and conversion at $n = 1$ and $L = 1$ may be taken as 441°C and 22.3%.

The same result would apply at $n = 0$ and 2, because the entering temperature is 400°C up to a radial position of $n = 3(r/r_0 = 0.6)$, as noted in

Fig. 13-13. At $n = 3$ the situation changes because $T_{4,0} = 376°C$. Let us make the stepwise calculations at this radial position. Starting with

$$r_{3,0} = 0.055$$

we assume $\bar{r}_P = 0.046$. Then, from Eq. (A),

$$T_{3,1} = 400 + 0.404[\tfrac{1}{3}(376 - 400) + 376 - 2(400) + 400] + 798(0.046)$$
$$= 400 - 13 + 37 = 424°C$$

$$x_{3,1} = 0 + 4.38(0.046) = 0.201$$

From Fig. 13-11 at 424°C and 20.1% conversion, $r_{3,1} = 0.037$, and so

$$\bar{r}_P = \frac{0.055 + 0.037}{2} = 0.046$$

Continuing the calculations at $n = 4(r/r_0 = 0.8)$, where $T_{4,0} = 376°$ and $x_{4,0} = 0$, we have

$$r_{4,0} = 0.029$$

and we assume $\bar{r}_P = 0.015$. Then

$$T_{4,1} = 376 + 0.404[\tfrac{1}{4}(197 - 376) + 197 - 2(376) + 400] + 798(0.015)$$
$$= 376 - 83 + 12 = 305°C$$

$$x_{1,1} = 0 + 4.38(0.015) = 0.066$$

From Fig. 13-11 at 305°C and $x = 0.066$ it is evident that the rate is close to zero; thus

$$\bar{r}_P = \frac{0.029 + 0}{2} = 0.015$$

which agrees with the assumed value. Hence at $n = 4$ and $L = 1$ the calculated temperature will be 305°C and the conversion 6.6%.

Since at $n = 5$ the wall is reached, the temperature remains 197°C. The rate is zero at this temperature, and so there will be no conversion due to reaction. Hence $T_{5,1} = 197°C$, and $x_{5,1} = 0$. At higher bed depths the conversion at the wall will not be zero, not because of reaction, but because of diffusion of the product SO_3 from the center of the tube.

The computations have now been made across the radius of the reactor at $L = 1(z = 0.05$ ft). The temperature results are indicated by the six points marked × in Fig. 13-13. The results computed by this stepwise procedure do not form a smooth curve at low bed depths. It is desirable before proceeding in the next increment to draw a smooth curve for this bed depth, as indicated in Fig. 13-13. The computed values and corresponding smooth conversion curve are shown in Fig. 13-14. The temperatures and conversions read from the smoothed curves, and to be used in the calculations at $L = 2$, are given in Table 13-6.

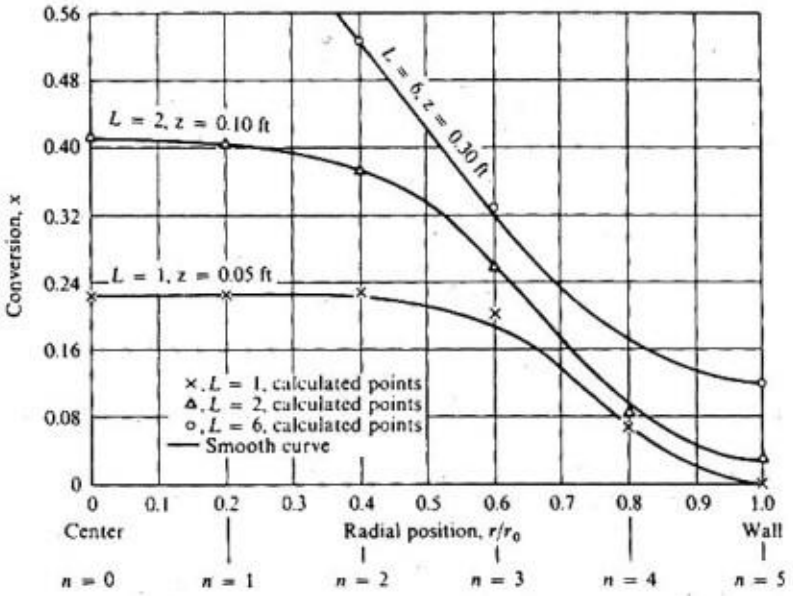

Figure 13-14 Calculated conversions in an SO_2 reactor.

Table 13-6 Temperatures and conversions for SO_2 oxidation by the two-dimensional model

Bed depth, ft	Radial position					
	0(center)	0.2	0.4	0.6	0.8	1.0 (wall)
	Temperature, °C					
$L = 0, z = 0$	400	400	400	400	376	197
$L = 1, z = 0.05$	441	441	437	418	315	197
$L = 2, z = 0.10$	475	471	458	390	298	197
$L = 3, z = 0.15$	496	488	443	378	285	197
$L = 4, z = 0.20$	504	476	437	360	278	197
$L = 5, z = 0.25$	470	466	415	350	269	197
$L = 6, z = 0.30$	451	435	412	334	265	197
	Conversion					
$L = 0, z = 0$	0	0	0	0	0	0
$L = 1, z = 0.05$	0.223	0.223	0.216	0.186	0.066	0
$L = 2, z = 0.10$	0.411	0.402	0.380	0.258	0.090	0.027
$L = 3, z = 0.15$	0.557	0.540	0.464	0.293	0.110	0.053
$L = 4, z = 0.20$	0.658	0.607	0.510	0.311	0.130	0.072
$L = 5, z = 0.25$	0.686	0.638	0.527	0.318	0.150	0.096
$L = 6, z = 0.30$	0.684	0.650	0.525	0.337	0.173	0.122

Results for successive increments ($L = 2$ to 6) By similar calculations temperature and conversion profiles may be obtained for successive bed lengths. The results at $L = 2$ are also plotted in Figs. 13-13 and 13-14. The computed values fall more nearly on a smooth curve than those at $L = 1$. The quantities at $L = 2$ shown in Table 13-6 were read from the smooth curves. These, rather than the computed points, are used in the calculations for the next bed depth. At high bed depths the tabulated values are those directly computed from the equations. A conversion of 68% is reached at the center when $z = 0.30$ ft, and 12% is obtained at the wall. The temperature reaches a maximum value of 504°C at $z = 0.20$ ft and then decreases at higher bed depths because the radial transfer of heat toward the wall exceeds the heat evolved due to reaction. The temperature and conversion profiles at $z = 0.30$ are also plotted in Figs. 13-13 and 13-14.

Mean conversion and temperature The bulk mean conversions and temperatures at any bed depth are obtained by graphical integration of the radial temperature and conversion profiles. The bulk mean temperature is the value resulting when the stream through the reactor is completely mixed in the radial direction. Hence the product of the heat capacity and the temperature at each radial position should be averaged. For an element dr the heat capacity of the flowing stream will be $G(2\pi r\, dr)c_p$. Thus the bulk mean temperature is given by the equation

$$\bar{T}_b = \frac{\int_0^{r_0} G(2\pi r\, dr)c_p T}{\pi G r_0^2 \bar{c}_p} = \frac{2\int_0^{r_0} Tc_p r\, dr}{r_0^2 \bar{c}_p}$$

If the variable $n = r/r_0$ is substituted for r, this expression becomes

$$\bar{T}_b = \frac{2}{\bar{c}_p}\int_0^1 Tc_p n\, dn \qquad \text{(E)}$$

In Eq. (E) c_p is the specific heat at the temperature T and $\bar{c}_p$ is for the bulk mean temperature $\bar{T}_b$. Equation (E) can be integrated by plotting the product $Tc_p n$ vs. n and evaluating the area under the curve.

Similarly, the bulk mean conversion $\bar{x}_b$ corresponds to complete radial mixing of the flow through the reactor. The moles of SO_2 converted in an element of thickness dr are $x(G/\bar{M})y_0\, 2\pi r\, dr$, where $G/\bar{M}$ represents the total moles per unit area entering the reactor and y_0 is the mole fraction SO_2 in the feed.

Integrating over all radial elements gives

$$\frac{\pi G r_0^2 y_0 \bar{x}_b}{\bar{M}} = \int_0^{r_0} x \frac{G}{\bar{M}} y_0 2\pi r\, dr$$

$$\bar{x}_b = \frac{2\int_0^{r_0} xr\, dr}{r_0^2}$$

Table 13-7 Data for calculation of mean conversion at $L = 6$ ($z = 0.30$ ft)

n	x	xn
0	0.684	0
0.2	0.650	0.130
0.4	0.525	0.210
0.5	0.422	0.211
0.6	0.337	0.202
0.8	0.173	0.139
1.0	0.122	0.1222

If r/r_0 is replaced by n, then†

$$\bar{x}_b = 2\int_0^1 xn\, dn \qquad \text{(F)}$$

From the data in Table 13-6, graphs can be made of $Tc_p n$ and xn vs. n to represent the values of the integrals in Eqs. (E) and (F). Actually, the mean conversion is the quantity of interest. Table 13-7 shows xn at a bed depth of $z = 0.30$ ft. These data are plotted in Fig. 13-15, and the area is

$$\int_0^1 xn\, dx = 0.150$$

† The velocity does not appear in Eqs. (E) and (F) because it is assumed that G is constant across the diameter of the reactor.

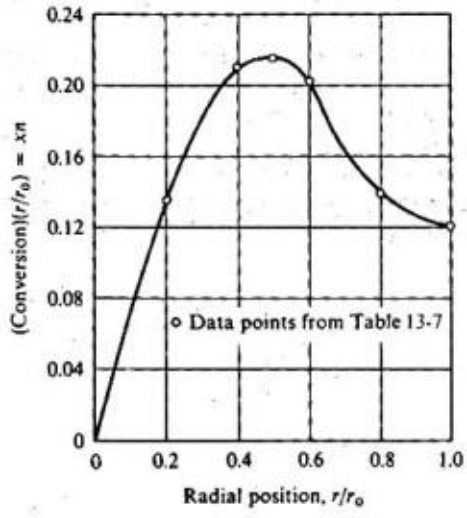

Figure 13-15 Graph for obtaining mean conversion.

Then, from Eq. (F),

$$\bar{x}_b = 2(0.150) = 0.300 \qquad \text{or } 30\% \text{ conversion}$$

Similar evaluations of the mean conversion have been made at the other bed depths. The results are plotted in Fig. 13-12, which also shows the measured conversions and the conversions calculated by the simplified method of Example 13-6. The two-dimensional method has resulted in better agreement than the one-dimensional model, but the computed conversions are still less than the experimental results. Young and Finlayson† have suggested that it is not valid to apply Eqs. (13-27) and (13-28) to the experimental conditions of this example. They have predicted conversions that agree well with Fig. 13-12 with a model that includes axial dispersion of heat and mass. Also, Ahmed and Fahien‡ have obtained good agreement neglecting axial dispersion but with $(D_e)_r$ and $(k_e)_r$ that vary radially.

Some of the deviations in Fig. 13-12 may be due to uncertainties in the radial diffusivity and thermal conductivity. The predicted results are based upon three independent sets of experimental data: global rates of reaction (Fig. 13-11), $(D_e)_r$ and $(k_e)_r$. The effective thermal conductivity and global rate, particularly, must be accurately known if any model is to predict reliable results.

The temperatures shown in Fig. 13-8 as solid curves represent experimental data for the conditions of this example. The computed values for r/r_0 of 0.0 and 0.6 have been taken from Table 13-6 and plotted as dashed lines on the figure for comparison. Referring to the centerline ($r/r_0 = 0$), we see that the computed results are about 10 to 20°C below the experimental values, although the location of the hot spot is predicted accurately. The comparison at $r/r_0 = 0.6$ is not as good.

When more than one reaction occurs the calculation procedures are similar to those illustrated in Example 13-7. A difference equation is written for each component and these equations are solved simultaneously with the difference equation for the conservation of energy. Froment§ and Carberry and White¶ have used one- and two-dimensional models to predict conversion and temperatures in a fixed-bed reactor for the oxidation of *o*-xylene to phthalic anhydride, CO, and CO_2, with a V_2O_5 catalyst. The reaction scheme is

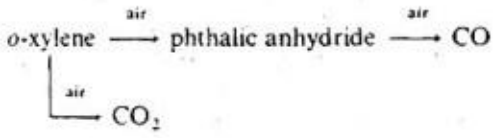

Calculations were made by Froment for a reactor containing a bundle of 2500 one-inch tubes packed with catalyst pellets and surrounded by molten salt to

† Loc. cit.

‡ M. Ahmed and R. W. Fahien, *Chem. Eng. Sci.*, **35**, 889, 897 (1980).

§ G. F. Froment, *Ind. Eng. Chem.*, **59**, 18 (1967).

¶ J. J. Carberry and D. White, *Ind. Eng. Chem.*, **61**(7), 27 (1969).

absorb the heat of reaction. The results showed that even with tubes of only 1 in. diameter, radial temperature gradients are severe for this extremely exothermic system. Carberry and White considered a reactor of 5 cm ID packed with 0'5-cm catalyst particles operating at a Reynolds number, $d_p G/\mu$, of 184. Here, too, axial and radial gradients of temperature were severe. It was demonstrated that the radial diffusivity had little effect on conversion to phthalic anhydride but that it was sensitive to the value of $(k_e)_r$.

A thorough study of a nonisothermal fixed-bed reactor for the reaction

$$C_6H_6 + 3H_2 \rightarrow C_6H_{12}$$

has been carried out by Otani.† An experimental differential reactor was used to obtain an equation of the Langmuir-Hinshelwood form [e.g., Eq. (9-32)] for the intrinsic rate, and then conversion and temperature measurements were made for cylindrical catalyst pellets (5 × 5 mm), for which the effectiveness factor was about 0.12. Then the *global* rate equation and estimated values of $(k_e)_r$ and $(D_e)_r$ were used to predict temperature and conversion data in the integral reactor tubes. The model was that described by Eqs. (13-27) and (13-28) and used in Example 13-7. The agreement between the predicted and experimental results was good in this case.

13-7 Dynamic Behavior

Thus far we have considered only steady-state operation of fixed-bed reactors. The response to variations in feed composition, temperature, or flow rate is also of significance. The dynamic response of the reactor to these involuntary disturbances determines the control instrumentation to be used. Also, if the system is to be put on closed-loop computer control, a knowledge of the response characteristics is vital for developing a control policy.

The solution of the steady-state form of the mass- and energy-conservation equations for fixed-bed reactors has been found to be complex. When transient conditions are considered the situation becomes more difficult. For the special case of isothermal operation only the mass-conservation equation is required. Then it is possible for many types of kinetics to obtain solutions for conversion at any point in the reactor in response to fluctuations in the feed. However, the nonisothermal case is most important because of the possibility of instabilities, and it is just this problem that is difficult to solve. For this reason effort has been directed more toward finding criteria for predicting when disturbances in the feed would grow and when they die out, instead of trying to solve the whole problem of conversion and temperature at any point in the reactor. We saw in Example 13-5 (Fig. 13-10) that sharp hot spots can develop when an exothermic reaction occurs in a cooled fixed-bed reactor. In that example conditions were such that the temperature rise was moderately large. Given other combinations of the heat of reaction, activation energy, rate equation, and heat-transfer rate to the surroundings, the temperature rise could be more pronounced. In such instances a positive

† S. Otani, "Some Practices in Petrochemical Process Development," presented at Sixty-fourth Annual Meeting of AIChE, New Orleans, March, 1969.

fluctuation in feed temperature or composition could cause so large a temperature rise in the reactor that reaction would be complete within a short section of the bed. Such behavior could be undesirable because of catalyst deactivation and reduced selectivity, but most important, the reactor would become uncontrollable. It is clear that a means for predicting the conditions at which this instability could occur would be helpful.

A number of criteria have been proposed for predicting instability,†—‡¶ and a review is available.¶ A simple proposal is that of Wilson.†† This criterion states that instability cannot occur if

$$\frac{E(T_{max} - T_{sur})}{R_g T_{max}^2} < 1 \tag{13-39}$$

where T_{max} and T_{sur} are the maximum and surroundings (cooling-medium) temperatures. For example, using the results of Example 13-5, $E/R_g = 2958°K^{-1}$, at the hot spot we have

$$\frac{E(T_{max} - T_{sur})}{R_g T_{max}^2} = \frac{2.958(527 - 427)}{(527)^2} = 1.06$$

According to this criterion, the reactor operation is at the point of instability, so that a perturbation in the feed could cause an uncontrollable situation.

The calculations of Froment‡‡ for a reactor for the oxidation of *o*-xylene illustrate the effect of a small fluctuation in feed temperature. The results showed that a 3°C rise in feed temperature (from 357 to 360°C) would lead to a continuous increase of the center temperature with reactor length, instead of the stable behavior of a rise and fall in temperature (for example as in Fig. 13-10). Such an unstable situation for this reaction results in a great loss in selectivity; the xylene is converted almost entirely to CO and CO_2 rather than to phthalic anhydride.

13-8 Variations of Fixed-Bed Reactors

Monolith catalyst beds The removal of oxidizable pollutants from air has stimulated the development of *monolithic* catalysts for use in a fixed-bed arrangement. The catalyst support is a partially or wholly continuous phase rather than consisting of individual particles. Many forms have been developed. Such structures are designed to have a high external surface area and to give a small pressure drop for the air flow. In one type, the support is prepared from crimped metal ribbon and arranged in mat-like sheets. In another form the catalyst base is a honeycomb structure. A third type consists of a bank of airfoil-shaped rods. The

† J. Beek, in T. B. Drew, J. W. Hoopes, Jr., and Theodore Vermeulen (eds.), "Advances in Chemical Engineering," vol. 3, Academic Press, Inc., New York, 1962.

‡ C. H. Barkelew, *Chem. Eng. Progr., Symp. Ser.*, 55, 37 (1959).

§ J. B. Agnew and O. E. Potter, *Trans. Inst. Chem. Eng.* 44, 216 (1966).

¶ V. Hlavacek, *Ind. Eng. Chem.*, 62(7), 9 (1970).

†† K. B. Wilson, *Trans. Inst. Chem. Eng.*, 24, 77 (1946).

‡‡ G. F. Froment, *Ind. Eng. Chem.*, 59, 18 (1967).

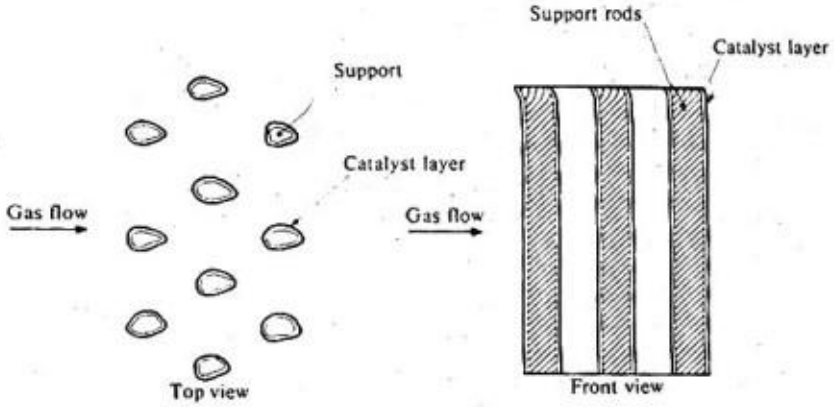

Figure 13-16 Cross-flow monolithic reactor.

air flows around the outer surface of the rods as indicated in Fig. 13-16. Such structures are made of either metal or ceramics.

The chief impetus for development of monolithic catalyst beds has been to reduce automobile exhaust emissions,† particularly unburned hydrocarbons and carbon monoxide. The oxidation catalyst, normally a platinum or platinum-palladium, can be electrolytically deposited on the support. Alternately, a thin layer of alumina impregnated with platinum may be deposited on the support. Since the reactions are strongly exothermic and have a sizable activation energy, the reaction rate is high. Hence, the reactive gases diffuse but a short distance into a porous catalyst before reaction is nearly complete. Hence, only a thin layer of catalytic material is usable. On the other hand, in an automobile exhaust line the catalyst bed must be mechanically strong to withstand mechanical and thermal shock and have a low pressure drop. These requirements are more closely satisfied in a monolithic arrangement than in the conventional bed of individual catalyst particles.

Since the catalyst layer is thin, intraparticle temperature and concentration gradients are not significant. Also, the high reaction rates imply that gas-to-solid mass- and heat-transfer resistances may be significant. The continuous nature of the solid phase introduces the possibility of heat transfer through the solid by conduction. Finally, the high temperature level and sharp changes in temperature in the direction of flow, suggest that heat transfer by radiation can be important. For these reasons models for predicting temperature and conversion in monolithic reactors are different from those in conventional fixed beds. Mathematical models based upon these concepts have been discussed.‡–¶ When all the

† F. G. Dwyer, *Cat. Rev.*, 6(2), 261 (1972).

‡ L. L. Hegedus, *AIChE J.*, 21, 849 (1975).

§ S. T. Lee and R. Aris, Proceedings of the Fourth International Symposium on Chemical Reaction Engineering, Heidelberg, Section VI, 232 (1976).

¶ V. Hlavacek, Proceedings of the Fourth International Symposium on Chemical Reaction Engineering, Heidelberg, Section VI, 240 (1976).

significant processes are included the solution of the conservation equations and boundary conditions is difficult, even by numerical methods.

We illustrate some of the aspects of the design problem by considering a simple model that ignores radiation. Suppose the catalyst is continuous in the direction of air flow (as indicated in Fig. 13-17; Fig. 13-16 shows a cross-flow arrangement) and suppose that the air moves in plug flow. Suppose also that the oxygen is in excess so that the rate is first order in the concentration of pollutant. Then Eq. (3-1) for a section of reactor of length dz gives, for the gas phase,

$$Q\frac{dC}{dz} + k_m a_L(C - C_s) = 0 \tag{13-40}$$

where Q is the volumetric flow rate, k_m the mass transfer coefficient from gas-to-catalyst surface, and a_L the mass- or heat-transfer area per unit *length* of reactor. For the solid phase, mass conservation of pollutant requires

$$k_m a_L(C - C_s) = k\,\delta C_s \tag{13-41}$$

where k ($k = Ae^{-E/R_g T_s}$) is the reaction-rate constant per unit mass of catalyst (evaluated at T_s) and δ is the mass of catalyst per unit length of reactor.

The energy conservation equation is obtained by applying Eq. (5-1) to the gas and to the catalyst phase. Allowing for axial conduction of heat in the catalyst phase the result is, for the gas,

$$Q\rho c_p\frac{dT}{dz} + ha_L(T - T_s) = 0 \tag{13-42}$$

and, for the catalyst,

$$(\Delta x)a_L\frac{d^2T_s}{dz^2} + ha_L(T - T_s) + (-\Delta H)k\,\delta C_s = 0 \tag{13-43}$$

where (Δx) is the thickness of the solid support (Fig. 13-17).

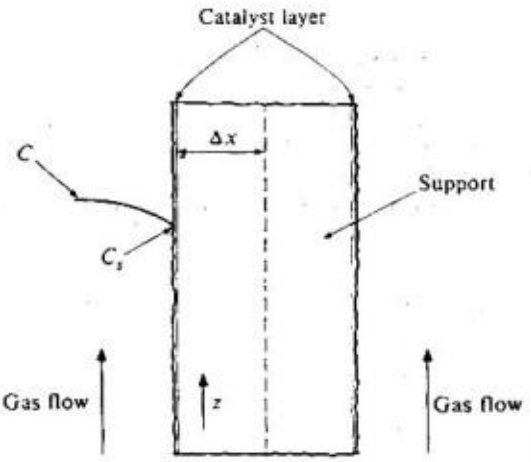

Figure 13-17 Axial section of monolithic catalyst.

If the heat loss from the end of the catalyst at $z = 0$ can be neglected, and the feed concentration and temperature are C_f and T_f, the boundary conditions are

$$C = C_f,\ T = T_f,\ \text{and}\ dT_s/dz = 0 \quad \text{at} \quad z = 0 \tag{13-44}$$

$$dT_s/dz = 0 \quad \text{at} \quad z = L \tag{13-45}$$

The boundary-value problem defined by the four equations (13-40) to (13-43), with the boundary conditions, can be solved for C, C_s, T, and T_s as a function of bed length z. Since k is a nonlinear function of T_s, numerical methods are required.

If the temperature is constant ($T = T_s =$ a constant) only Eqs. (13-40) and (13-41) are required. Now the solution is simple. If Eq. (13-41) is solved for C_s and the result substituted in Eq. (13-40), one obtains

$$\frac{dC}{dz} = -\left(\frac{1}{k\delta} + \frac{1}{k_m a_L}\right)^{-1} \frac{C}{Q}$$

This can be integrated directly to obtain the following solution for the conversion as a function of bed length.

$$1 - x = \frac{C}{C_f} = \exp\left[-\left(\frac{1}{k\delta} + \frac{1}{k_m a_L}\right)^{-1} \frac{z}{Q}\right] \tag{13-46}$$

Autothermal reactors† When an exothermic reaction requires a high temperature [examples are the ammonia or methanol synthesis, water-gas shift reaction ($CO + H_2O = H_2 + CO_2$)] the heat of reaction can be used to preheat the feed. This can be accomplished in several ways in fixed-bed reactors. A separate external heat exchanger can be employed to transfer the heat of reaction, residing in the effluent, to the feed stream (Fig. 13-18*a*). Alternately, the exchanger may be an integral part of the reactor (Fig. 13-18*b*). Another possibility is to recycle part of the high-temperature effluent, Fig. 13-18*c*. Such heat-transfer and reaction systems are termed autothermal. Their advantage is that they can be essentially self-sufficient in energy, even though high temperature is required for the reaction to occur at a reasonable rate. An external source of heat is needed during the startup period while the system is coming to thermal equilibrium.

For the operating procedures shown in Fig. 13-18*a* or 13-18*c*, the reactor itself would operate adiabatically or with heat transfer to the surroundings. Then the conservation equations developed in Secs. 13-4 to 13-6 are applicable. When the heat exchanger is an integral part of the reactor (Fig. 13-18*b*) the equation for conservation will be different, but can be derived by applying Eq. (5-1). Conservation equations and their solution for various types of autothermal systems are available for both fixed-bed catalytic reactors‡§ and homogeneous reactors.¶

† C. van Heerden, *Ind. Eng. Chem.*, **45**, 1242 (1953).

‡ B. F. Baddour, P. L. T. Brian, B. A. Logeais, and J. P. Eymery, *Chem. Eng. Sci.*, **20**, 281 (1965). These authors used a one-domensional model to predict reactor temperature profiles for an ammonia-synthesis reactor of the type shown in Fig. 13-18*a*.

§ J. Caha, V. Hlavacek, and M. Kubicek, *Chem. Ing. Techn.*, **45**, 1308 (1973).

¶ T. G. Smith and J. T. Banchero, *J. Heat Transfer*, **95**, 145 (1973).

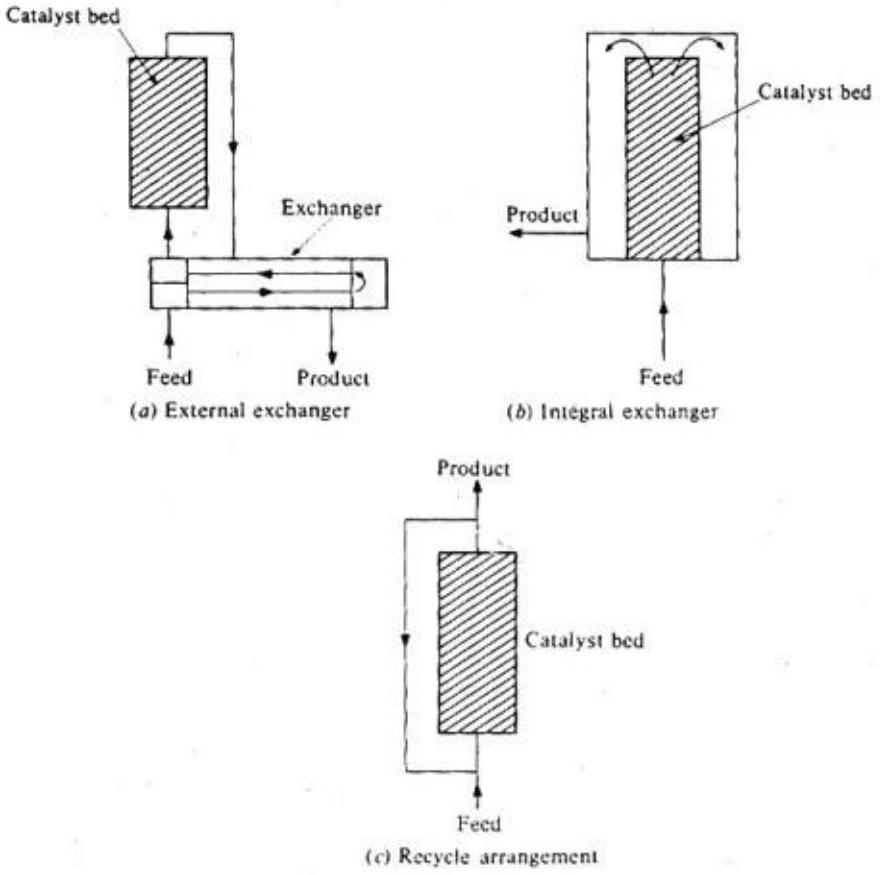

Figure 13-18 Autothermic reactor arrangements.

An interesting feature of autothermal systems is that they may exhibit more than one steady state, much like the phenomena found in Sec. 5-5 for stirred-tank reactors.

13-9 Importance of Transport Processes in Fixed-Bed Reactors

The procedure followed in this chapter for design of *fixed-bed* reactors has presumed that we know the *global* rate. Then only intrareactor transport processes in the radial and axial directions need be considered. As an aid in deciding on an appropriate model for the overall design, it is helpful to assign a relative importance to all the transport processes, including those that affect the global rate.

We divide the processes into three divisions, intrareactor (radial and axial dispersion of heat and mass), interphase (fluid-to-outer-surface of the catalyst particle), and intraparticle. It is impossible to summarize the importance of trans-

Table 13-8 Relative importance of transport effects in fixed-bed reactors

Mass transfer	Heat transfer	Importance of transport process
Intraparticle (effectiveness factor)	Intrareactor [radial direction $(k_e)_r$]	Most severe
Intrareactor [radial direction $(D_e)_r$]	Interphase (k_m)	Intermediate severity
Interphase (k_m)	Intrareactor [(axial direction $(k_e)_z$]	Least severe
Intrareactor [axial direction $(D_e)_z$]	Intraparticle	

port effects in a way that is applicable to all reaction systems because of differences in such factors as bed length, fluid velocity, temperature level, catalyst particle size. However, for many cases, the relative importance follows the arrangement in Table 13-8. Some of the conclusions suggested in the table have been discussed separately: for example the relatively low importance of interphase mass transfer (Sec. 10-3) and the great importance of radial heat transfer (Sec. 13-6). The table is arranged so as to apply to a nonadiabatic, nonisothermal reactor for which the two-dimensional model (Sec. 13-6) is necessary. For isothermal reactors none of the heat-transfer effects are pertinent, and for adiabatic reactors radial transport is not involved.

One approach to modeling the reactor would be to include only the transport effects of great and intermediate severity. Then we would neglect the effects of intraparticle temperature differences, axial dispersion of heat and mass, and fluid-to-particle (interphase) concentration differences.

FLUIDIZED-BED REACTORS

In Chap. 10 we discussed the effect of increasing velocity (Fig. 10-6) on the movement of gas and particles in a fluidized bed and also heat-transfer rates between fluid and particles (Sec. 10-6). Now we want to consider how to predict the behavior of the fluidized bed as a catalytic reactor; that is, we want to predict the conversion in the effluent from a proposed model for the reactor.

The particles in a fluidized bed are so small that intraparticle concentration and temperature gradients are negligible. As was noted in Sec. 10-6, heat- and mass-transfer rates between fluid and particles are very high so that external temperature and concentration differences are negligible. Thus, the global reaction rate is equal to the intrinsic rate, evaluated at bulk values of the temperature and concentration. This means that the reactor design problem is essentially one of modeling the flow conditions in the reactor as a whole (interactor model).

Most fluidized-bed reactors operate in the bubbling regime as sketched in Fig. 10-6. Under these conditions the upward motion of the "gas bubbles" causes enough mixing in the dense phase that the temperature is nearly uniform in the entire reactor. This effect of the gas bubbles is favorable. However, there is little reaction within the bubbles (because of the low catalyst particle concentration). Hence, the bubbles are unfavorable in that they serve as channels for gas to bypass the catalyst and leave the reactor more or less unreacted. Models have been proposed† for predicting the conversion under these conditions. Such models should, in general, include the extent of reaction in the gas bubbles, in the dense phase, velocities and magnitudes of bubble and dense phases, and extent of mass transfer between the two phases. One of the most attractive proposals is the bubbling-gas model.‡ This approach actually includes a third region, a cloud of particles, surrounding the bubble and within which gas recirculates but does not mix rapidly with the gas in the dense phase. Quantitative treatment for this three-phase model is described in detail by Kunii and Levenspiel. Discussions of the nature of the cloud region and its relation to the bubble and dense phases are available.§¶ Also the model has been carefully compared with other models using experimental data.†† The model includes several parameters: apparent reaction rate constants in the bubble, in the cloud, and in the dense phase, and transport rate constants for the reactant from bubble gas to cloud and from bubble gas to emulsion phase. The useful feature of the model is that these parameters may be estimated solely from the diameter of the gas bubbles. Kunii and Levenspiel‡‡ suggest correlations for obtaining numerical values. One of the requirements for valid models is that they be able to predict a conversion less than that corresponding to complete mixing of the entire reactor contents. If the apparent rate constant in the bubbles is low, because of low particle concentration, and if a significant portion of the total gas flow is in such bubbles, the model successfully predicts these low conversions. Figure 13-19 shows how experimental conversions can be less than those for either an ideal stirred-tank or plug-flow reactor, at higher average gas velocities. The deviation between the fluidized bed and ideal stirred-tank conversions presumably increases with velocity because the extent of bypassing in the gas bubbles increases.

We will not give the quantitative development of the rather complex three-region model. The equations can be illustrated with a two-region ("two-phase") model as applied by Pavlica and Olson.§§ Also these same equations can be used for treating trickle-bed reactors later in this chapter.

An even simpler, "single-phase" model considers the entire reactor volume to

† J. F. Davidson and D. Harrison, "Fluidized Solids," Cambridge University Press, London, 1963; J. R. Grace, AIChE Symposium Series, 67(116), 159 (1971).

‡ D. Kunii and O. Levenspiel, *Ind. Eng. Chem. Fundam.*, 7, 446 (1968); *Ind. and Eng. Chem. Proc. Des. Dev.*, 7, 481 (1968).

§ J. F. Davidson and D. Harrison, loc. cit.

¶ P. N. Rowe and B. A. Partridge, *Proc. Symp. on Interaction Between Fluids and Particles, Inst. Chem. Eng. (London)*, June 1962.

†† Colin Fryer and O. E. Potter, *AIChE J.*, 22, 38 (1976).

‡‡ Loc. cit.

§§ R. T. Pavlica and J. H. Olson, *Ind. Eng. Chem.*, 62(12), 45 (1970).

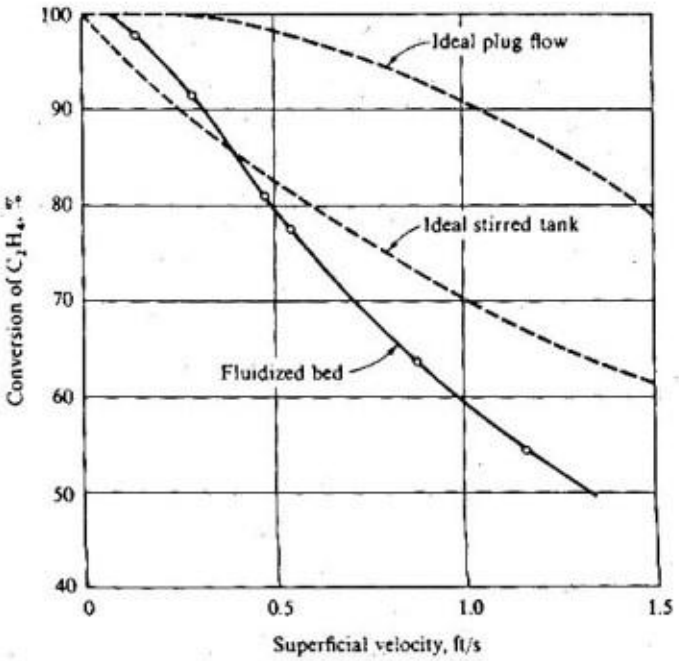

Figure 13-19 Hydrogenation of ethylene in a fluidized-bed reactor [*from W. K. Lewis, E. R. Gilliland, and W. Glass, AIChE J., 5, 419 (1959)*].

have a uniform concentration of catalyst particles. Deviations from plug-flow behavior is accounted for by introducing an axial dispersion term in the mass conservation equation. Then the results are the same in form as those for the isothermal, fixed-bed reactor. Equation (13-14) is the appropriate conservation equation where D_L is an axial dispersion coefficient applicable for a fluidized bed (see Prob. 13-14). The conversion for first-order kinetics is given by Eq. (6-47). A conversion less than that for a stirred tank cannot be obtained with this model.

13-10 Two-Phase Fluidized-Bed Model

Suppose an irreversible catalytic reaction occurs in a fluidized-bed reactor operating in the bubbling-gas regime, as shown in Fig. 13-20. Radial variations in concentrations within the two phases are neglected and isothermal operation is assumed. Suppose that the catalyst particle concentration within the bubbles is so low that reaction in the bubbles can be neglected. Also, assume that the bubbles move in plug flow up through the reactor. Then conservation of mass of reactant requires that the net flow rate of reactant into an element of reactor volume of height Δz be equal to the rate of mass transfer from bubble to dense phase. Application of Eq. (3-1) to the bubble phase gives

$$u_b \frac{dC_b}{dz} + k_m a_v (C_b - C_d) = 0 \tag{13-47}$$

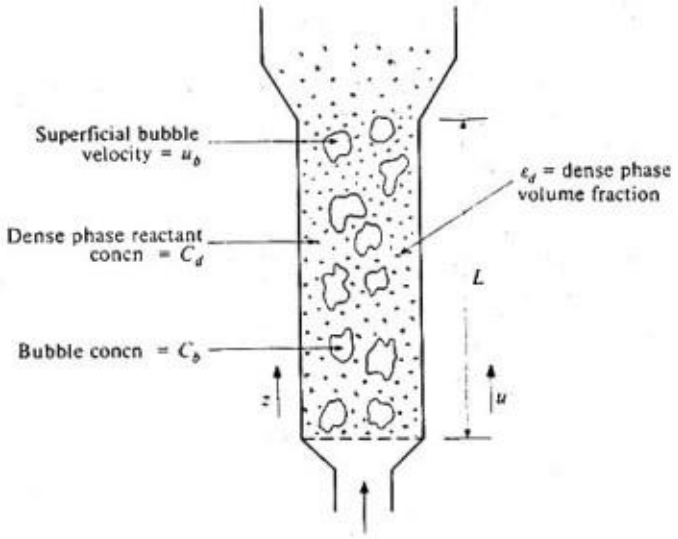

Figure 13-20 Two-phase model of fluidized-bed reactor.

where u_b = superficial velocity of the gas bubbles
(u_b = gas flow rate divided by cross-sectional area of reactor)
C_b, C_d = concentration of reactant in gas bubbles or in the dense phase
k_m = mass-transfer coefficient between bubble and dense phases
a_v = mass-transfer area between bubble and dense phases per unit volume of reactor

Suppose that mixing of the reactant gas in the dense phase can be accounted for with the dispersion model. Then the mass conservation equation for reactant in the dense phase will be similar to Eq. (13-47) but include a term for axial mixing and for reaction. Equation (3-1) under these conditions may be written

$$-u_d \frac{dC_d}{dz} + \varepsilon_d D_L \frac{d^2C_d}{dz^2} - \varepsilon_d \rho_d [kf(C_d)] + k_m a_v (C_b - C_d) = 0 \qquad (13\text{-}48)$$

where $kf(C)$ represents the reaction rate per unit mass of catalyst
ρ_d is the density of catalyst particles in the dense phase
u_d = superficial velocity of the gas in the dense phase, and
ε_d = fraction of reactor cross section occupied by the dense phase (the holdup of the dense phase)

These equations with appropriate boundary conditions describe the concentrations in the two phases as a function of reactor height z. With known values for the parameters ε_d, D_L, a_v, k_m, and the reaction rate, they can be solved for the effluent concentrations C_b and C_d. These concentrations can be combined to give the conversion. However, the experimental evidence suggests that the net upward gas

velocity in the dense phase is low and that mixing in this phase is very good. As an approximation, the process may be visualized as the feed stream forming gas bubbles as it enters the reactor and these bubbles flowing upward through the dense phase. This means that the dense region behaves as a well-mixed *batch* phase so that the first two terms in Eq. (13-48) disappear. With this simplification, and for a first-order reaction $[kf(C) = kC]$, Eq. (13-48) reduces to

$$\varepsilon_d \rho_d k C_d = k_m a_v (C_b - C_d) \tag{13-49}$$

Now we can solve Eq. (13-49) for C_d in terms of C_b and substitute this result in Eq. (13-47) for immediate integration. Doing this, Eq. (13-47) becomes

$$u_b \frac{dC_b}{dz} = -\left[\frac{1}{\varepsilon_d k \rho_d} + \frac{1}{k_m a_v}\right]^{-1} C_b \tag{13-50}$$

If the feed concentration is C_f (at $z = 0$), the integrated form of Eq. (13-50) is

$$1 - x = \frac{C}{C_f} = \exp\left[-\left(\frac{1}{\varepsilon_d k \rho_d} + \frac{1}{k_m a_v}\right)^{-1} \frac{z}{u_b}\right] \tag{13-51}$$

Note that this result is similar to Eq. (13-46) for a monolithic reactor. Both reactor models represent the same type of interaction between reaction and mass transport processes.

Example 13-8 The effect of bypassing in a bubbling fluidized bed is determined by the fraction $(1 - \varepsilon_d)$ of the reactor volume that consists of bubbles and by the relative values of the reaction rate and mass transfer rate. The quantities k_m, ε_d, u_b, and a_v all depend upon the bubble diameter. In a particular case suppose that these parameters have the following values, for a first-order reaction operating isothermally in the bubbling regime:

$\rho_d = 0.01$ g/cm^3
$(k_m a_v) = 0.60$ s^{-1}
$k = 50$ cm^3/(g)(s)
$u_b =$ velocity of feed $= 10$ cm/s
Reactor height, $z = L = 40$ cm
$\varepsilon_d = 0.80$ (that is, 20% of the reactor volume is occupied by gas bubbles and 80% by the dense phase)

A. Calculate the conversion in the effluent.

B. For comparison, calculate the conversion for plug-flow and stirred-tank reactors operating with the same apparent bubble residence time.

SOLUTION

A. The terms in parentheses in Eq. (13-51) may be regarded as time constants that measure the time required for reaction, $1/\varepsilon_d k \rho_d$, and for mass transport between bubble and dense phases, $1/k_m a_v$.

For $\varepsilon_d = 0.80$ Eq. (13-51) gives

$$x = 1 - \exp\left[-\left(\frac{1}{0.80(50)(0.01)} + \frac{1}{0.60}\right)^{-1}\frac{40}{10}\right]$$

$$x = 1 - \exp\left[-4(2.50 + 1.67)^{-1}\right]$$

$$x = 1 - 0.38 = 0.62\ (62\%)$$

The time constant for mass transfer (1.67 s) is only a little less than the time constant for reaction (2.50 s). In this case mass transport from gas bubble to dense phase has an important effect on reactor performance.

B. Equations (4-18) and (4-17) give the conversion for first-order reactions in plug-flow and in stirred-tank reactors. In these equations the residence time is V/Q. Hence, for the same apparent bubble residence time as in the fluidized bed,

$$\frac{V}{Q} = \frac{L}{u_b} = \frac{40}{10} = 4\ \text{s}$$

Also, the rate constant per unit volume in these equations is equal to $k\rho_d = 0.50\ \text{s}^{-1}$. Then Eqs. (4-18) and (4-17) give

$$\text{Plug flow reactor } x = 1 - [\exp - 4(0.5)]$$

$$= 1 - 0.14 = 0.84\ (84\%)$$

$$\text{Stirred tank } x = \frac{0.50(4)}{1 + 0.50(4)} = 0.667\ (67\%)$$

For these conditions we see that bypassing of reactant in the gas bubbles has reduced the conversion below that expected if the whole reactor contents were well mixed (stirred-tank performance).

We have been concerned with but one reaction. If multiple reactions occur, the mass-transfer term in Eq. (13-51) can affect selectivity. The situation is the same as discussed in Sec. 10-5 for the effect of external mass transport on selectivity. If the reactions are consecutive the mass-transfer term $1/k_m a_b$ in Eq. (13-51) has an adverse effect on selectivity. If the reactions are of the parallel type selectivity is unaffected.

13-11 Operating Characteristics

Fluidized beds are particularly suitable when frequent catalyst regeneration is required, or for reactions with a very high heat effect. Often the reactors are vessels of large diameter (10 to 30 ft is not unusual for catalytic cracking units in the petroleum industry). A typical system is shown in Fig. 13-21. The movable catalyst permits continuous regeneration in place. Part of the catalyst is continuously withdrawn from the reactor in line *A* and flows into the regenerator. The regenerator shown in the figure is another fluidized bed, from which reactivated catalyst is returned to the reactor through line *B*. It is not necessary to carry out the regener-

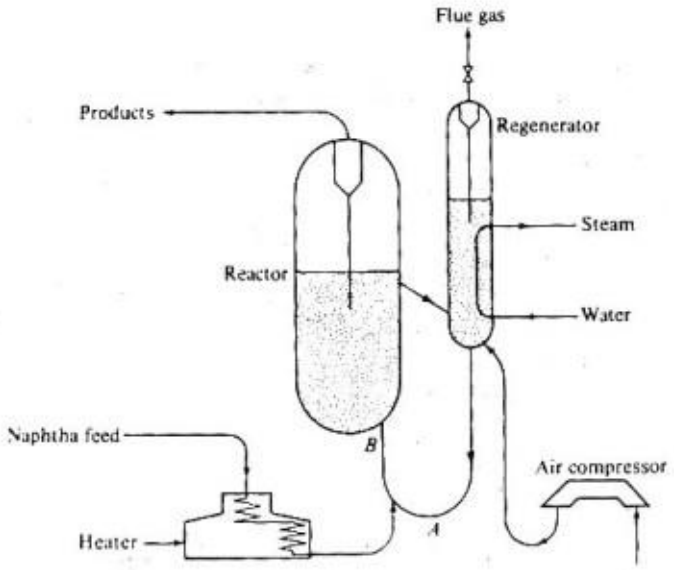

Figure 13-21 Flow diagram for a fluid hydroformer, a fluidized-bed reactor-generator combination (*by permission from Esso Standard Oil Company, Baton-Rouge, La.*).

ation in a fluidized bed, as catalyst could be withdrawn continuously, and reactivated catalyst returned with the regeneration accomplished by any procedure. However, the process is most economical if both reaction and regeneration are carried out in fluidized beds by means of the integral setup illustrated in Fig. 13-21.

An important feature of the fluidized-bed reactor is that it operates at a nearly constant temperature and hence is easy to control. There is no opportunity for hot spots to develop, as in the case of the fixed-bed unit. The fluidized bed does not possess the flexibility of the fixed bed for adding or removing heat. A diluent can be added to control the temperature level, but this may not be desirable for other reasons (requires separation after the reactor, lowers the rate of reaction, increases the size of the equipment). A heat-transfer fluid can be circulated through a jacket around the reactor, but if the reactor is large in diameter, the energy exchange by this method is limited.†

Catalyst loss due to carryover with the gas stream from the reactor and regenerator may be an important problem. Attrition of particles decreases their size to a point where they are no longer fluidized, but move with the gas stream. It has been customary to recover most of these catalyst fines by cyclone separators and electrical precipitation equipment placed in the effluent lines from reactor and regenerator.

† A heat-transfer fluid also may be circulated through tubes placed within the fluidized bed.

Deterioration of lines and vessels due to the abrasive action of the sharp, solid particles in the fluidized cracking process has caused concern. This problem has been particularly severe in the small-diameter transfer lines, where the particle velocity is high. These and other matters relating to the commercial operation of fluidized catalytic cracking plants have been discussed in the literature.†

It has been mentioned that catalytic cracking of petroleum gas-oil is the most frequent application of fluidized-reactor technology. In this area the development of synthetic zeolite (molecular-sieve) catalysts has greatly increased the intrinsic rates of the cracking reactions. As a result, much of the reaction may occur in the transfer line (line *AB* is Fig. 13-20) *before* the hydrocarbon enters the reactor proper. Such "transfer-line" reactors are moving-bed units with a very high void fraction. The system consists of two moving phases. Reactor design models can be developed by writing conservation equations for each phase much like was done for the two-phase model of fluid-bed reactors [Eqs. (13-47) and (13-48)]. An important factor in such reactors is the slip velocity, or relative velocity between particles and gas.

SLURRY REACTORS

Slurry reactors are similar to fluidized-bed reactors in that a gas is passed through a reactor containing solid catalyst particles suspended in a fluid. In slurries the catalyst is suspended in a liquid; in fluidized-beds the suspending fluid is the reacting gas itself. The advantages of slurry reactors over fixed beds are similar to those of fluidized beds: more uniform temperature, better temperature control for highly exothermic reactions, and low intraparticle diffusion resistance. For very active catalysts this last factor means that the global rate can be much higher than for fixed-bed reactors. In order to eliminate the retardation of the global rate due to intraparticle diffusion the particles must be very small. This is because diffusivities in *liquid*-filled pores are relatively low, of the order of 10^{-5} cm^2/s in comparison with 10^{-2} cm^2/s for gases. For example, in studies of adsorption of benzene in aqueous slurries of activated carbon‡ it was found that intraparticle diffusion reduced the global rate for carbon particles as small as 160 microns. For slower intrinsic rates (the rate for physical adsorption of benzene was very fast), intraparticle diffusion would be less important.

The most serious disadvantage of slurry reactors is the difficulty in retaining the catalyst in the vessel. Screens and other devices placed in the outlet lines tend to clog or otherwise be unreliable. In some instances,§ the catalyst can be so active that it need not be retained in the reactor. If the production rate of product per unit mass of catalyst is very high, there may be no need to separate the small amount of finely divided catalyst from the effluent. The concentration of catalyst particles in the product is too small to be troublesome.

† E. V. Murphree, et al., *Trans. AIChE.* 41, 19 (1945); A. L. Conn, et al., *Chem. Engr. Progr.*, 46, 176 (1950).

‡ Takehiko Furusawa and J. M. Smith, *Ind. Eng. Chem. Fundam.*, 12, 197 (1973).

§ For example, ethylene polymerization.

As pointed out in Chap. 10, when one reactant is a gas and a second is a liquid, reactions catalyzed by a solid must be carried out in a three-phase system. Then, the meaningful comparison of slurry reactors is not with fluid-solid fixed-bed units but with trickle-bed reactors. The latter is the three-phase version of the fixed-bed arrangement. This comparison is taken up later in the chapter after the design of trickle-bed units has been discussed.

13-12 Slurry Reactor Models

In Chap. 10 global rate equations were developed (for the overall transfer of reactant from gas bubble to catalyst surface) in terms of the individual mass-transfer and chemical-reaction steps [Eqs. (10-38) and (10-39)]. The purpose there was to show how the global rate $\mathbf{r}_v$ (per unit volume of bubble-free slurry) was affected by such variables as the gas-bubble–liquid interface a_g, the liquid-solid catalyst interface a_c, and the various mass-transfer coefficients, and the intrinsic rate for the chemical step. Now the objective is to utilize the results for the global rate to predict the performance of the reactor as a whole. For this purpose we need a model to describe the flow and mixing characteristics of the gas, liquid, and solid phases. With three phases there are a large number of possible operating conditions. We first list some of the possibilities and then, as an illustration, quantitatively examine one common form of slurry system.

With respect to reactor modeling we could propose that both gas and liquid could be in plug flow or could be well mixed, while the catalyst phase remains in the tank-type reactor. Alternatively, the liquid phase could remain in the reactor, as in batch operation with continuous flow of gas in and out of the reactor. Regardless of the arrangement, the design procedure is to write mass conservation equations, for the reactant, according to Eq. (3-1), for each reaction.† If the reactant exists in both gas and liquid phases, separate conservation equations may be necessary for each phase. If the global rate is used, these equations will be in terms of bulk concentrations. Hence, the solution gives the relation between extent of reaction and reactor volume, analogous to the results for single-phase reaction systems developed in Chap. 4.

As an example, consider a continuous slurry reactor in which the reactants are both in the gas phase, and the liquid is inert.‡ The purpose of the liquid is simply to suspend the catalyst particles. The overall catalytic reaction is

$$A(g) + B(g) \rightarrow C(g)$$

For a reactor model suppose that the slurry is well agitated so that concentrations in the liquid, both of dissolved reactants and of catalyst particles, are uniform. Suppose also that the gas bubbles are discrete§ and rise in plug flow through the slurry as indicated in Fig. 13-22. We may write a mass conservation equation for

† As mentioned in Chaps. 5 and 10, for tank-type reactors mixing results in a uniform temperature unless internals, such as cooling coils, interfere with mixing.

‡ Examples are the hydrogenation of gases with a slurry of nickel particles as catalyst, or oxidation of gases such as SO_2 or H_2S in aqueous slurries of activated carbon particles.

§ That is, they rise individually through the slurry rather than coalesce.

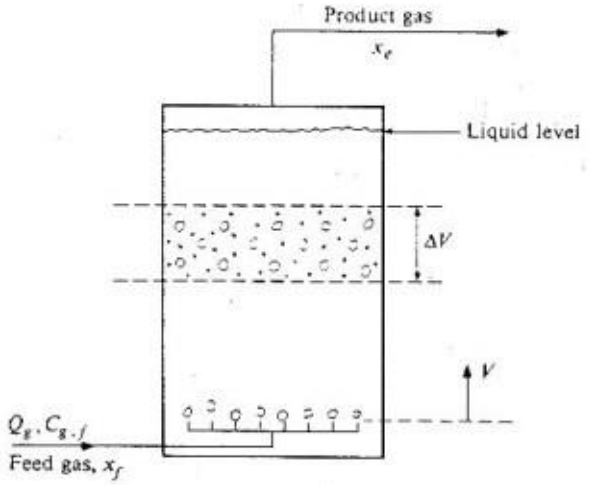

Figure 13-22 Slurry reactor (batch liquid, continuous-flow gas).

an element of reactor volume, dV, extending across the entire cross section of the slurry. This is because the liquid-phase concentrations are uniform and because we suppose that the gas-flow rate, Q_g is distributed uniformly. For the limiting reactant, at steady state, Eq. (3-1), applied to the gas phase is identical with Eq. (3-14) for a plug-flow reactor. If $\mathbf{r}_v$ is a positive value (rate of disappearance of reactant)

$$-d(Q_g C_g) - \mathbf{r}_v \, dV = 0$$

As noted in Chap. 3, if the conservation equation is to be applicable for a reaction with a change in moles (i.e., variable Q_g), it is advantageous to express $-d(Q_g C_g)$ as $F_A \, dx$. Then we may write

$$\frac{V}{F_A} = \int_{x_f}^{x_e} \frac{dx}{\mathbf{r}_v} \tag{13-52}$$

This is the same as Eq. (3-18) except that V is the volume of bubble-free slurry in the reactor, and $\mathbf{r}_v$ is the global rate of reaction per unit volume of liquid, as defined in Chap. 10. If the reaction is first-order and irreversible, $\mathbf{r}_v$ is given by Eq. (10-38).

Equation (13-52) may be used to calculate the volume of slurry liquid required to obtain a conversion x for a molal feed rate F_A of reactant. For a first-order reaction, and if Henry's law is valid, Eq. (10-39) displays how the various rate constants k_g, k_c, and k, and areas a_g and a_c, influence the process.

If there is no change in moles in the gas phase as a result of reaction, Eq. (13-52) can be easily integrated. Noting that $C_g = C_{gf}(1 - x)$ and $F_A = Q_g C_{gf}$, and using Eq. (10-38) for $\mathbf{r}_v$, Eq. (13-52) becomes, for $x_f = 0$,

$$\frac{V}{Q_g C_{gf}} = \int_0^{x_e} \frac{dx}{k_0 a_c C_{gf}(1 - x)}$$

or

$$\frac{V}{Q_g} = \frac{-1}{k_0 a_c} \ln (1 - x_e) \tag{13-53}$$

which is similar to Eq. (4-18). If the reaction had not been first-order, the simple relation between $\mathbf{r}_v$ and the various rate constants, as given by Eqs. (10-38) and (10-39) would not have been valid. Then the global rate would not be a simple function of gas-phase concentration like Eq. (10-38). Numerical methods would have been needed to eliminate the liquid and surface concentrations, C_L and C_s, and express $\mathbf{r}_v$ in terms of C_g. The procedure for doing this is the same as illustrated in Example 10-2 for two-phase systems. Once $\mathbf{r}_v$ is obtained as a function of C_g, Eq. (13-52) could be integrated numerically to obtain the exit conversion.

Only the gas phase has been considered in our application because both reactants were in the gas phase. If the slurry liquid were reacting, as in hydrogenation of oils, then mass conservation expressions would need to be written for liquid and gas phases. For a batch liquid system the problem becomes a dynamic one because the concentrations in the liquid will change with time. If the process is continuous, and at steady state with respect to the liquid, there would be a combination of plug flow of gas and stirred-tank behavior for the liquid. The method of solution is the same, in principle, for these cases: conservation equations are written for gas and liquid phases and solved for final and/or effluent values (see Prob. 13-20). Quantitative treatments for these forms of slurry reactors are available.† ‡

Examples 13-9 and 13-10 illustrate the calculation of conversion in slurry reactors.

Example 13-9 Ethylene is to be hydrogenated by bubbling mixtures of H_2 and C_2H_4 through a slurry of Raney nickel catalyst particles suspended in toluene. The gas bubbles are formed at the bottom of a tubular reactor and rise in plug flow through the slurry. The slurry is well mixed, so that its properties are the same throughout the tube. A large concentration of small catalyst particles will be used. The temperature and pressure are to be 50°C and 10 atm. At these conditions the overall rate has been shown to be determined by the rate of diffusion of hydrogen from the bubble interface to the bulk liquid.§ This means that $\mathbf{r}_v$ is first order in the gas-phase concentration of hydrogen, regardless of the intrinsic kinetics at the catalyst site.

Estimate the volume of bubble-free slurry required to obtain a conversion of 30% for a hydrogen feed rate of 100 ft^3/min (at 60°F and 1 atm). By a light-transmission technique, Calderbank measured gas-liquid interfacial areas of 0.94 to 2.09 cm^2/cm^3 for bubble sizes likely to be encountered in this system. Suppose for this illustration $a_g = 1.0$ cm^2/cm^3 of bubble-free slurry.

† Hiroo Niiyama and J. M. Smith, *AIChE J.*, **22**, 961 (1976).

‡ Takehiko Furusawa and J. M. Smith, *Ind. Eng. Chem. Fundam.*, **12**, 360 (1973).

§ P. H. Calderbank, F. Evans, R. Farley, G. Jepson, and A. Poll, "Catalysis in Practice," *Symp. Inst. Chem. Engrs. (London)*, 1963.

The Henry's law constant for hydrogen in toluene at 50°C is 9.4 (g mol cm^3)/(g mol/cm^3), and its diffusivity is 1.1×10^{-4} cm^2/s. The density and viscosity of toluene at 50°C are 0.85 g/cm^3 and 0.45 centipoises, respectively. Equimolal feed rates of ethylene and hydrogen will be used.

SOLUTION For the reaction

$$C_2H_4(g) + H_2(g) \rightarrow C_2H_6(g)$$

the number of moles of each component at a conversion level x is

$$H_2 = F(1 - x)$$

$$C_2H_4 = F(1 - x)$$

$$C_2H_6 = Fx$$

$$\text{Total moles} = F(2 - x)$$

where F is the molal feed rate of H_2 or C_2H_4. Then the concentration of H_2 in the gas bubbles is

$$(C_{H_2})_g = \frac{p_t}{R_g T} y_{H_2} = \frac{p_t}{R_g T} \frac{1 - x}{2 - x} \tag{A}$$

Equation (13-52) is applicable to this reactor with $\mathbf{r}_v$ given by Eq. (10-38). Substituting Eqs. (A) for C_g in Eq. (10-38), Eq. (13-52) becomes

$$\frac{V}{F} = \frac{R_g T}{k_o a_c p_t} \int_0^{x_e} \frac{2 - x}{1 - x} dx \tag{B}$$

Integrating from zero to the exit conversion gives

$$\frac{V}{F} = \frac{1}{k_o a_c} \frac{R_g T}{p_t} [x_e - \ln (1 - x_e)] \tag{C}$$

The overall rate constant k_o would, in general, be a function of several rate parameters. Since it is known that only the resistance to diffusion of hydrogen from the bubble interface is significant, Eq. (10-39) reduces to

$$\frac{1}{k_o} = \frac{a_c}{a_g} \frac{H}{k_L}$$

or

$$k_o a_c = \frac{a_g k_L}{H} \tag{D}$$

Hence Eq. (C) may be written

$$\frac{V}{F} = \frac{H}{a_g k_L} \frac{R_g T}{p_t} [x_e - \ln (1 - x_e)] \tag{E}$$

Everything in Eq. (E) is known except the mass-transfer coefficient for hydrogen in the liquid. This may be estimated from Eq. (10-46), since this

correlation was based on data for gas bubbles rising through a liquid phase. Thus

$$k_L\left[\frac{0.45\times10^{-2}}{0.85(1.1\times10^{-4})}\right]^{2/3}=0.31\left[\frac{(0.85-0.8\times10^{-3})(0.45\times10^{-2})(32.2)}{0.85^2}\right]^{1/3}$$

$$k_L=\frac{0.31}{13.2}(0.55)=0.013\ \text{cm/s}$$

Substituting this result for k_L and the other numerical value in Eq. (E) gives

$$\frac{V}{F}=\frac{9.4}{1.0(0.013)}\frac{82(273+50)}{10}[0.3-\ln(1-0.3)]$$

$$=1.25\times10^6\ \text{cm}^3/(\text{g mol/s})$$

For a hydrogen feed rate of 100 ft^3/min, at 60°F and 1 atm, the slurry volume required would be

$$V=\frac{100}{379}\left(\frac{454}{60}\right)(1.25\times10^6)(10^{-3})\left(\frac{1}{28.32}\right)=88\ \text{ft}^3$$

In this example many important properties of the slurry have been omitted. For example, the questions of bubble diameter and volume fraction of gas in the slurry have been avoided by giving a directly measured value of a_g. Alternately, the interfacial area can be estimated from Eqs. (10-50) and (10-52).

Example 13-10 An aqueous slurry of 3×10^{-5} m (0.03 mm) (diameter) carbon particles is to be used, at 25 C and 1 atm pressure, to remove SO_2 from a gas stream. The gas contains 2.3% SO_2 and 97.7% air, and its rate is 2.75 m^3/s. The density ρ_p of the carbon particles is 0.80×10^3 kg/m^3 (0.80 g/cm^3) and their concentration, m_s will be 70 kg/(m^3 of water) or 0.07 g/cm^3. For the distributor to be used the gas bubble size will be 3×10^{-3} m (3 mm). The gas holdup, or bubble volume per unit volume of liquid, is estimated to be 0.08. Assume that the gas bubbles are uniformly distributed across the diameter of the reactor and rise individually in plug flow. The slurry will be well mixed. Calculate the volume of bubble-free liquid needed to convert 70% of the SO_2 to H_2SO_4. Base the calculations on the steady-state period before the H_2SO_4 concentration has increased enough to retard significantly the reaction rate.

Use the mass-transfer coefficients found for the same system in Example 10-7. The intrinsic rate at the carbon site under these operating conditions is first-order in oxygen and zero order in SO_2. In terms of a rate, $\mathbf{r}_v$, per unit volume of bubble-free liquid, it is given by†

$$(\mathbf{r}_v)_{O_2}=\tfrac{1}{2}(\mathbf{r}_v)_{SO_2}=(k\eta)a_c C_s \qquad (A)$$

† Hiroshi Komiyama and J. M. Smith, *AIChE J.*, **21**, 664 (1975).

where $k = 0.0033 \times 10^{-2}$ m/s
$\eta = 0.86$†(for $d_p = 3 \times 10^{-5}$ m)
C_s = concentration of oxygen in the liquid at a carbon site, kg mol/m^3

SOLUTION For 70% conversion, the concentration of SO_2 in the gas will decrease by 2.3 (0.7) = 1.6 mol/(100 mole of gas). By the reaction

$$SO_2 + \tfrac{1}{2}O_2 \rightarrow SO_3$$

the oxygen concentration will change by $\frac{1}{2}(1.6)$ mol. Hence, the oxygen concentration will fall from 97.7(0.21) = 20.5% to 20.2%. This small change will not affect the rate significantly. We may use a constant, arithmetic average value of 20.3%, and in so doing introduce less error than the uncertainty in the various rate constants. The kinetics are independent of the SO_2 concentration. This means that the rate will be the same throughout the reactor. Then Eq. (13-52) can be immediately integrated to give

$$V = F_A \frac{(x_e - 0)}{\mathbf{r}_v} = \frac{F_A x_e}{\mathbf{r}_s} \tag{B}$$

The product $F_A x_e$ is equal to the moles reacted in the entire reactor per unit time. We can express this product as $Q_g C_{gf} x_e$ and evaluate it in terms of either SO_2 or O_2, as long as $\mathbf{r}_v$ is on the same basis. In terms of SO_2, Eq. (B) becomes

$$V = \frac{Q_g (C_{gf})_{SO_2} (x_e)_{SO_2}}{(\mathbf{r}_v)_{SO_2}} \tag{C}$$

The required volume is calculable from Eq. (C) once the global rate has been determined.

Since oxygen is but slightly soluble in water at 25°C, the resistance for mass transfer from gas to liquid is determined by the liquid-side coefficient k_L. Also, Henry's law is valid for oxygen in water at 25°C. [H = 35.4(mol/cm^3 of gas)/(mol/cm^3 of liquid)]. Then Eqs. (10-40) and (10-41) give the global rate in terms of the two mass-transfer coefficients k_L, k_c, and the intrinsic rate constant ($k\eta$). For spherical carbon particles and spherical gas bubbles, using Eqs. (C) and (10-50) of Example 10-7,

$$a_c = \frac{6m_s}{d_p \rho_p} = \frac{6(70)}{3 \times 10^{-5}(0.80 \times 10^3)} = 175 \times 10^2 \text{ m}^2/\text{m}^3$$

$$a_g = \frac{6}{d_b} V_B = \frac{6}{3 \times 10^{-3}}(0.08) = 1.6 \times 10^2 \text{ m}^2/\text{m}^3$$

Then Eq. (10-40) becomes

$$\frac{1}{k_o H} = \frac{175}{1.6}\left(\frac{1}{k_L}\right) + \frac{1}{k_c} + \frac{1}{k\eta} \tag{D}$$

† For 0.03-mm particles the effectiveness factor in the liquid-filled pores of activated carbon was found to be 0.86 (loc. cit.)

We could estimate k_L and k_c from Eq. (10-42) and Fig. 10-10. However, conditions are essentially the same as in Example 10-7. In that example, for bubbles of the same size, k_L was found to be 0.08×10^{-2} m/s. The liquid-to-particle coefficient was $k_c = 0.027 \times 10^{-2}$ m/s for 0.542-mm particles. According to Fig. 10-10, the effect of particle size on k_c is very small (the effects of d_p on Re and on Sh about cancel each other). Using these values and the intrinsic rate constant, Eq. (D) gives

$$\frac{1}{k_o H} = \frac{175}{1.6}\left(\frac{10^2}{0.08}\right) + \frac{10^2}{0.027} + \frac{10^2}{0.86(0.0033)}$$

$$= (1370 + 37 + 352) \times 10^2 = 1759 \times 10^2$$

$$k_o H = 5.7 \times 10^{-6} \text{ m/s}$$

The global rate from Eq. (10-41) is

$$(r_v)_{O_2} = k_o a_c H(C_L) = (k_o H) a_c [(C_g)_{O_2}/H]$$

Substituting numerical values,

$$(r_v)_{SO_2} = 2(r_v)_{O_2} = 2(5.7 \times 10^{-6})(175 \times 10^2)\left[\frac{1(0.203) \times 10^3}{82(298)35.4}\right]$$

$$= 4.68 \times 10^{-5} \text{ kg mol/(s)(m}^3 \text{ of liquid)}$$

With this global rate, Eq. (C) gives for the required volume of water

$$V = \frac{2.75\left[\frac{1(0.023)}{82(298)} \times 10^3\right]0.7}{4.68 \times 10^{-5}} = 39 \text{ m}^3$$

In this example, mass transfer from gas to liquid has a greater effect on the global rate than either liquid-to-particle mass transfer or the intrinsic rate. The relatively small effect of liquid-to-particle mass transfer is due to the large ratio, $a_c\ a_g$, which is over 100 (i.e., 175/1.6). For lower concentrations of particles this ratio would decrease. Also, larger carbon particles would increase the resistance of liquid-to-particle mass transport. Note that the resistance to the reaction at a site also would become relatively larger, because η decreases as d_p increases. For example, it was found† that η decreased from 0.86 to 0.098 when the particle size increased from 0.03 to 0.54 mm.

It should not be inferred from Examples 13-9 and 13-10 that diffusion from the bubble to the bulk liquid always controls the global rate. For example, data for different slurry reactions given by Sherwood and Farkas‡ show other results. For the hydrogenation of α-methyl styrene containing a slurry of palladium black (diameter 55 microns), the global rate was controlled by k_L and k_c, with the significance of k_L decreasing at low catalyst concentrations. For catalyst concentrations below about 0.5 g of catalyst per liter of slurry, and at temperatures less

† Hiroshi Komiyama and J. M. Smith, loc. cit.

‡ T. K. Sherwood and E. J. Farkas, *Chem. Eng. Sci.*, **21**, 573 (1966).

than 30°C, the rate of diffusion of dissolved hydrogen to the catalyst particles (that is, k_c) essentially controlled the rate. Results for the hydrogenation of cyclohexene in an aqueous suspension of 30-micron palladium-black particles indicated again that the predominant resistance was the diffusion to catalyst particles. However, the data of Kolbel and Maennig† for the slower hydrogenation of ethylene in a slurry of Raney nickel particles in a paraffin oil show different results. Here the catalyst particles were small enough (5 microns) and their concentration high enough that $k_c a_c$ was very large. Sherwood and Farkas were able to correlate these data by assuming that the chemical step on the catalyst particles controlled the rate.

TRICKLE-BED REACTORS

In Chap. 10 we discussed the characteristics of cocurrent down-flow of gas and liquid over a fixed bed of catalyst particles (see Fig. 10-16). In Secs. 10-10 to 10-12, correlations were presented for mass transfer from gas to liquid and from liquid to solid for the trickling-flow regime (continuous gas phase and liquid rivulets cascading *down* over the particles). Now we wish to use this information, along with intrinsic kinetics and a reactor model, to predict the behavior of trickle-bed reactors. Since the catalyst particle sizes in these reactors are relatively large, intraparticle resistances will be more significant than for slurry reactors. On the other hand, there is no difficulty in retaining the large particles in the bed, in contrast to the situation in slurries.

As in Chap. 10, the treatment will be limited to the trickling flow regime and to isothermal operation. Also, it will be assumed that flowing liquid completely covers the particles so that reaction can occur only by reactant mass transfer through the liquid-particle interface. Isothermal conditions and complete liquid coverage are reasonable assumptions for many trickle-bed processes, except at very low liquid rates. Capillary forces normally draw liquid into the pores of the particles. Therefore, in evaluating intraparticle mass-transfer effects (effectiveness factors) it is satisfactory to use liquid-phase diffusivities.

The main need for three-phase reactors is when one reactant is too volatile to liquefy and a second is too nonvolatile to vaporize. Hence, the main emphasis will be for the case of a gaseous component reacting with a second reactant in the liquid phase; that is for a reaction of the form:

$$aA(g) + B(l) \rightarrow C(g \text{ or } l) + D(g \text{ or } l) \qquad (13\text{-}54)$$

This general form would include hydrogenation (e.g., hydrodesulfurization of petroleum fractions, hydrogenation of oils) and oxidation (oxidation of pollutants dissolved in liquids) reactions.

† H. Kolbel and H. G. Maennig, *Elektrochem.*, 66, 744 (1962).

13-13 Trickle-Bed Reactor Model

For isothermal operation and uniform distribution of gas and liquid phases across the reactor diameter, there will be no radial gradients of concentration or velocity for the gas or liquid, except on a particle-size scale. Of course there will be concentration and velocity changes near the phase boundaries, as shown in Fig. 10-14. However, the concentrations and velocities will be the same in the *bulk* fluid at any radial position if the flow distribution is uniform.†

With no radial gradients, a one-dimensional, isothermal model is adequate. The mass-conservation equations are of the same form as those developed in Sec. 13-10 for the "two-phase," fluid-bed reactor, except that equations must be written for both reactants A and B. For most applications axial dispersion in the gas phase is negligible, and such dispersion may be unimportant in the liquid.‡ Let us write the conservation equations for plug-flow of gas and use a dispersion model (with axial dispersion coefficient D_L) for the liquid. For reactant A in the gas phase, at steady state, and for a volume element that extends across the reactor (Fig. 13-23),

$$u_g \frac{d(C_A)_g}{dz} + (K_L a_g)_A[(C_A)_g/H_A - (C_A)_L] = 0 \tag{13-55}$$

where $(C_A)_g/H_A$ is the liquid-phase concentration in equilibrium with the bulk gas concentration; K_L is an *overall* mass-transfer coefficient between gas and liquid; u_g is the superficial velocity of the gas. Since Henry's law has been assumed to be applicable for A, K_L is related to the individual films coefficients k_L and k_g by the equation:

$$\frac{1}{K_L} = \frac{1}{Hk_g} + \frac{1}{k_L} \tag{13-56}$$

As noted in Chap. 10, for many trickle-bed processes, A is slightly soluble in the liquid (H is large) so that $K_L \approx k_L$.

For reactant A in the liquid phase, the conservation equation is

$$D_L \frac{d^2(C_A)_L}{dz^2} - u_L \frac{d(C_A)_L}{dz} + (K_L a_g)_A[(C_A)_g/H_A - (C_A)_L] - (k_c a_c)_A[(C_A)_L - (C_A)_s] = 0 \tag{13-57}$$

† In a trickle bed, the gas is distributed uniformly across the diameter, but the liquid tends to flow toward the reactor wall. Approximately, a reactor-to-particle diameter ratio of 18 or more will ensure uniform liquid distribution. Correlations for predicting the flow distribution and the catalyst bed depth required to achieve the equilibrium distribution are available [Mordechay Herskowitz and J. M. Smith, *AIChE J.*, **24**, 439 (1978)].

‡ Criteria for the importance of axial dispersion are available, e.g., D. E. Mears, *Chem. Eng. Sci.*, **26**, 1361 (1971).

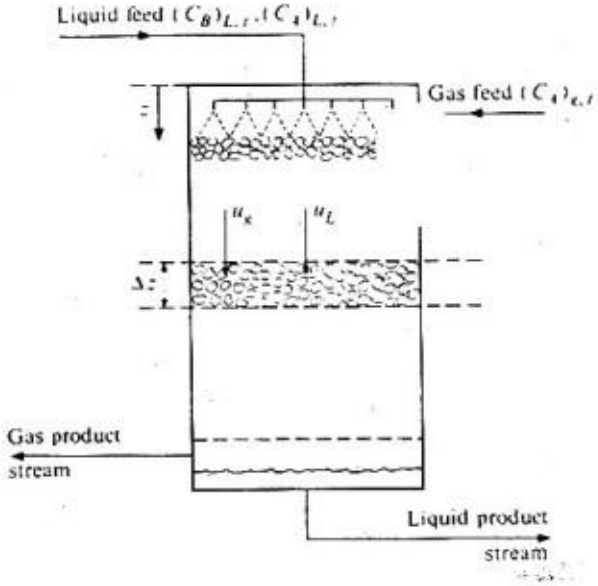

Figure 13-23 Trickle-bed for catalytic reaction $aA(g) + B(l) \rightarrow$ product.

which includes terms for mass transfer from gas-to-liquid and from liquid-to-particle (coefficient $k_c a_c$). The third mass-conservation equation needed is that for reactant B in the liquid phase:

$$(D_L)_B \frac{d^2(C_B)_L}{dz^2} - u_L \frac{d(C_B)_L}{dz} - (k_c a_c)_B[(C_B)_L - (C_B)_s] = 0 \qquad (13\text{-}58)$$

Here it has been assumed that B is nonvolatile. The velocity u_L is the superficial value for the liquid, and $(C)_s$ is the liquid-phase concentration at the outer surface of the catalyst particle. The areas per unit volume of empty reactor a_g and a_c are the same as those used in Secs. 10-10 to 10-12.

The reaction rate expressed in terms of surface concentrations provides the relationship between $(C)_s$ and $(C)_L$. From the definition of the effectiveness factor η in Chap. 11 [Eq. (11-42)], we may express the required equality of mass-transfer and reaction rates, $\mathbf{r}_A$ and $\mathbf{r}_B$ as

$$(k_c a_c)_A[(C_A)_L - (C_A)_s] = \mathbf{r}_A = \rho_B \eta f[(C_A)_s, (C_B)_s] \qquad (13\text{-}59)$$

$$(k_c a_c)_B[(C_B)_L - (C_B)_s] = \mathbf{r}_B = \frac{\mathbf{r}_A}{a} = \frac{\rho_B}{a} \eta f[(C_A)_s, (C_B)_s] \qquad (13\text{-}60)$$

where $f[(C_A)_s, (C_B)_s]$ represents the intrinsic rate of reaction, per unit mass of catalyst, for the disappearance of A, and ρ_B is the bulk density of the catalyst particles in the bed.

With appropriate boundary conditions, the five equations [Eqs. (13-55), (13-57) to (13-60)] can be solved for the five concentrations, $(C_A)_g$, $(C_A)_L$, $(C_B)_L$, $(C_A)_s$, $(C_B)_s$ as a function of reactor bed depth z. It is necessary to know all the

mass-transfer coefficients, the intrinsic rate equation, $f[C_A, C_B]$, and the effectiveness factor.

The problem becomes much simpler (an initial-value rather than a boundary-value problem) if axial dispersion in the liquid can be neglected (plug flow of liquid). Then the terms involving the second derivative in Eqs. (13-57) and (13-58) can be omitted. The boundary conditions for the three first-order equations [Eqs. (13-55), (13-57), and (13-58) with dispersion terms omitted] are, at $z = 0$,

$$(C_A)_g = (C_A)_{g,f} \quad \left.\right\} \text{ feed concn} \qquad (13\text{-}61)$$

$$(C_A)_L = (C_A)_{L,f} \quad \left.\right\} \text{ feed concn} \qquad (13\text{-}62)$$

$$(C_B)_L = (C_B)_{L,f} \quad \left.\right\} \text{ feed concn} \qquad (13\text{-}63)$$

Both the axial dispersion and plug-flow models have been solved and compared with experimental data for the oxidation of aqueous solutions of formic† and of acetic acids with air.‡ Plug-flow solutions for design of trickle-bed reactors are illustrated in the examples that follow. When the intrinsic kinetics are first order, analytical solutions for the conversion are possible. Otherwise, the set of differential equations must be solved numerically.

Example 13-11 A hydrocarbon oil is to be desulfurized prior to catalytic cracking. Of the various sulfur compounds present (mercaptans, sulfides, disulfides, etc.) one of the most difficult to desulfurize is thiophene. With a sulfided, cobalt-molybdenum oxide catalyst on alumina, thiophene reacts with hydrogen to form butane and H_2S.

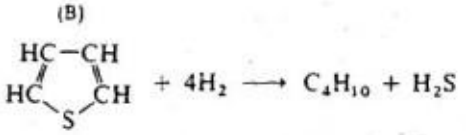

A trickle-bed reactor is to be designed on the supposition that if the refractory thiophene is reacted, the other sulfur compounds will also have been hydrogenated.

Pure hydrogen and the hydrocarbon liquid will be fed to the top of the catalyst bed, operating at 200°C and 40 atm. Neglect the vaporization of thiophene from the liquid at these conditions.

A. For the first case assume that the reaction rate at the catalyst sites and the mass-transfer rate from liquid to catalyst particle are slow enough that the liquid is saturated with hydrogen throughout the column. While the reaction probably is second order, assume that the thiophene concentration is relatively large with respect to that of hydrogen dissolved in the oil. Then the intrinsic rate will be pseudo-first-order in hydrogen. Also, the intrinsic rate is slow enough that the effectiveness factor is unity. Derive an expression for the

† S. Goto and J. M. Smith, *AIChE J.*, **21**, 706 (1975).
‡ J. Levec and J. M. Smith, *AIChE J.*, **22**, 159 (1976).

fractional removal (conversion) of thiophene from the oil, assuming plug flow of liquid.

B. For very low thiophene concentrations the intrinsic kinetics will become first order in C_B. Consider the extreme case where the intrinsic rate is independent of hydrogen concentration. What will be the expression for the fractional removal of thiophene?

C. Calculate the catalyst bed depth required, for conditions of parts A and B, to remove 75% of the thiophene. For part A, the feed concentration of thiophene is 1000 ppm and for part B suppose it is 100 ppm. The superficial liquid velocity will be 5.0 cm/s. The first-order rate constants are $k_H = 0.11$ cm^3/(g)(s), and $k_B = 0.07$ cm^3/(g)(s), and the volumetric mass-transfer coefficients from liquid to particle are $(k_c a_c)_{H_2} = 0.50\ s^{-1}$ and $(k_c a_c)_B = 0.3\ s^{-1}$ (estimated from correlations in Sec. 10-11), $\rho_B = 0.96$ g/cm^3.

SOLUTION

A. Since the liquid is saturated with hydrogen, and pure hydrogen is used as the gas stream, Eqs. (13-57) and (13-55) are not needed; the concentration of hydrogen in the liquid $(C_{H_2})_L$ is a constant and equal to $(C_{H_2})_g/H_{H_2}$. Further, the intrinsic rate is independent of the thiophene concentration so that the function, $f[(C_A)_s, (C_B)_s]$, is the first-order form:

$$f[(C_A)_s, (C_B)_s] = k_H(C_{H_2})_s \tag{A}$$

Then Eq. (13-59) for hydrogen is

$$(k_c a_c)_{H_2}[(C_{H_2})_L - (C_{H_2})_s] = \rho_B k_H (C_{H_2})_s$$

or

$$(C_{H_2})_s = \frac{(k_c a_c)_{H_2}}{(k_c a_c)_{H_2} + \rho_B k_H}(C_{H_2})_L = \frac{(k_c a_c)_{H_2}}{(k_c a_c)_{H_2} + \rho_B k_H}\left[\frac{(C_{H_2})_g}{H_{H_2}}\right] \tag{B}$$

Hence, Eq. (13-60) for thiophene (B) may be written

$$(k_c a_c)_B[(C_B)_L - (C_B)_s] = \frac{\rho_B}{4}\frac{(k_c a_c)_{H_2} k_H}{(k_c a_c)_{H_2} + \rho_B k_H}\left[\frac{(C_{H_2})_g}{H_{H_2}}\right] \tag{C}$$

Since $(C_{H_2})_g$ is constant, Eq. (C) shows that the rate of mass transfer of thiophene from liquid to particle (and the rate of reaction) is the same throughout the reactor. Equation (C) can be substituted in Eq. (13-58) and the result easily integrated to determine how C_B varies with catalyst bed depth. Thus, for plug flow of liquid, Eq. (13-58) becomes

$$u_L \frac{d(C_B)_L}{dz} + \tfrac{1}{4}(k_H^\circ)\frac{(C_{H_2})_g}{H_{H_2}} = 0 \tag{D}$$

where the overall coefficient is given by

$$\frac{1}{k_H^\circ} = \frac{1}{(k_c a_c)_{H_2}} + \frac{1}{\rho_B k_H} \tag{E}$$

The boundary (feed) condition is $(C_B)_L = (C_B)_{L,f}$ at $z = 0$. Then the integrated form of Eq. (D) is

$$(C_B)_L - (C_B)_{L,f} = -\left(\frac{k_H^\circ z}{4u_L}\right)\frac{(C_{H_2})_g}{H_{H_2}}$$

and the fractional removal of thiophene is

$$x = \frac{(C_B)_{L,f} - (C_B)_L}{(C_B)_{L,f}} = \left(\frac{k_H^\circ z}{4u_L}\right)\frac{(C_{H_2})_g/H_{H_2}}{(C_B)_{L,f}} \tag{F}$$

where z is the catalyst bed depth.

B. In this case the intrinsic rate function (for *thiophene*) becomes

$$f[(C_A)_s, (C_B)_s] = k_B(C_B)_s \tag{G}$$

Now, Eq. (13-59) for hydrogen is not involved. Equation (13-60) may be written

$$(k_c a_c)_B[(C_B)_L - (C_B)_s] = \rho_B k_B (C_B)_s$$

or

$$(C_B)_s = \frac{(k_c a_c)_B}{(k_c a_c)_B + \rho_B k_B}(C_B)_L \tag{H}$$

Substituting this result in Eq. (13-58) gives, for plug flow of liquid,

$$u_L\frac{(dC_B)_L}{dz} + k_B^\circ(C_B)_L = 0 \tag{I}$$

where, now,

$$\frac{1}{k_B^\circ} = \frac{1}{(k_c a_c)_B} + \frac{1}{\rho_B k_B} \tag{J}$$

Integrating Eq. (I) with the boundary condition at $z = 0$ gives

$$x = 1 - \exp\left(-\frac{k_B^\circ z}{u_L}\right) \tag{K}$$

C. For part A, Eq. (F) is applicable. The hydrogen concentration at 40 atm and 200°C is

$$(C_{H_2})_g = \frac{P_{H_2}}{RT} = \frac{40}{82(473)} = 1.03 \times 10^{-3} \text{ g mol/cm}^3$$

From hydrogen solubility data it is estimated that H_{H_2} at 200°C is 50[g mol/(cm^3 gas)]/[g mol/(cm^3 in liquid)]. From the rate constant data and Eq. (E),

$$\frac{1}{k_H^\circ} = \frac{1}{0.50} + \frac{1}{0.96(0.11)} = 11.5 \text{ s}$$

The concentration of thiophene in the feed (100 ppm) is $(1000/84) \times 10^{-6} = 1.19 \times 10^{-5}$ g mol/cm^3. Substituting these results in Eq. (F) gives

$$z = x\left(\frac{4u_L}{k_H^\circ}\right)\frac{(C_B)_{L,f}}{(C_{H_2})_g/H} = 0.75\,\frac{4(5)}{(1/11.5)}\,\frac{1.19 \times 10^{-5}}{1.03 \times 10^{-3}/50}$$

$$z = 100 \text{ cm}$$

For part B, we first must calculate k_B° for thiophene. From data given, Eq. (J) gives

$$\frac{1}{k_B^\circ} = \frac{1}{0.3} + \frac{1}{0.96(0.07)} = 18.2 \text{ s}$$

Then Eq. (K) is applicable:

$$0.75 = 1 - \exp\left[-\frac{(1/18.2)z}{(5)}\right]$$

Solving for z yields

$$z = 126 \text{ cm}$$

Example 13-12 Reconsider Example 13-11, part A, but do not assume that the liquid is saturated with hydrogen. The hydrogen concentration in the feed liquid is zero, and the gas-to-liquid mass-transfer coefficient is $(K_L a_g)_{H_2} = (k_L a_g)_{H_2} = 0.030 \text{ s}^{-1}$.

Derive an expression for the fractional removal of thiophene. Also calculate the bed depth required for removal of 75% of the thiophene for the conditions of Example 13-11.

SOLUTION Since pure hydrogen is used, Eq. (13-55) is again unnecessary; $(C_{H_2})_g$ is constant and equal to the value in the feed. Equation (13-57) for plug flow of liquid becomes

$$-u_L\frac{d(C_{H_2})_L}{dz} + (K_L a_g)_{H_2}\left[\frac{(C_{H_2})_g}{H_{H_2}} - (C_{H_2})_L\right] - (k_c a_c')_{H_2}[(C_{H_2})_L - (C_{H_2})_s] = 0 \tag{A}$$

For the first-order (in hydrogen) kinetics, Eq. (A) of Example 13-11 is applicable. Then, $(C_{H_2})_s$ from Eq. (13-159) is

$$(C_{H_2})_s = \frac{(k_c a_c)_{H_2}}{(k_c a_c)_{H_2} + \rho_B k_H}(C_{H_2})_L \tag{B}$$

Using this expression for $(C_{H_2})_s$, we may write

$$(C_{H_2})_L - (C_{H_2})_s = \frac{\rho_B k_H}{(k_c a_c)_{H_2} + \rho_B k_H}(C_{H_2})_L \tag{C}$$

Then Eq. (A) may be written solely in terms of $(C_{H_2})_L$ as a variable:

$$-u_L\frac{d(C_{H_2})_L}{dz}+(K_La_g)_{H_2}\left[\frac{(C_{H_2})_g}{H_{H_2}}-(C_{H_2})_L\right]-k_H^\circ(C_{H_2})_L=0 \qquad \text{(D)}$$

where k_H° is given by Eq. (E) of Example 13-11.

Equation (D) can be integrated to give the following equation for $(C_{H_2})_L$ as a function of z:

$$(C_{H_2})_L=\frac{(C_{H_2})_g/H_{H_2}}{1+[k_H^\circ/(K_La_g)_{H_2}]}\left\{1-\exp\left[-\{(K_La_g)_{H_2}+k_H^\circ\}\frac{z}{u_L}\right]\right\} \qquad \text{(E)}$$

Next we want to integrate Eq. (13-58) to find the thiophene concentration at any bed depth. To do this the surface concentration in the term in brackets must be eliminated. This is done by using Eq. (13-60). Thus, from Eq. (B) and Eq. (A) of Example (13-11), Eq. (13-60) becomes

$$(k_ca_c)_B[(C_B)_L-(C_B)_s]=\frac{\rho_Bk_H}{4}(C_{H_2})_s=\frac{\rho_Bk_H}{4}\frac{(k_ca_c)_{H_2}}{(k_ca_c)_{H_2}+\rho_Bk_H}(C_{H_2})_L$$

$$=\frac{k_H^\circ}{4}(C_{H_2})_L \qquad \text{(F)}$$

Substituting Eq. (E) for $(C_{H_2})_L$ in Eq. (F),

$$(k_ca_c)_B[(C_B)_L-(C_B)_s]=\frac{k_H^\circ(C_{H_2})_g/H_{H_2}}{4(1+\{k_H^\circ/(K_La_g)_{H_2}\})}$$

$$\times\left\{1-\exp\left[-\{(K_La_g)_{H_2}+k_H^\circ\}\frac{z}{u_L}\right]\right\} \qquad \text{(G)}$$

$$=\alpha[1-\exp(-\beta z)] \qquad \text{(H)}$$

where α and β are constants defined by comparing Eqs. (G) and (H).

Now we can use Eq. (H) to write Eq. (13-58), for plug flow of liquid, in terms of only $(C_B)_L$:

$$u_L\frac{d(C_B)_L}{dz}+\alpha[1-\exp(-\beta z)]=0 \qquad \text{(I)}$$

Integrating, with the boundary condition $(C_B)_L=(C_B)_{L,f}$ at $z=0$, gives

$$(C_B)_L-(C_B)_{L,f}=-\alpha\frac{z}{u_L}-\frac{\alpha}{\beta u_L}(e^{-\beta z}-1)$$

In terms of fractional removal of thiophene this is

$$x=\frac{\alpha}{(C_B)_{L,f}}\left[\left(\frac{z}{u_L}\right)+\frac{1}{\beta u_L(C_B)_{L,f}}(e^{-\beta z}-1)\right] \qquad \text{(J)}$$

If the expressions for α and β are inserted, Eq. (J) becomes,

$$x=\frac{k_H^\circ[(C_{H_2})_g/H_{H_2}(C_B)_{L,f}]}{4[1+\{k_H^\circ/(K_La_g)_{H_2}\}]}\left\{\frac{z}{u_L}+\frac{\exp[-\{(K_La_g)_{H_2}+k_H^\circ(z/u_L)\}]-1}{[(K_La_g)_{H_2}+k_H^\circ]}\right\} \qquad \text{(K)}$$

From Example 13-11, $k_H^\circ = 1/11.5 = 0.087$ s, $(C_{H_2})_g = 1.03 \times 10^{-3}$ g mol/cm^3, and $(C_B)_{L,f} = 1.19 \times 10^{-6}$ g mol/cm^3. Substituting these values in Eq. (K),

$$x = 0.75$$

$$0.75 = \frac{0.087[(1.03 \times 10^{-3}/50)1.19 \times 10^{-5}]}{4[1 + (0.087/0.030)]} \times \left\{\frac{z}{5} + \frac{\exp -(0.03 + 0.087)(z/5) - 1}{0.03 + 0.087}\right\}$$

$$77.7 = \frac{z}{5} + 8.55(e^{-0.023z} - 1)$$

Solving this expression for z gives

$$z = 430 \text{ cm}$$

All of the increase from 100 (obtained in Example 13-11) to 430 cm is not due to the mass-transfer resistance between gas and liquid. In Example 13-11 it was supposed that the liquid was always saturated with hydrogen. In the present example, the concentration of hydrogen in the liquid feed was taken as zero. If the boundary condition for Eq. (D) were the saturated condition, $(C_{H_2})_L = (C_{H_2})_{g,f}/H_{H_2}$ at $z = 0$. Then, the bed depth required is $z = 270$ cm. The increase in z from 100 to 270 cm is the result of the mass-transfer resistance from gas to particle. The change from 430 to 270 cm reflects the effect of saturating the hydrocarbon liquid with hydrogen before it enters the reactor.

In the previous two examples, the gas-phase conservation expression [Eq. (13-55)] was not needed, because the gas was pure hydrogen. This is not so when a trickle-bed reactor is used to remove pollutants from a gas stream. Example 13-13 is an illustration of this type of application.

Example 13-13 Sulfur dioxide is to be removed from air in a bed of activated carbon particles at 25°C and 1 atm pressure. The reactor will be of the trickle-bed type in which the gas stream, containing 3% SO_2, 18% O_2, and 79% N_2, and pure water are fed to the top of the reactor. Activated carbon catalyzes the oxidation of SO_2 to SO_3, and the SO_3 dissolves in the water to produce H_2SO_4. It has been suggested† that the intrinsic rate of reaction is controlled by the rate of adsorption of oxygen on the carbon and is independent of the SO_2 concentration.

Derive equations for steady-state operation which give the fraction of the SO_2 from the gas stream removed by reaction, as a function of the catalyst bed depth. Assume that liquid and gas streams are in plug flow and that the feed water is in equilibrium with the gas feed with respect to oxygen. To simplify the mass balances written for the *entire* reactor, neglect the difference in oxygen content of the liquid feed and effluent streams.

† Hiroshi Komiyama and J. M. Smith, *AIChE J.*, 21, 664 (1975).

SOLUTION Equations (13-55) and (13-57) with the second derivative omitted, and Eq. (13-59) are applicable when applied to oxygen. For simplicity, we omit the subscript A so that C designates the oxygen concentration. The intrinsic rate function is

$$r_{O_2} = \rho_B \eta f[(C_A)_s, (C_B)_s] = \rho_B \eta k C_s \tag{A}$$

Then Eq. (13-59) becomes

$$(k_c a_c)(C_L - C_s) = \rho_B \eta k C_s$$

Solving for C_s,

$$C_s = \frac{k_c a_c}{k\eta\rho_B + k_c a_c} C_L = \alpha C_L \tag{B}$$

If this value for C_s is substituted into Eq. (13-57), with the second derivative omitted, there is obtained

$$-u_L \frac{dC_L}{dz} + K_L a_g \left(\frac{C_g}{H} - C_L\right) - k_c a_c (1 - \alpha) C_L = 0 \tag{C}$$

Equation (13-55) may be rearranged to the form

$$\frac{C_g}{H} - C_L = -\left(\frac{u_g}{K_L a_g}\right)\frac{dC_g}{dz} \tag{D}$$

or

$$C_L = \frac{C_g}{H} + \left(\frac{u_g}{K_L a_g}\right)\frac{dC_g}{dz} \tag{E}$$

Differentiation of Eq. (E) yields

$$\frac{dC_L}{dz} = \left(\frac{1}{H}\right)\frac{dC_g}{dz} + \left(\frac{u_g}{K_L a_g}\right)\frac{d^2 C_g}{dz^2} \tag{F}$$

If Eqs. (D), (E), and (F) are substituted in (C), a second-order equation is obtained with C_g as the only dependent variable. The expression may be written:

$$\frac{d^2 C_g}{dz^2} + \beta \frac{dC_g}{dz} + \gamma C_g = 0 \tag{G}$$

where the constant coefficients are

$$\beta = \frac{u_g + u_L/H + k_c a_c (1 - \alpha) u_g / K_L a_g}{u_L u_g / K_L a_g} \tag{H}$$

$$\gamma = \frac{(k_c a_c) K_L a_g (1 - \alpha)}{H u_L u_g} \tag{I}$$

$$\alpha = k_c a_c / (k\eta\rho_B + k_c a_c) \tag{J}$$

The boundary conditions (for oxygen) are

$$\text{at } z = 0, \qquad C_g = C_{g,f} \tag{K}$$

$$C_L = C_{g,f}/H \qquad \text{(equilibrium)} \tag{L}$$

Boundary condition (L) can be written in terms of C_g by applying Eq. (E) at $z = 0$. This gives

$$\text{at } z = 0, \qquad \frac{dC_g}{dz} = 0 \tag{M}$$

Equation (G) with boundary conditions (K) and (M) can be solved by standard methods to give

$$\left(\frac{C_g}{C_{g,f}}\right)_{O_2} = \frac{1}{m_2 - m_1}\left[m_2 e^{m_1 z} - m_1 e^{m_2 z}\right] \tag{N}$$

where

$$m_1 = -\frac{\beta}{2} + \frac{1}{2}(\beta^2 - 4\gamma)^{1/2} \tag{P}$$

$$m_2 = -\frac{\beta}{2} - \frac{1}{2}(\beta^2 - 4\gamma)^{1/2} \tag{Q}$$

The reactions involved are

$$SO_2 + \tfrac{1}{2}O_2 \rightarrow SO_3$$

$$SO_3 + H_2O \rightarrow H_2SO_4$$

Neglecting the change in O_2 concentration of the liquid between feed and effluent, the first reaction requires that the SO_2 removed from the gas stream by reaction be twice that of oxygen; that is,

$$(C_{g,f} - C_g)_{SO_2} = 2(C_{g,f} - C_g)_{O_2}$$

Then the fractional removal of SO_2 is

$$\left(\frac{C_{g,f} - C_g}{C_{g,f}}\right)_{SO_2} = 2\frac{(C_{g,f})_{O_2}}{(C_{g,f})_{SO_2}}\left[1 - \left(\frac{C_g}{C_{g,f}}\right)_{O_2}\right] \tag{R}$$

Equation (R) with Eq. (N) for $(C_g/C_{g,f})_{O_2}$ can be used to calculate the fractional removal of SO_2 from the gas by reaction. This does not account for the SO_2 that might be removed in the effluent liquid. Problem 13-23 is a numerical illustration for this type of trickle-bed reactor.

A more realistic approach to the hydrodesulfurization process in Examples 13-11 and 13-12 would have been to use nonlinear kinetics, particularly when the concentrations of thiophene and hydrogen in the liquid are of the same magnitude. However, an analytical solution for the effluent concentrations cannot be obtained. Another example of nonlinear kinetics is the catalytic oxidation of aqueous solutions of formic acid. The kinetics of the reaction

$$HCOOH(aq) + \tfrac{1}{2}O_2(g) \rightarrow H_2O(l) + CO_2$$

using a CuO·ZnO catalyst have been found† to be second order with a rate equation

$$r_{O_2} = \eta \rho_B k_{O_2} (C_{O_2})_s (C_F)_s$$

where $(C_F)_s$ represents the concentration of formic acid in the liquid at the catalyst site. For this case the five equations (13-55) and (13-57) to (13-60) become, for plug flow of liquid:

$$u_g \frac{d(C_{O_2})_g}{dz} + (K_L a_g)_{O_2} \left[\frac{(C_{O_2})_g}{H_{O_2}} - (C_{O_2})_L \right] = 0 \tag{13-64}$$

$$-u_L \frac{d(C_{O_2})_L}{dz} + (K_L a_g)_{O_2} \left[\frac{(C_{O_2})_g}{H_{O_2}} - (C_{O_2})_L \right] - (k_c a_c)_{O_2} [(C_{O_2})_L - (C_{O_2})_s] = 0 \tag{13-65}$$

$$-u_L \frac{d(C_F)_L}{dz} - (k_c a_c)_F [(C_p)_L - (C_F)_s] = 0 \tag{13-66}$$

$$(k_c a_c)_{O_2} [(C_{O_2})_L - (C_{O_2})_s] = r_{O_2} = \eta \rho_B k_{O_2} (C_{O_2})_s (C_F)_s \tag{13-67}$$

$$(k_c a_c)_F [(C_F)_L - (C_F)_s] = 2 r_{O_2} = 2 \eta \rho_B k_{O_2} (C_{O_2})_s (C_F)_s \tag{13-68}$$

The required boundary conditions are the feed concentrations; that is, Eqs. (13-61) to (13-63) with $A = O_2$ and $B =$ formic acid.

These equations can be solved numerically in the following way. Starting at $z = 0$ where $(C_F)_L$ and $(C_{O_2})_L$ are known, calculate $(C_F)_s$ and $(C_{O_2})_s$. Then Eqs. (13-64) to (13-66) can be solved for the first increment, for example by the Runge-Kutta method, to give $(C_{O_2})_g$, $(C_{O_2})_L$ and $(C_F)_L$ at the end of the increment chosen for z. Repetition of the process ultimately gives the concentrations at any bed depth.

A complication arises if intraparticle diffusion is not negligible (i.e., $\eta \neq 1.0$). This is because η is a function of the surface concentrations when the intrinsic kinetics are not first order (see Fig. 11-8). This means that η will vary with bed depth. A method of accounting for this variation is available‡ as well as a detailed description of the solution procedure for the concentration profiles in the reactor. For the linear kinetics considered in Example 13-13, this complication did not exist. The effectiveness factor is independent of concentration [Fig. 11-8 or Eq. (11-52)] so that η is a constant throughout the reactor.

We have not discussed countercurrent flow in packed-bed reactors. The equations for predicting the performance for this flow arrangement are essentially the same (only the signs of some of the terms in the conservation equations are different) as those for trickle beds, and the results are similar. A comparison has been made of the performance of slurries, trickle-beds and countercurrent packed beds as examples of 3-phase reactors.§ The three types were compared for the

† G. Baldi, S. Goto, C. K. Chow, and J. M. Smith, *Ind. Eng. Chem., Proc. Des. Dev.*, **13**, 447 (1974).
‡ S. Goto and J. M. Smith, *AIChE J.*, **21**, 706 (1975).
§ S. Goto and J. M. Smith, *AIChE J.*, **24**, 286 (1978).

removal of SO_2 from a gas stream. The differences in performance are due primarily to the different values for the mass transfer effects. For the same reactor volume and flow rates, the countercurrent packed bed gave somewhat higher SO_2 removal. For the same mass of catalyst, the slurry reactor gave the greatest removal. Practical factors, such as the problem of retaining small particles in the slurry reactor, were not considered.

OPTIMIZATION

Although we shall not consider the quantitative aspects of optimization, some general comments are necessary in order to give proper emphasis to the material that has been covered. As indicated in Sec. 1-1, the purpose of this text has been to present the concepts necessary to design a reactor. We started with chemical kinetics (Chap. 2) and then discussed physical processes in terms of the process-design features of large-scale reactors, first for homogeneous reactions (Chaps. 3 to 6) and then for heterogeneous catalytic reactions (Chaps. 7 to 13). The general approach was that the reactor form was known, and the objective was to predict the performance for a single set of operating conditions. Nevertheless, aspects of optimum performance were often introduced. As early as Chap. 1, the interrelationship between kinetics and thermodynamics for an exothermic reversible reaction was employed. We saw that the maximum attainable conversion in such reactions decreases as the temperature increases, but the rate of reaction increases. These contrasting effects suggest that improved conversion (per unit volume of reactor) could be obtained by operating the system at different temperatures: first in a high-temperature reactor, where most of the conversion is obtained at a high rate, and then in a second reactor operated at a lower temperature to achieve the higher conversion dictated by thermodynamics. In Chap. 4, Secs. 4-4 and 4-5, conclusions were reached about operating conditions and reactor types for maximum yield of the desired product in multiple-reaction systems. Optimum temperature profiles for exothermic reactions in a tubular reactor were discussed in Sec. 5-7. More on these subjects is available.†

The term "optimizing the performance" does not properly describe the goal, since the ultimate objective concerns economics. However, this term does indicate a dilemma of optimization studies. Rarely can the profit from a chemical reactor be described quantitatively in terms of operating conditions. First, the reactor is probably only one unit of a plant, and the most economical operation of the reactor may conflict with the economy of subsequent separation processes. Hence overall economy may in fact require operating the reactor at nonoptimum conditions. Second, market conditions for the reaction products, even when they are known, are subject to fluctuation. Hence the economics of the entire plant may be time dependent or uncertain. Third, it is difficult to establish valid figures for *all* the costs that accrue to a reactor or a plant. Because of these uncertainties, most

† R. Aris, "The Optimal Design of Chemical Reactors," Academic Press, Inc., New York, 1961; K. G. Denbigh, "Chemical Reactor Theory," chap. 5, Cambridge University Press, Cambridge, 1965; H. Kramers and K. R. Westerterp, "Elements of Chemical Reactor Design and Operation," chap. VI, Academic Press, Inc., New York, 1963.

published optimization studies have dealt with conversion and selectivity rather than with profits. While this approach does not take into consideration any of the cost factors, it does provide a constant solution to the *technical* problem. For *economic* studies a unit value must be applied to each product, determined on the basis of operating and initial costs and marketing uncertainties. Such studies require a knowledge of how operating conditions, such as temperatures, pressures, and feed compositions, affect the production rate of the products, and the problem is to determine the particular operating conditions that will give the maximum profit.

It is supposed that the most profitable reactor type has already been chosen, and the question is: What conditions will afford the most profitable operation of this type? Actually, complete optimization would require simultaneous solution for both considerations. Consider a highly exothermic catalytic reaction (such as air oxidation of naphthalene to phthalic anhydride) which must be carried out below an upper temperature limit to prevent undesirable side reactions (oxidation to CO_2 and H_2O). Several choices of reactor exist. A single, large-diameter, adiabatic fixed bed could be used, with an excess of inert diluent added to the feed to absorb the heat of reaction. This would reduce the initial cost of the reactor. Alternately, a large number of parallel small tubes, packed with catalyst pellets and surrounded by a cooling fluid, might be employed; in this case the diluent might be reduced, and the temperature rise would be limited by heat transfer to the cooling fluid. Operating costs might be reduced, but the initial cost would be high for a reactor consisting of hundreds of small tubes manifolded together. Another possibility would be a large-diameter fluidized bed, either with extensive diluent in the feed and no internal cooling tubes, or with less diluent but a bank of tubes in the bed through which a cooling medium flowed. To decide among these types, optimization studies and a comparison of the results for each would be necessary. More study of this broader type of optimization could be rewarding.

Let us return to the problem of optimizing total conversion and selectivity. To begin with, it is important to note the relation between the two quantities. For a single reaction optimum operation corresponds to the maximum production rate of the product per unit mass of catalyst. When two or more reactions are involved the situation is more complicated, because both total conversion and selectivity, that is, the production rate of each product, are likely to be important. Moreover, this importance may depend on factors other than the reactor, specifically the difficulty (cost) of separation and recycling unreacted feed components and the separation of desirable and undesirable products. Sometimes separation is not feasible.

As an example, consider the catalytic reforming of naphtha to gasoline in a fixed bed of platinum catalyst. The aromatization and cracking processes that occur with the naphtha feed (which itself contains many components) lead to a product that contains literally hundreds of individual components. An overall measure of selectivity is usually all that is possible, and this is generally the octane number of product; separation of individual products is not attempted.† The

† Automated chromatographs with improved resolution have simplified greatly the analysis of mixtures of a large number of individual components.

profitability of the reactor depends on the total production of reformed product and its selectivity (octane number). As temperature increases, total conversion increases, but octane number decreases (many other operating conditions, of course, affect these two measures of performance). Hence a profit function giving appropriate emphasis to total conversion and octane number must be calculated, and then operating conditions that maximize this function must be determined. A complete mathematical analysis, taking into account all the reactions, is impossible—in this case because all the reactions and their kinetics are not known, and not because of the magnitude of the calculations. In simpler situations involving only a few variables, complete analysis is not difficult. Kramers and Westerterp† consider several cases; for example, maximizing the production rate of B in the reaction $A \rightarrow B \rightarrow C$ in an ideal stirred-tank reactor for various temperature conditions, and maximizing the profit in a tubular-flow reactor where three reactions occur, $A \rightarrow B$, $A \rightarrow C$, and $A \rightarrow D$, and B is the valuable product. For somewhat more complex cases with more variables, solutions are still feasible with machine computation for the extensive calculations. In these cases mathematical concepts such as those embodied in the optimality theory of Bellman‡ or the "method of steepest descent"§ are useful.

In summary, the requirement for economical commercial operation suggests the need for further optimization studies. Mathematical procedures are available for carrying out almost any reactor optimization problem. The limitations appear to reside not so much in optimization methods as in formulation of the profit function and complete knowledge of the technical aspects of the process.

PROBLEMS

13-1 The vapor-phase hydration of ethylene is being carried out in a commercial-scale, fixed-bed reactor using spherical, phosphoric acid-on-kieselguhr catalyst pellets whose diameter is d_p. Ethylene and steam (15 moles of steam per mole of ethylene) enter the reactor at 150°C. The heat of reaction

$$C_2H_4(g) + H_2O(g) \rightarrow C_2H_5OH(g)$$

is essentially constant; $\Delta H_R = -22{,}000$ cal/g mol.

The system pressure is 40 lb/in.^{2} abs and at these conditions no liquid phase is present. Also no reaction occurs in the absence of the catalyst.

External mass transfer (bulk-gas-to-pellet-surface) and intrapellet diffusion both can affect the performance of the reactor. The intrinsic rate at a catalyst site is first order in ethylene and first order in water vapor. Neglect the reverse reaction.

A. Derive an explicit equation for the conversion of ethylene leaving the reactor in terms of the mass-transfer coefficient, k_m, based upon the outer surface area of the pellet, the effectiveness factor, η, and other quantities as needed. Assume that there is no axial dispersion in the tubular reactor, no radial gradients of concentration or velocity, and assume isothermal conditions. Neglect pressure drop through the catalyst bed.

B. Calculate the conversion of C_2H_4 in the reactor effluent for the following conditions:

† H. Kramers and K. R. Westerterp, "Elements of Chemical Reactor Design and Operation," chap. 6. Academic Press, Inc., New York, 1963.

‡ See R. Aris, *Chem. Eng. Sci.*, **13**, 18 (1960).

§ F. Horn and U. Trolten, *Chem. Eng. Techol.*, **32**, 382 (1960).

1. Effective diffusivity of ethylene in the catalyst pellets at 150°C and 40 lb/in.^{2} abs = 1.05 cm^2/s
2. Pellet diameter, $d_p = \frac{1}{4}$ in.
3. External mass-transfer coefficient, $k_m = 1.0$ cm/s
4. Intrinsic rate constant for second-order reaction at a catalyst site, $k_2 = 2.13 \times 10^5$ cm^6/(s)(mol)(g of catalyst)
5. Density of catalyst pellet, $\rho_p = 1.5$ g/cm^3 of pellet
6. Density of bed of catalyst pellets, $\rho_B = 1.2$ g/(cm^3 of reactor volume)
7. Diameter of reactor, $2R = 6$ in.
8. Length of catalyst bed = 5 ft
9. Total volumetric flow rate entering the reactor, at 150°C and 40 lb/in.^{2} abs, $Q_F = 9.0$ ft^3/s

13-2 Suppose it were possible to operate an ethyl benzene-dehydrogenation reactor under approximately isothermal conditions. If the temperature is 650°C, prepare a curve for conversion vs. catalyst-bed depth which extends to the equilibrium conversion. The catalyst to be used is that for which rate data were presented in Example 13-3. Additional data are:

Average pressure = 1.2 atm
Diameter of catalyst tube = 3 ft
Feed rate of ethyl benzene per tube = 8.0 lb mol/h
Feed rate of steam per tube = 225 lb mol/h
Bulk density of catalyst as packed = 90 lb/ft^3

Equilibrium-constant data are given in Example 13-3.

13-3 In this case assume that the reactor in Prob. 13-2 operates adiabatically and that the entrance temperature is 650°C. If the heat of reaction is $\Delta H = 60{,}000$ Btu/lb mol, compare the curve for conversion vs. bed depth with that obtained in Prob. 13-2.

13-4 Begley† has reported temperature data taken in a bed consisting of $\frac{1}{4} \times \frac{1}{4}$-in. alumina pellets packed in a 2-in. pipe (actual 2.06 in. ID) through which heated air was passed. No reaction occurred. The tube was jacketed with boiling glycol to maintain the tube wall at about 197°C. For a superficial mass velocity (average) of air equal to 300 lb/(h)(ft^2) the experimental temperatures at various packed-bed depths are as follows:

Radial position	Experimental temperature, °C				
	0.076 ft	0.171 ft	0.255 ft	0.365 ft	0.495 ft
0.0	378.7	354.7	327.8	299.0	279.3
0.1	377.2	353.7	327.0	298.0	278.9
0.2	374.6	349.9	324.1	294.7	277.0
0.3	369.5	343.9	319.7	289.2	273.2
0.4	360.3	336.3	313.8	282.1	267.6
0.5	347.7	327.4	306.4	274.0	260.8
0.6	331.9	316.1	298.2	265.0	252.7
0.7	313.2	300.7	287.9	254.8	243.8
0.8	291.0	282.8	273.1	242.2	234.5
0.9	256.5	257.9	244.2	224.8	224.6

Calculate the effective thermal conductivity (k_r), vs. radial position from these data. Neglect axial dispersion.

† J. W. Begley, master's thesis, Purdue University, Purdue, Ind., February, 1951.

13-5 The temperature-profile data in Prob. 13-4 are to be represented by a constant k_e (across the tube diameter) and a wall heat-transfer coefficient h_w. Estimate the values of $(k_e)_r$ and h_w which best fit the temperature data. Note that at the boundary layer between the wall and the central core of the bed the following relation must apply:

$$h_w(T_i - T_w) = -(k_e)_r\left(\frac{\partial T}{\partial r}\right)_i$$

where $(k_e)_r$ is constant for central core of bed

T_i = temperature at the interface between film and central core

$\left(\frac{\partial T}{\partial r}\right)_i$ = gradient in central core at the interface between core and wall film

13-6 The rate of the catalytic hydrogenation of carbon dioxide to produce methane is [*Ind. Eng. Chem.*, **47**, 140 (1955)]:

$$\text{Rate} = \frac{k p_{CO_2} p_{H_2}^4}{[1 + K_1 p_{H_2} + K_2 p_{CO_2}]^5}$$

where p_{CO_2} and p_{H_2} are partial pressures in atmospheres.

At a total pressure of 30 atm and 314°C, the values of the constants are

$$k = 7.0 \text{ kg mol of } CH_4/(\text{kg catalyst})(\text{h})(\text{atm})^{-5}$$
$$K_1 = 1.73 \text{ (atm)}^{-1}$$
$$K_2 = 0.30 \text{ (atm)}^{-1}$$

A. For an isothermal tubular-flow, fixed-bed, catalytic reactor with a feed rate of 100 kg mol/h of CO_2 and stoichiometric rate of hydrogen, calculate the mass of catalyst required for 20% conversion of the carbon dioxide. Assume that there are no diffusional or thermal resistances (i.e., the global rate is given by the above equation) and that axial dispersion in the reactor is negligible.

B. Repeat part A neglecting the change in total moles due to reaction.

13-7 In the German phthalic anhydride process† naphthalene is passed over a vanadium pentoxide (on silica gel) catalyst at a temperature of about 350°C. Analysis of the available data indicates that the rate of reaction (pound moles of naphthalene reacted to phthalic anhydride per hour per pound of catalyst) can be represented empirically by the expression

$$r = 305 \times 10^5 p^{0.38} e^{-28{,}000/RT}$$

where p is partial pressure of naphthalene in atmospheres and T is in degrees Kelvin. The reactants consist of 0.10 mole % naphthalene vapor and 99.9% air. Although there will be some complete oxidation to carbon dioxide and water vapor, it is satisfactory to assume that the only reaction (as the temperature is not to exceed 400°C) is

$$C_{10}H_8 + 4.5O_2 \rightarrow C_8H_4O_3 + 2H_2O + 2CO_2$$

The heat of this reaction is $\Delta H = -6300$ Btu/lb of naphthalene, but use a value of -7300 Btu/lb in order to take into account the increase in heat release owing to the small amount of complete oxidation. The properties of the reaction mixture may be taken as equivalent to those for air.

The reactor will be designed to operate at a conversion of 80% and have a production rate of 6000 lb/day of phthalic anhydride. It will be a multitude type (illustrated in Fig. 13-1) with heat-transfer salt circulated through the jacket. The temperature of the entering reactants will be raised to 340°C by preheating, and the circulating heat-transfer salt will maintain the inside of the reactor-tube walls at 340°C.

Determine curves for temperature vs. catalyst-bed depth for tubes of three different sizes: 1.0, 2.0, and 3.0 in. ID. In so doing, ascertain how large the tubes can be without exceeding the maximum

† *FIAT Repts. 984, 649; BIOS Repts. 1597, 957, 753, 666; CIOS Rept. XXVIII 29; XXVII 80, 89.*

permissible temperature of 400°C. The catalyst will consist of 0.20 by 0.20-in. cylinders, and the bulk density of the packed bed may be taken as 50 lb/ft^3 for each size of tube.† The superficial mass velocity of gases through each tube will be 400 lb/(h)(ft^2 tube area). Use the one-dimensional design procedure.

13-8 In order to compare different batches of catalysts for fixed-bed cracking operations it is desired to develop a numerical catalyst activity by comparing each batch with a so-called "standard catalyst" for which the x-vs.-W/F curve is known. If the activity of a batch is defined as the rate of reaction of that batch divided by the rate for the standard catalyst at the same conditions, which of the following two procedures would be the better measure of catalyst activity?

(*a*) Determine from the curves the values of W/F required to obtain the same conversion x, and call the activity the ratio

$$\frac{(W/F)_{\text{standard}}}{(W/F)_{\text{actual}}}$$

(*b*) Determine from the curves the values of x at the same W/F, and define the activity as

$$\frac{x_{\text{actual}}}{x_{\text{standard}}}$$

Sketch the x-vs.-W/F curve for a standard catalyst and a curve for a catalyst with an activity less than unity.

13-9‡ Design a reactor system to produce styrene by the vapor-phase catalytic dehydrogenation of ethyl benzene. The reaction is endothermic, so that elevated temperatures are necessary to obtain reasonable conversions. The plant capacity is to be 20 tons of crude styrene (styrene, benzene, and toluene) per day. Determine the bulk volume of catalyst and number of tubes in the reactor by the one-dimensional method. Assume that two reactors will be needed for continuous production of 20 tons/day, with one reactor in operation while the catalyst is being regenerated in the other. Also determine the composition of the crude styrene product.

With the catalyst proposed for the plant, three reactions may be significant:

$$C_6H_5C_2H_5 \overset{k_1}{\rightleftharpoons} C_6H_5CH{=}CH_2 + H_2$$

$$C_6H_5C_2H_5 \overset{k_2}{\rightleftharpoons} C_6H_6 + C_2H_4$$

$$H_2 + C_6H_5C_2H_5 \overset{k_3}{\rightleftharpoons} C_6H_5CH_3 + CH_4$$

The mechanism of each reaction follows the stoichiometry indicated by these reactions. The forward rate constants determined for this catalyst by Wenner and Dybdal are

$$\log k_1 = \frac{-11{,}370}{4.575T} + 0.883$$

$$\log k_2 = \frac{-50{,}800}{4.575T} + 9.13$$

$$\log k_3 = \frac{-21{,}800}{4.575T} + 2.78$$

where T is in degrees Kelvin, and

k_1 = lb mol styrene/(h)(atm)(lb catalyst)
k_2 = lb mol benzene/(h)(atm)(lb catalyst)
k_3 = lb mol toluene/(h)(atm)^2(lb catalyst)

† This represents an approximation, since the bulk density will depend to some extent on the tube size, especially in the small-diameter cases.

‡ From an example suggested by R. R. Wenner and F. C. Dybdal, *Chem. Eng. Progr.*, **44**, 275 (1948).

The overall equilibrium constants for the three reversible reactions are as follows:

t, °C	K_1	K_2	K_3
400	1.7×10^{-3}	2.7×10^{-2}	5.6×10^{4}
500	2.5×10^{-2}	3.1×10^{-1}	1.4×10^{4}
600	2.3×10^{-1}	2.0	4.4×10^{3}
700	1.4	8.0	1.8×10^{3}

The reactor will be heated by flue gas passed at a rate of 6520 lb/(h)(tube) countercurrent (outside the tubes) to the reaction mixture in the tubes. The flue gas leaves the reactor at a temperature of 1600°F. The reactant stream entering the reactor will be entirely ethyl benzene. The reactor tubes are 4.03 in. ID, 4.50 in. OD, and 15 ft long. The feed, 425 lb of ethyl benzene/(h)(tube), enters the tubes at a temperature of 550°C and a pressure of 44 lb/in.^{2} abs; it leaves the reactor at a pressure of 29 lb/in.^{2} abs. The heat-transfer coefficient between the reaction mixture and the flue gas is 9.0 Btu/(h)(ft^2)(°F) (based on outside area) and $\rho_B = 61$ lb/ft^3.

The thermodynamic data are as follows:

Average specific heat of reaction mixture = 0.63 Btu/(lb)(°F)
Average specific heat of flue gas = 0.28 Btu/(lb)(°F)
Average heat of reaction 1, $\Delta H_1 = 53{,}600$ Btu/lb mol
Average heat of reaction 2, $\Delta H_2 = 43{,}900$ Btu/lb mol
Average heat of reaction 3, $\Delta H_2 = -27{,}700$ Btu/lb mol

To simplify the calculations assume that the pressure drop is directly proportional to the length of catalyst tube. Point out the possibility for error in this assumption, and describe a more accurate approach.

13-10 A pilot plant for the hydrogenation of nitrobenzene is to be designed on the basis of Wilson's rate data (see Example 13-5). The reactor will consist of a 1-in.-ID tube packed with catalyst. The feed, 2.0 mol % nitrobenzene and 98 % hydrogen, will enter at 150°C at a rate of 0.25 lb mol/h. To reduce temperature variations the wall temperature of the tube will be maintained at 150°C by a constant-temperature bath. The heat-transfer coefficient between reaction mixture and wall may be taken equal to 20 Btu/(h)(ft^2)(°F).

Determine the temperature and conversion as a function of catalyst-bed depth for the conversion range 0 to 90%. Convert the rate equation in Example 13-4 to a form in which r_p is expressed as lb mol nitrobenzene reacting/(h)(lb catalyst) by taking the void fraction equal to 0.424 and the bulk density of catalyst as 60 lb/ft^3. The heat of reaction is $-274{,}000$ Btu/lb mol. The properties of the reaction mixture may be assumed to be the same as those for hydrogen.

13-11 Use the two-dimensional method to compute the conversion for bed depths up to 0.30 ft for the oxidation of sulfur dioxide under conditions similar to those described in Examples 13-6 and 13-7. The same reactor conditions apply, except that the superficial mass velocity in this case is 147 lb/(h)(ft^2), and the temperature profile at the entrance to the reactor is as shown below:

t, °C	352.0	397.5	400.4	401.5	401.2	397.4	361.2	197.0
Radial position	0.797	0.534	0.248	0.023	0.233	0.474	0.819	1.00

The measured conversions are given for comparison:

Catalyst-bed depth, in.	0	0.531	0.875	1.76	4.23	5.68
% SO_2 converted	0	26.9	30.7	37.8	41.2	42.1

13-12 A monolithic catalyst for a catalytic muffler is made using a metal support of high thermal conductivity. Suppose that the catalyst temperature T_s is constant along the entire reactor length. The air entering the reactor has a pollutant concentration C_f and temperature T_f. Using the nomenclature of Sec. 13-8, derive equations for the conversion and temperature in the air leaving the reactor. Assume that the rate of oxidation is first order (and irreversible) in pollutant concentration and that there is a large excess of oxygen. Hence, $r = 4[\exp(-E/RT_s)]C_s$, where C_s is the pollutant concentration in the air at the catalyst surface. Neglect heat loss from the reactor.

Also, derive an equation for the constant surface temperature.

13-13 A fluid-bed reactor has been suggested for the oxidation of ethylene to ethylene oxide. The operating conditions would be 280°C and 1 atm pressure. The feed gas whose composition is $C_2H_4 = 8\%$, $O_2 = 19\%$ and 73% N_2 has a superficial velocity in the reactor of 2 ft/s at 280°C.

With the silver catalyst available the intrinsic reaction rate, g mol of ethylene oxide/(s)(g catalyst), is given by

$$r = 5.0C_{C_2H_4}$$

Two competing reactions occur:

$$C_2H_4 + \tfrac{1}{2}O_2 \rightarrow C_2H_4O$$

$$C_2H_4 + 3O_2 \rightarrow 2CO_2 + 2H_2O$$

The selectivity of ethylene oxide with respect to carbon dioxide is independent of conversion and equal to 1.5.

A. Calculate the conversion as a function of reactor height using the bubbling-gas model. Neglect the catalyst concentration in the bubbles, assume that the dense phase is a well-mixed batch fluid and that the gas bubbles rise in plug flow. Other properties of the fluidized bed are:

Density of catalyst particles in the dense phase = 0.04 g/cm^3
Mass-transfer coefficient, bubble to dense phase, $k_m a_v = 0.30$ s^{-1}
Volume fraction occupied by gas bubbles, $1 - \varepsilon_d = 0.10$

B. For comparison, calculate the conversion in a plug-flow reactor and in a stirred-tank reactor for the same bubble-phase residence time.

13-14 An irreversible first-order gaseous reaction $A \rightarrow B$ is carried out in a fluidized-bed reactor at conditions such that the rate constant is $k_1 = 0.076$ ft^3/(s)(lb catalyst). The superficial velocity is 1.0 ft/s and the bulk density of catalyst in the bed is 5.25 lb/ft^3. In this case assume that the entire bed has a uniform particle density ("single phase" rather than bubbling-gas concept) and that the mixing conditions correspond to plug flow modified by axial dispersion. The extent of dispersion can be evaluated from Gilliland and Mason's† equation

$$\frac{u}{D_L} = 2.6\left(\frac{1}{u}\right)^{0.61}$$

where u is superficial velocity, in feet per second, and D_L is axial diffusivity, in square feet per second.

What will be the conversion in the effluent from a reactor with a catalyst-bed depth of 5.0 ft? What would the conversion be if plug-flow behavior were assumed?

13-15 A first-order gaseous reaction $A \rightarrow B$ is carried out in a fluidized bed at 500°F and 2 atm pressure. At this temperature $k_1 = 0.05$ ft^3/(s)(lb catalyst). The bulk density of the catalyst bed is 3 lb/ft^3 and the superficial mass velocity of gas is 0.15 lb/(s)(ft^2). If the bed height is 10 ft, what will be the exit conversion? The molecular weight of component A is 44.

13-16 Repeat Prob. 13-15 for a reversible reaction for which the equilibrium constant is 0.6. Compare results obtained for plug flow of gas through the bed and by using the axial dispersion model (with D_L given by the correlation suggested in Prob. 13-14).

† E. R. Gilliland and E. A. Mason, *Ind. Eng. Chem.*, **41**, 1191 (1949).

13-17 A reaction $2A \rightarrow B$ is being studied in a fluidized-bed reactor at atmospheric pressure and 200°F. The global rate of reaction may be approximated by a second-order irreversible equation

$$r_p = k_2 p_A^2$$

where k_2 = lb mol/(s)(atm^2)(lb catalyst). Assume that the "single phase" model described in Prob. 13-14 is applicable. At the operating temperature, $k_2 = 4.0 \times 10^{-6}$. The superficial gas velocity is 1.0 ft/s, and the bulk density of the fluidized catalyst 4.0 lb/ft^3. (*a*) Calculate the conversion of *A* for plug flow of gas, with bed heights of 5, 10, and 15 ft. (*b*) Correct for the effect of longitudinal diffusion, using the diffusivity data given in Prob. 13-14.

13-18 In the slurry reactor of Example 13-10, an arithmetic average concentration of oxygen in the gas bubbles was used. Then the reaction rate was constant throughout the reactor. To evaluate the error introduced by this assumption, calculate the volume of bubble-free liquid required if the change in oxygen concentration is taken into account.

13-19 A. Reconsider Example 13-10 for a carbon particle size of $d_p = 0.542$ mm; the mass concentration, m_s, of particles will be the same, 0.070 g/(cm^3 of water), and the size of the gas bubbles is unchanged so that k_L is 0.08 cm/s. For the 0.542 mm particles the effectiveness factor is 0.098 (note that for the 0.03 mm particles of Example 13-10, $\eta = 0.86$). What volume of water would be required? All other conditions are the same as in Example 13-10.

B. If m_s were reduced to 0.03 g/(cm^3 of water) and the reactor volume was that found in part A, what would be the conversion of SO_2 to H_2SO_4?

13-20 A laboratory-scale, continuous slurry reactor is used for the polymerization of ethylene. A slurry of catalyst in cyclohexane is fed to the reactor at a rate of 10^3 cm^3/min and the volume of liquid in the vessel is 10^4 cm^3. Pure ethylene gas at a rate of 10^3 cm^3/min is bubbled into the bottom of the vessel and is dispersed into bubbles which are uniformly distributed throughout the slurry.

At the operating conditions, the values of the transport coefficients are

$$k_L = 0.07 \text{ cm/s}$$

$$k_c = 0.03 \text{ cm/s}$$

The catalyst particle concentration is 0.10 g/cm^3 of 0.10 mm particles (particle density $\rho_p = 1.0$ g cm^3). The bubbles will be about 3 mm in diameter and the bubble volume per unit volume of liquid will be 0.09.

While the kinetics are complex, assume that the rate of disappearance of ethylene is controlled by the first-order reaction

$$r_{C_2H_4} = k a_c (C_L) \qquad \text{mol } C_2H_4/(\text{s})(\text{cm}^3 \text{ of liquid})$$

$$k = 0.01 \text{ cm/s}$$

The effectiveness factor for the catalyst particles is unity. Henry's law constant for ethylene is 5 [mol/(cm^3 of gas)]/[mol/(cm^3 of liquid)].

Calculate the production rate of polymer in terms of moles of ethylene reacted per second. The entering slurry of cyclohexane and catalyst contains no dissolved ethylene or polymer.

13-21 In Example 13-9 the catalyst concentration was so large that the rate of hydrogenation was determined solely by the mass-transfer rate of hydrogen from the gas bubble to the liquid. Reconsider this example by accounting for the effect of liquid-to-particle mass transfer. For the catalyst particle size of 0.5 mm and for the agitation conditions, Fig. 10-10 gives $k_c = 0.02$ cm/s. The density of the particles is $\rho_p = 0.9$ cm^3/s. What would be the minimum particle concentration (m_s) in the slurry if inclusion of liquid-to-particle mass transfer is not to change the overall rate of hydrogenation by more than 5%.

13-22 Reconsider Example 13-12 for a gas feed of 50% H_2 and 50% N_2. Neglect the solubility of nitrogen in the liquid. Note that for this case the mass balance for hydrogen in the gas phase is required.

A. Derive an equation for the fractional removal of thiophene as a function of catalyst bed depth.

B. Calculate the bed depth required for removal of 75% of the thiophene. The superficial gas velocity is 20 cm/s (at 200°C and 40 atm).

13-23 The removal of SO_2 from air is being investigated in a laboratory trickle-bed reactor as described in Example 13-13. Using the results of that example, and the following data, calculate the fractional removal of SO_2 from the air by reaction:

$$(H)_{O_2} = 5.0[\text{g mol/(cm}^3\text{ of gas)}]/[\text{(g mol/(cm}^3\text{ of liquid)}]$$
$$\text{Liquid flow rate} = 1.0\ \text{cm}^3/\text{s}$$
$$\text{Gas flow rate} = 1.0\ \text{cm}^3/\text{s}$$
$$(k_c a_c) = 0.20\ \text{s}^{-1}$$
$$(K_L a_g) = 0.02\ \text{s}^{-1}$$
$$\text{Intrinsic reaction rate constant, } k = 0.2\ \text{cm}^3/(\text{g})(\text{s})$$
$$\text{Catalyst particle effectiveness factor} = 0.5$$
$$\text{Density of catalyst bed, } \rho_B = 1.0\ \text{g/cm}^3$$
$$\text{Cross-sectional area of empty volume} = 5.0\ \text{cm}^2$$

13-24 A laboratory trickle-bed reactor is to be designed for the catalytic oxidation of dilute, aqueous solutions of acetic acid using air. A commercial iron-oxide catalyst, for which the intrinsic reaction rate is given by Eq. (A) of Example 10-10, is to be used. Operating conditions will be 67 atm and 252°C. The reactor, 2.54 cm ID, will be packed with 0.0541 cm catalyst particles. Liquid and gas-flow rates are 0.66 cm^3/s and 3.5 cm^3/s, measured at reactor temperature and pressure. For these catalyst particles the effectiveness factor is unity. The density, ρ_B, of the particles in the bed is 1.17 g/cm^3 and the density of the particles themselves is 2.05 g/cm^3. Oxygen is slightly soluble so that it is the limiting reactant in the oxidation:

$$CH_3COOH(aq) + 2O_2(g) \rightarrow 2CO_2(aq) + 2H_2O$$

Henry's law constant for oxygen is 2.78 [(g mol)/(cm^3 of gas)]/[(g mol)/(cm^3 of liquid)] when the concentration in the gas is reported in terms of a volume measured at 252°C and 5.5 atm. The mass-transfer coefficients may be taken as those found in Example 10-9

$$(K_L a_g)_{O_2} = (k_L a_g)_{O_2} = 0.024\ \text{s}^{-1}$$
$$(k_c a_c)_{O_2} = 2.2\ \text{s}^{-1}$$
$$(k_c a_c)_{HA} = 1.5\ \text{s}^{-1}$$

where HA designates acetic acid.

The feed concentrations in the liquid are 2.40×10^{-7} g mol/cm^3 for oxygen and 33.7×10^{-7} g mol/cm^3 (about 200 ppm) for acetic acid. The gas feed is saturated with water vapor at 252°C (p_{H_2O} = 40.8 atm) so that its oxygen partial pressure is (67 − 40.8)0.21 = 5.5 atm. Calculate the conversion of acetic acid as a function of catalyst bed depth. Assume plug flow of liquid.

A numerical solution of the mass-conservation equations and boundary conditions is required. These equations are similar to Eqs. (13-64) to (13-68) and (13-61) to (13-63), except that the intrinsic rate is not second order.